Open Research Online

The Open University's repository of research publications
and other research outputs

Tetracycline and its Analogues as Drugs Against Protein Aggregation and Amyloid Formation

Thesis

How to cite:

Beeg, Marten (2010). Tetracycline and its Analogues as Drugs Against Protein Aggregation and Amyloid Formation. PhD thesis The Open University.

For guidance on citations see FAQs.

© 2010 The Author

https://creativecommons.org/licenses/by-nc-nd/4.0/

Version: Version of Record

Link(s) to article on publisher's website:
http://dx.doi.org/doi:10.21954/ou.ro.0000f22d

Copyright and Moral Rights for the articles on this site are retained by the individual authors and/or other copyright owners. For more information on Open Research Online's data policy on reuse of materials please consult the policies page.

oro.open.ac.uk

UNRESTRICTED

Candidate:

Marten Beeg

The Open University, UK
— Advanced School of Pharmacology —
Dean, Enrico Garattini M D
Mario Negri Institute for
Pharmacological Research
2/04/2010

Tetracycline and its Analogues as Drugs against Protein Aggregation and Amyloid Formation

---

Registered degree:

Doctor of Philosophy at the Open University

Affiliated Research Center:

Istituto di Ricerche Farmacologiche Mario Negri (Milan, Italy)

Milan, November 2009

DATE OF SUBMISSION : 30 Nov 200
DATE OF AWARD : 24 MAR 201

ProQuest Number: 13837656

All rights reserved

INFORMATION TO ALL USERS
The quality of this reproduction is dependent upon the quality of the copy submitted.

In the unlikely event that the author did not send a complete manuscript
and there are missing pages, these will be noted. Also, if material had to be removed,
a note will indicate the deletion.

ProQuest 13837656

Published by ProQuest LLC (2019). Copyright of the Dissertation is held by the Author.

All rights reserved.
This work is protected against unauthorized copying under Title 17, United States Code
Microform Edition © ProQuest LLC.

ProQuest LLC.
789 East Eisenhower Parkway
P.O. Box 1346
Ann Arbor, MI 48106 – 1346

Abstract

With more than 20 million cases worldwide, Alzheimer's disease (AD) is now the most common neurodegenerative disease. The two defining features of this disease are extracellular plaques and intracellular neurofibrillary tangles.

Although no AD treatment is available, researchers are making encouraging progress, including the use of small compounds which interact with amyloid-β (Aβ) and affect its self aggregation. Tetracyclines (TCs) are thought to have an anti-amyloidogenic effect on Aβ peptides. But the inconsistency of results in literature prompted us to further investigate the behaviour of various fragments of Aβ (Aβ1-40; Aβ1-42; guest-host-peptide Aβ14-24) which were synthesised as depsi-peptides, in the presence of TCs. Due to their superior solubility the depsi-peptides allowed us to prepare reliable and seed-free stock solutions with reproducible properties. These allowed the preparation of different well-characterised Aβ1-42 species (initial state, oligomers, and fibrils), and to investigate the binding of Aβ ligands (Aβ monomers or TCs) to them or to study the modulation of the kinetics of fibril formation in the absence or presence of TCs, by Surface Plasmon Resonance (SPR), Circular Dichroism (CD) or Thioflavine-T (ThT) fluorescence.

Binding of Aβ1-42 monomers to immobilised fibrils could be well described by the "Dock and Lock" mechanism. TCs do not bind to the prepared Aβ species nor do they alter the highly reproducible kinetics of fibril formation or disaggregated preformed amyloidogenic structures. Consistent with the inactivity of TCs against amyloid β-sheet structures the treatment of APP/PS1tg mice with doxycycline (DC) after plaque formation did not change the plaque load in this mouse model compared to the control mice. These findings suggest that toxic Aβ species other than these considered in this study or the common neuroprotection seen for TCs might be responsible for the positive effects in-vivo in previously reported studies.

Content

CONTENT I

ACKNOWLEDGMENTS V

LIST OF FIGURES VI

LIST OF TABLES IX

LIST OF ABBREVIATIONS X

1 INTRODUCTION 1

1.1 MISFOLDING DISEASES 2

1.1.1 Mechanism of fibril formation 3

1.2 ALZHEIMER'S DISEASE 6

1.2.1 From APP to β-amyloid plaques in-vivo 9

1.2.2 Molecular and cellular processes of AD pathogenesis: What goes wrong? 12

1.2.3 Kinetics of fibril formation in-vitro 13

1.2.4 Other Aβ oligomers 17

1.2.5 Mutations in AD and early on-set of the disease 18

1.2.6 Surface-induced formation of Aβ assemblies 20

1.2.7 Metals in AD 20

1.3 CHEMICAL SYNTHESIS OF PROTEINS 22

1.4 DISAGGREGATION AND PEPTIDE PREPARATION 27

1.5 AGGREGATION INHIBITORS: A STRATEGY IN AD TREATMENT 28

1.5.1 β-sheet binding compounds 29

1.5.2 β-sheet breaker peptides 29

1.5.3 Modulation of structural transitions 30

1.5.4 Current clinical trials using aggregation modulators 31

1.5.5 Tetracyclines (TCs): small compounds for AD treatment? 32

1.6 TETRACYCLINE 35

1.6.1 Nomenclature and structure 35

1.6.2 Physical and chemical properties 36

2 AIM OF THE THESIS 45

3 MATERIAL AND METHODS 48

3.1 MATERIAL 49

3.2 PEPTIDE SYNTHESIS 49

3.2.1 Automated peptide synthesis 49

3.2.2 Manual peptide synthesis 50

3.2.3 Kinetics of native sequence formation 52

3.3 IN-VITRO BINDING AND KINETICS OF FIBRIL FORMATION STUDIES 52

3.3.1 Thioflavine T (ThT) fluorescence 52

3.3.2 Circular Dichroism (CD) analysis 52

3.3.3 CD spectra of Doxycycline (DC) depending on pH 53

3.3.4 Titration of Aß assemblies with ligands (TCs) by following changes in the CD bands upon ligand binding 54

3.3.5 Fluorescence Microscopy 54

3.3.6 Atomic force microscopy (AFM) 54

3.3.7 Size exclusion chromatography (SEC) 55

3.3.8 Surface Plasmon Resonance (SPR) 55

3.4 TOXICITY OF AB ASSEMBLIES 56

3.4.1 Preparation of primary hippocampal neurons 56

3.4.2 MTT assay 57

3.5 TREATMENT OF APP/PS1TG MICE WITH DC 57

4 RESULTS 58

4.1 THE INITIAL STATE AND SAMPLE PREPARATION 59

4.1.1 The improvement in reproducibility of the initial state CD spectrum by use of depsi-Aß 60

4.1.2 The initial state of various Aß fragments 65

4.1.3 Native peptide formation slightly basic condition permits the preparation of high concentrated Aß stock solution 67

4.1.4 Preparation and characterization of specific Aß1-42 assemblies (initial state, oligomers, fibrils) 69

4.1.5 Toxicity of the various assemblies on neuronal cells *73*

4.2 KINETICS OF FIBRIL FORMATION 74

4.2.1 Sedimentation of aggregated assemblies during the CD experiments interfere with the secondary structure measurements under non agitating (quiescent) condition *75*

4.2.2 Kinetics of aggregation of Aβ1-42 and the impact of the variation in concentration *77*

4.2.3 Stirring-induced alignment of amyloid fibrils revealed by CD *79*

4.2.4 Determination of optimal condition for the kinetic experiments *81*

4.2.5 Analysis of Aβ1-42 fibril elongation by Surface Plasmon Resonance *83*

4.2.6 Investigation of the kinetics of aggregation of a guest-host system Aβ14-24 permits the incubation at neutral pH under quiescent condition *86*

4.2.7 Differences in the aggregation propensity of Aβ1-40 MUT (A2V) compared to Aβ1-40 WT ... *90*

4.3 TETRACYCLINE AND THE SYNTHETIC AB FRAGMENTS 92

4.3.1 Solubility of TC and the changes of the CD spectra depending on the pH *93*

4.3.2 Binding of tetracycline to Aβ fibrils *95*

4.3.3 Tetracycline and the kinetics of fibril formation *97*

4.3.4 Stability of Tetracycline *99*

4.3.5 The influence of the Tetracycline instability upon CD and ThT measurements *101*

4.3.6 No disaggregation of preformed aggregates *104*

4.3.7 DC does not reduce the plaque load in an animal model *106*

5 DISCUSSION **108**

5.1 REFINEMENT OF PEPTIDE PREPARATIONS FOR KINETICS OF FIBRIL FORMATION 109

5.2 PREFORMED ASSEMBLIES AND TOXICITY 112

5.3 TC AND ITS BINDING TO AB ASSEMBLIES 113

5.4 TCS AND THE KINETICS OF FIBRIL FORMATION OF AB 115

6 CONCLUSION **121**

7 APPENDIX **124**

7.1 SECONDARY STRUCTURE OF AB RELATED FRAGMENTS DETERMINED BY VARIOUS TECHNIQUES 125

7.2 CHEMISTRY OF SOLID STATE PEPTIDE SYNTHESIS (ADAPTED FROM (KIRIN ET AL. 2007) 128

7.2.1 Fmoc deprotection *128*

7.2.2 Amino acid coupling *129*

7.2.3 Final deprotection from the resin and side chain deprotection *130*

7.3 INITIAL STATE AND SAMPLE PREPARATION 131

7.3.1 Preparation of stock solutions of Depsi-Aβ1-40/1-42 ..... *131*

7.3.2 Formation of native Aβ and sample preparations *131*

7.4 THE SEQUENCE DEPENDANT PROPERTIES WHICH INFLUENCE THE AGGREGATION OF THE AB MUTATION (A2V) COMPARED TO THE WT SEQUENCE 132

8 BIBLIOGRAPHY 133

Acknowledgments

This thesis is dedicated to my wife Anna and my two children Sveva and Timoteo, who offered me unconditional love and support, even of the numerous hours I was not present.

Furthermore this research project would not have been possible without the support of many people. The author wishes to express his gratitude to his supervisors, Dr. Mario Salmona (Head of the Department of Molecular Biochemistry, Istituto di Ricerche Farmacologiche Mario Negri) and Dr. Peter Bayley (National Institute for Biomedical Research, London) who were abundantly helpful and offered invaluable assistance, support and guidance with the freedom to grow as a researcher.

Special thanks also to all my group members; for sharing thoughts, literature and invaluable assistance. Especially Marco Gobbi for the fundamental advices and the awareness that writing is the best way for reasoning about results and to stay focused. Thanks also to all the senior scientists; Antonio Bastone, Laura Colombo, Alfredo Cagnotto, Ada DeLuigi and Luisa Diomede who offered a helping hand to teach me the skills and knowledge needed to accomplish my research project. Special thanks to Claudia Balducci for conducting the animal studies with Doxycycline, Alexandra Sclip for the toxicity study and for the help of Matteo Stravalacci during the SPR experiments. Finally, special thanks are also due to our collaborators, Fabrizio Tagliavini and Pietro DeFede from the Istituto Besta who gave me the possibility to be part of a very exciting scientific study.

This work wouldn't be possible without my parents Regina and Harald Beeg, who with their support and guidance over many years paved the way for my carrier. Furthermore, I feel deeply thankful for my parents in law Stefania Maranzana and Carlo Cattaneo, who gave always a helping hand when it was needed.

List of Figures

Fig. 1-1: Nucleation Polymerization A: The model B: The time dependant formation of fibrils with and without seeds (Harper and Lansbury, 1997) 4

Fig. 1-2: The nucleated conformational change (NCC) model (Serio et al., 2000) 5

Fig. 1-3 The different phases of AD (NIH, 2008) 6

Fig. 1-4: The hallmarks of AD A: plaques B: Neurofibrilar tangles http://edoc.hu-berlin.de/dissertationen/becker-matthias-2006-07-17/HTML/image005.jpg 7

Fig. 1-5 Changes in the brain due to AD A: healthy brain B: Severe AD (NIH, 2008) 9

Fig. 1-6: From APP to beta-amyloid plaque in-vivo 11

Fig. 1-7: Key players in the pathogenesis of AD (Mucke, 2009) 13

Fig. 1-8: Kinetics of fibril formation of Aβ1-42 (Roychaudhuri et al., 2009) 13

Fig. 1-9: The cleavage sites and loci of mutation of the Aβ sequence. (Thinakaran and Koo, 2008) 19

Fig. 1-10: Solid phase peptide synthesis (Amblard et al., 2006) 23

Fig. 1-11: Amide backbone modification strategies for the synthesis of difficult sequences 25

Fig. 1-12: Therapeutic strategies based on the "amyloid hypothesis" 28

Fig. 1-13: Acidic functional groups of Tetracycline a) C2 tricarbonyl system b) C4 Dimethylamino group (here bH+) protonated c) Keto-Enol-groupe of the BCD (Schmitt and Schneider, 2006) 38

Fig. 1-14: The various structures of TCs A: extended B: twisted 39

Fig. 4-1: Preparation of a reliable stock solution and the impact of vortexing 61

Fig. 4-2: Comparison of concentration determination of depsi-Aβ1-40 via absorbance measurements at 214 nm and 280 nm 64

Fig. 4-3: The initial state of Aβ1-40 compared to Aβ1-42 in CD 65

Fig. 4-4: The initial state of Aβ1-40 WT compared to Aβ1-40 MUT 66

Fig. 4-5 Formation of the native sequence or the art of clicking 68

Fig. 4-6: Characterization of different species of native Aβ1-42 by AFM, CD, ThT, and SEC: 70

Fig. 4-7: AFM and SEC of Aβ1-42 22°C oligomers 71

Fig. 4-8 Binding of Aβ1-42 monomers and 22°C oligomers to immobilised anti-bodies 6E10 and A11 72

Fig. 4-9 AFM of fibrils before and after sonication 72

Fig. 4-10: Concentration dependent cell viability neuronal cells after treatment with various Aβ1-42 assemblies for 24h compared to the cells treated only with the buffer. 73

Fig. 4-11: Kinetics of fibril formation of Aβ1-40 under quiescent condition 76
Fig. 4-12: The kinetics of fibril formation of Aβ1-42 under quiescent condition 78
Fig. 4-13: Stirring induced alignment of β-sheet assemblies determined by CD. 80
Fig. 4-14: Optimised kinetics of fibril formation of Aβ1-42 and Aβ1-40 82
Fig. 4-15: Aβ1-42 fibril elongation investigated by SPR: 83
Fig. 4-16 Global fitting of the sensorgrams obtained injecting Aβ1-42 monomers (three concentrations) over immobilised Aβ1-42 fibrils: 84
4-17: Design principles of host–guest switch-peptides that are derived from Aβ14-24 (guest) which contains two switch elements at the N and C termini, separating the guest sequence form the β-sheet formation favouring host sequence (SL-motif)(Camus et al., 2008) 86
Fig. 4-18: The kinetics of fibril formation of Aβ14-24: CD 88
Fig. 4-19: The kinetics of fibril formation of Aβ14-24: AFM and ThT 89
Fig. 4-20: In-situ ThT kinetics of fibril formation of 50 μM Aβ1-40 WT/MUT in 50 mM PB pH 7.4 at 37°C. 91
Fig. 4-21: The solubility of TC 93
Fig. 4-22: pH dependent changes in Doxycycline CD spectrum and absorbance spectrum 94
Fig. 4-23: Binding of TC to fibrils investigated by CD, SPR and fluorescence spectroscopy 96
Fig. 4-24 TCs and the kinetics of fibril formation 98
Fig. 4-25: The decomposition of TC 100
Fig. 4-26: Turbidity changes at 500 nm of Aβ1-40 during fibril formation in either presence of absence of RTC 101
Fig. 4-27: The decomposed TC influences the ThT fluorescence and the CD measurement 103
Fig. 4-28: No disaggregation of fibrils and 22°C oligomers by CD and ThT 105
Fig. 4-29: No differences in amyloid plaque deposition after doxycycline treatment of APP/PS1tg mice.107
Fig. 5-1:Alpha synuclein in the presence of different concentration of Tetracycline (A) original data (B) normalization by the final value (Ono and Yamada, 2006) 118
Fig. 5-2: Amount of β-structure, fibril length and intersheet stacking of Aβ11-25 with and without Tetracycline determined by X-ray diffraction patterns (adapted from Kirschner et al. (Kirschner et al., 2008)) 118
Fig. 7-1: Mechanism by arrow pushing of the removal of the Fmoc Nα-protecting group 128
Fig. 7-2: Mechanism by arrow pushing of the coupling reaction using TBTU in the presence of DIEA 129

Fig. 7-3: Mechanism by arrow pushing of deprotection reaction of tBu and cleavage of a peptide from Wang resin 130

Fig. 7-4: The amino acid dependant hydrophobicity, β-sheet propensity, contribution to a hydrophilic, hydrophobic pattern and α-helix propensity; Alanine (WT) and Valine (MUT) are highlighted..... 132

List of Tables

Table 1-1: Amyloid related diseases (Chiti and Dobson, 2006) 2

Table 1-2 Effects of Minocycline in AD (adapted from (Kim and Suh, 2009)) 34

Table 1-3. Chemical formula of various TCs 35

Table 1-4: Complexing agents for TCs (adapted from (Durckheimer, 1975) 40

Table 3-1: Condition for first coupling to Rink amide resin using guanidium based reagents 50

Table 3-2: Condition for first coupling to NovaPEG resin and ester bond formation between Boc-Ser-OH and the following AA on the resin by DIC/NMI method 51

Table 3-3: Condition for coupling of depsi-Dipeptide by DIC/HOBt method 51

Table 3-4: Condition for Fmoc deblocking 51

Table 3-5: Parameters for CD spectrum scan and timecourse experiment to monitor the changes at 215 nm 53

Table 3-6: Pipetting protocol to determine the changes in the CD spectrum upon ligand titration 54

Table 4-1: Extinction coefficient at 214 nm of various Aβ fragments based on the values suggested by Kuiper et al. (Kuipers and Gruppen, 2007) 64

Table 4-2: The kinetic parameters obtained in three independent runs, identical to the one shown here, are indicated in Table. The table reports the mean±SD of the kinetic parameters in three independent runs. The data for $A\beta_{1-40}$ are from Cannon et al. (16) and are shown here for comparison 85

Table 7-1: List of publication concerning the determination of the secondary structure of various Aβ fragments 125

List of Abbreviations

Aβ	amyloid-β
AD	Alzheimer's Disease
ADDL	Alzheimer derived diffusible ligands
AFM	Atomic force microscopy
APOE4	Apo lipoprotein E4
APP	Alzheimer parent protein
AU/A.U.	Arbitrary units
AUC	Area under the curve
BACE	beta-site APP-Cleaving Enzyme
Boc	butoxycarbonyl
BSA	Bovine serum albumin
CD	Circular Dichroism
CHC	Central Hydrophobic Core
COX	Cyclooxygenase
CR	Congo Red
CTC	Chlorotetracycline
DBU	Diazabicycloundecen
DC	Doxycycline
DCM	Dichloromethane
DIC	Diisopropylcarbodiimide
DIEA	Diisopropylethylamine
DMC	Demeclocycline
DMF	Dimethylformamide
DNA	Deoxyribonucleic acid
EM	Electronmicroscopy
EPR	Electron paramagnetic resonance
FAD	Familial Alzheimer's disease
Fmoc	Fluorenylmethyloxycarbonyl
FPLC	Fast protein liquid chromatography
HBTU	O-Benzotriazole-N,N,N',N'-tetramethyl-uronium-hexafluoro-phosphate
HCTU	O-(6-Chloro-1-hydrocibenzotriazol-1-yl)- -1,1,3,3-tetramethyluronium hexafluorophosphate
HOBt	Hydroxybenzotriazole
HPLC	High pressure liquid chromatography
LS	Light scattering
MC	Minocycline
MTT	Dimethyl thiazolyl diphenyl tetrazolium salt
MUT	Mutation
NCC	Nucleated conformational change
NGS	Normal goat serum
NM	NH2-terminal (N) and highly charged middle (M)) of the Sup35 prion
NMI	N-Methylimidazol
NMP	N-Methyl-2-pyrrolidone
NMR	Nuclear magnetic resonance
NO	Nitric oxide
NOs	Nitric oxides

NP	Nucleation polymerization
OTC	Oxythetracycline
PAF	Paraformaldeide
PB	Phosphate buffer
PBS	Phosphate buffer saline
PC12	cell line derived from a pheochromocytoma of the rat adrenal medulla
RNA	Ribonucleic acid
ROS	Reactive Oxygen Species
RT	Room temperature
RTC	Rolytetracycline
RU	Resonance Units
SD	Standard deviation
SDS	Sodium dodecyl sulfate
SEC	Size exclusion chromatography
SPPS	Solid phase peptide synthesis
SPR	Surface Plasmon resonance
STEM	Scanning transmission electron microscope
TBTU	O-Benzotriazole-1-yl-N,N,N',N'-tetramethyluronium tetrafluoroborate
tBu	tert-Butyl
TC	Tetracycline
TCs	Tetracycline derivatives
TFA	Trifluoroacetic acid
TGN	Trans Golgi Network
TNF	Tumour necrosis factors
TRIS	tris(hydroxymethyl)aminomethane
TTR	Transthyretin
UV	Ultraviolet
WT	Wildtype

1 Introduction

1.1 Misfolding diseases

A broad range of human diseases arises from the failure of a specific peptide or protein to adopt, or remain in, its native functional conformational state. The largest group of misfolding diseases, however, is associated with the conversion of specific peptides or proteins from their soluble states ultimately into highly organised fibrillar aggregates, but comprise many different proteins with no obvious sequence similarity (Chiti and Dobson, 2006). These structures are generally described as amyloid fibrils or plaques when they accumulate extracellularly, whereas the term "intracellular inclusions" has been suggested when formed inside the cell.

A list of known neurodegenerative diseases that are associated with the formation of extracellular amyloid fibrils or intracellular inclusions with amyloid-like characteristics is given in *Table 1-1*, along with the specific proteins which are the predominant component of the deposits. They may be globular proteins with rigid 3D-structure or belong to the class of natively unfolded (or intrinsically unstructured) proteins (Uversky and Fink, 2004). Despite these differences, the final fibrillar form of the different pathologies display many common properties including a core cross-β-sheet structure and there is an increasing belief that the capability to form fibril is a generic property of the peptide sequence (Chiti and Dobson, 2006).

Table 1-1: Amyloid related diseases (Chiti and Dobson, 2006)

Disease	**Involved protein**
Alzheimer's Disease	Amyloid ß-protein
Parkinson's disease	α-Synuclein
Creutzfeldt Jakob disease	Prion protein and fragments
Huntington's disease	Huntingtin
Frontotemporal dementia with Parkinsonism	Tau
Familial British dementia	ABri

There are conflicting evidences for the role of the fibrillar amyloid found in the deposits, since it not always correlates with the pathology. That is why oligomeric fibril precursors

are currently under investigation to establish their role in the progression of the diseases. These aggregates formed early in the aggregation process, have been reported in many different degenerative diseases. Other in-vitro formed stable aggregates different than fibrils and on-pathway oligomers are off-pathway oligomers and amorphous aggregates whose formation depends on the experimental conditions used.

1.1.1 Mechanism of fibril formation

Experimental studies have shown for a range of peptides and proteins that amyloid fibril formation is preceded by the appearance of organised assemblies usually termed protofibrils and smaller oligomeric species at yet earlier stages of the aggregation process. These oligomers appear initially to be relatively disordered, but then convert into species containing extensive β-sheet structure, that are often capable of stimulating fibril formation.

In the beginning the native monomeric structure of a protein is destabilised to form a partial folded state, which increases the population of non-native states prone to aggregate. This includes the unfolding of globular proteins to a partially unfolded state and the partial folding of native unstructured proteins like Alzheimer's disease (AD) peptide fragments to a more aggregation prone state, which is governed by the amino acid sequence and by the details of the protein environment. But the characterization of fibril formation solely based on the partially unfolded states is unlikely to provide a detailed description of the mechanism of aggregation. Additionally, a high aggregation propensity of sequence could direct the aggregation, independent of the extent and stability of the non-persistent structure of an unstructured sequence.

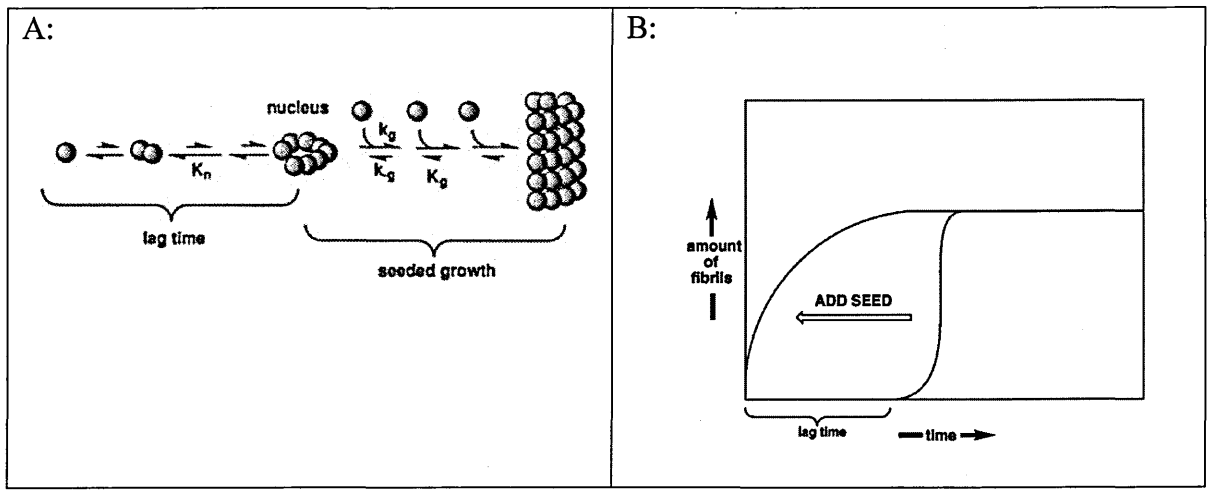

Fig. 1-1: Nucleation Polymerization A: The model B: The time dependant formation of fibrils with and without seeds (Harper and Lansbury, 1997).

Many of the polymerizing peptides are thought to follow a nucleation-dependent pathway (Harper and Lansbury, 1997), when the concentration of the solution is higher than the critical concentration. These processes are characterised by a slow nucleation phase the so called lag phase. During the lag phase the protein undergoes several unfavourable association steps of ordered monomers (nucleation barrier) to form an ordered oligomeric aggregate the nucleus. The initial phase is followed by the exponential growth phase, in which the nucleus rapidly grows to form larger assemblies until a plateau (steady state) is reached, in which the ordered aggregate and the monomer appear to be at equilibrium. If seeds are added during the lag phase or already present in the starting solution, the peptide polymerises immediately. Not all experimental results can be explained with nucleated polymerization (NP). Serio et. al. proposed a nucleated conformational change (NCC) mechanism for the polymerization of NM protein (NH2-terminal (N) and highly charged middle (M)) of the Sup35 prion protein (Serio et al., 2000). Monomeric NM possesses a high degree of conformational flexibility (random-structure) in aqueous buffers and is thought to coalesce into unordered "molten" aggregates in a first step, followed by reorganization to highly ordered oligomers.

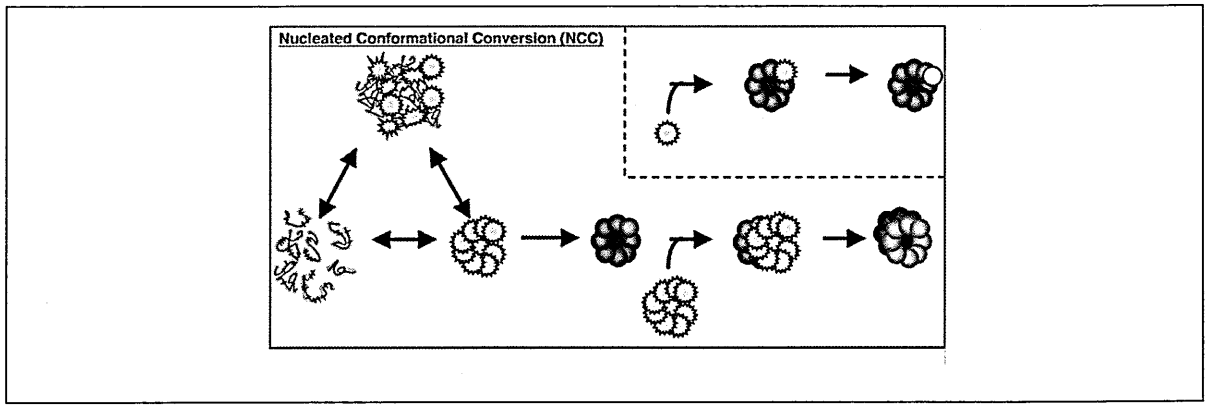

Fig. 1-2: The nucleated conformational change (NCC) model (Serio et al., 2000).

The fibril formation is then continued by addition of unordered monomer or unordered oligomers to the ordered nucleus. Unordered monomer addition, usually called "Dock and lock" mechanism, was proposed to explain the growth of Aβ and PrP 82-146 fibrils (Esler et al., 2000; Gobbi et al., 2006; Nguyen et al., 2007). According to this idea, the attachment of a monomer to ordered assembly is followed by a much slower and rate-limiting lock phase (reorganization).

Auer et al. proposed a unifying framework , which was tested by computer simulations (Auer et al., 2009). They found that the interplay between highly directional hydrogen bonds and nonspecific hydrophobic interactions explains the observed two-step condensation-ordering mechanism which corresponds to NCC. This mechanism was favoured at higher peptide concentration which additionally lowered or even abolished the nucleation barrier. Interestingly, at low concentrations or weak hydrophobicity, the formation of fibrillar structures proceed via the formation of polypeptide chains, converted directly into β-sheet structures, which compares to the NP-mechanism.

1.2 Alzheimer's disease

Alzheimer's disease (AD) is a devastating disease. The majority of AD cases belong to the sporadic or late-onset form of AD, which tends to occur later in life. One in 20 people over 65, and one in five over 85, have AD. Since the elderly population will increase three to four fold by 2050 in highly industrialised regions and the advancing age is the strongest risk factor to develop the disease, AD will result in a huge social and economic burden (Minati et al., 2009).

It is believed, that changes in the brain start decades before the symptoms. Although the course of Alzheimer's disease is unique for every individual, there are many common symptoms. Most commonly recognised symptom is memory loss. This mild cognitive impairment (MCI) can be revealed up to eight years before AD is diagnosed, because the brain is still capable to compensate for the changes. After the diagnosis the patient goes through three different stages, mild, moderate, severe AD. During the progress of the disease, symptoms include confusion, irritability and aggression, mood swings, language difficulties, and long-term memory loss. Gradually, body functions are lost, which in the end leads to death by aspiration pneumonia, because a person is not able to swallow properly and takes food or liquids into the lungs instead of air.

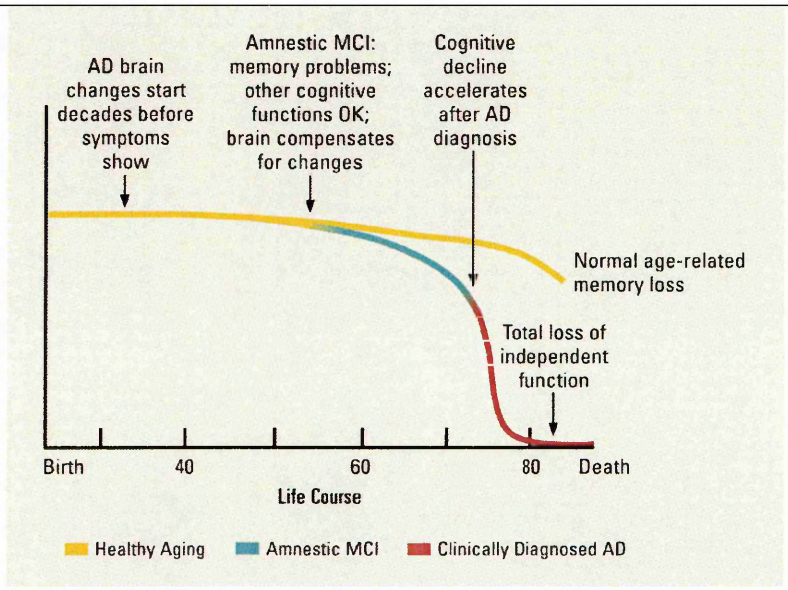

Fig. 1-3 The different phases of AD (NIH, 2008).

The cause and pathways leading to AD are not yet completely clear. But three major competing hypotheses are currently discussed. The oldest is the cholinergic hypothesis, which proposes that AD is caused by reduced synthesis of the neurotransmitter acetylcholine. The other two are derived from the deposits found in the patient's brain, first described by Dr. Alois Alzheimer, a German neurologist and psychiatrist in 1906 (Alzheimer, 1907). He examined the brain tissue of a 51 year old woman, Auguste D., and found tangled bundle of fibrils within neurons (neurofibrillary tangles) (Honson and Kuret, 2008) and numerous patches of sticky proteins (β-amyloid (Aβ)) (Hardy and Selkoe, 2002) in the space between neurons (Fig. 1-4). Both are hallmarks of AD.

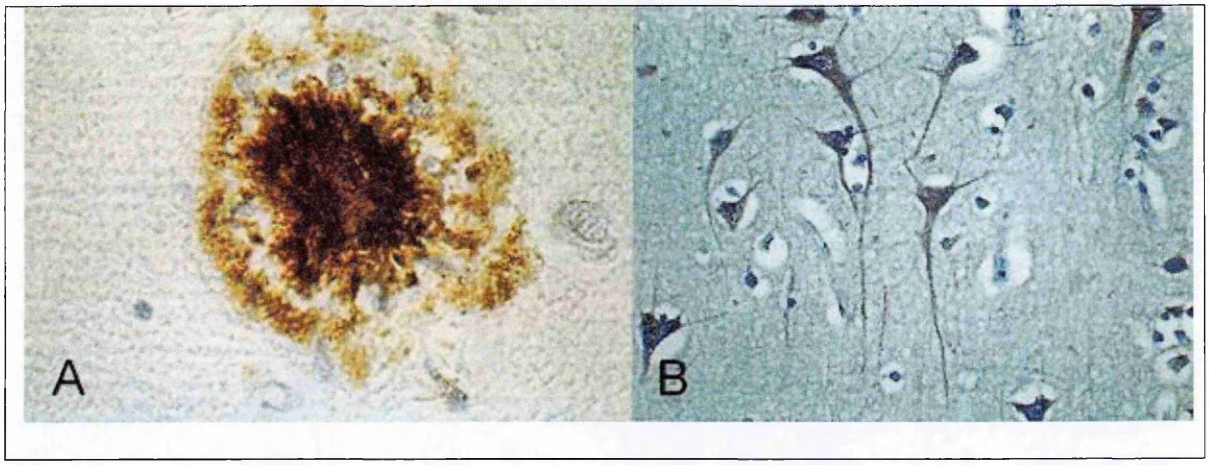

Fig. 1-4: The hallmarks of AD A: plaques B: Neurofibrilar tangles http://edoc.hu-berlin.de/dissertationen/becker-matthias-2006-07-17/HTML/image005.jpg.

Neurofibrillary tangles are mainly composed of the tau protein. In a healthy brain tau stabilises microtubules. For this tau usually contains a certain number of phosphate molecules. In AD the protein gets "hyperphosphorylated" and detaches from the microtubules to form paired helical filaments which enmeshed with each other to form the tangles. As a result the microtubules disintegrate and the neuronal internal transport network collapses with a tremendous impact on the communication abilities of neurons. This abnormal aggregation of the tau protein and the lack of correlation between the amount of amyloid plaques and neuronal loss in some cases, suggested the formulation of "Tau-hypothesis", which is based on the assumption that tau is the major culprit of the

disease (Honson and Kuret, 2008). Nevertheless, genetic, pathological and biochemical clues suggest that the progressive production and subsequent accumulation of β-amyloid (Aβ), a proteolytic fragment (Aβ1-40 or Aβ1-42) of the membrane-associated amyloid precursor protein (APP), play a central role which led to the "Amyloid hypothesis" (Hardy and Selkoe, 2002). Support for this hypothesis comes from the location of the gene for the amyloid beta precursor protein (APP) on chromosome 21, and the fact that patients with trisomy 21 (Down Syndrome) who have an extra gene copy or the duplication of the APP locus (Rovelet-Lecrux et al., 2006) almost universally develop AD and that most of the familiar AD mutations are located inside the Aβ sequence (Miyoshi, 2009). Furthermore most of the early onset AD cases are related to mutation of the AD gene and also APOE4, the major genetic risk factor for AD, leads to excess amyloid build-up in the brain before AD symptoms arise (Kim et al., 2009). Thus in these cases, Aβ deposition precedes clinical AD.

AD is characterised by loss of neurons and synapses in the cerebral cortex and certain subcortical regions (NIH, 2008). It begins in the entorhinal cortex part of the temporal lobe, where healthy neurons begin to work less efficiently, lose their ability to communicate and finally die. Then, the hippocampus is afflicted and the ventricles increase their size. After the diagnosis of AD more and more parts of the cerebral cortex are affected and the number of plaques and tangles grows and the shrinkage of the concerned brain areas progresses further. Finally, when severe AD pathology is developed, the deposits of protein aggregates are widespread throughout the brain and further enlargement of the ventricles and an overall shrinkage of the brain is observed (Fig. 1-5).

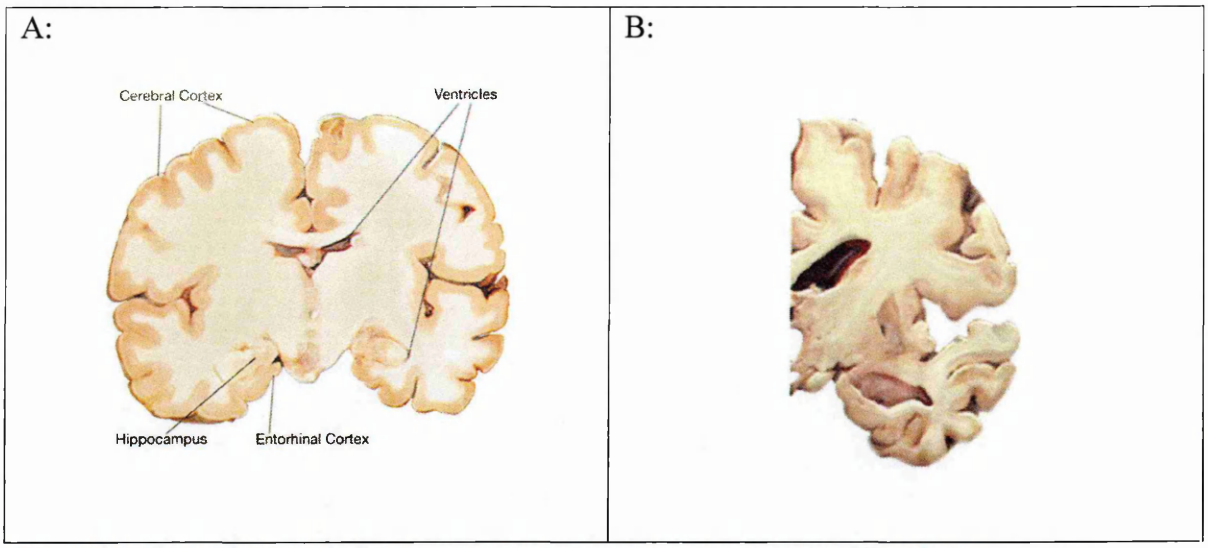

Fig. 1-5 Changes in the brain due to AD A: healthy brain B: Severe AD (NIH, 2008).

1.2.1 From APP to β-amyloid plaques in-vivo

After the isolation and determination of the Aβ fragment as a main constituent of the extracellular plaques in 1984 (Glenner and Wong, 1984), it was found that these fragments are part of a much longer protein encoded on Chromosome 21 called the Amyloid precursor protein (APP) (Goldgaber et al., 1987).

APP is a transmembrane glycoprotein expressed in many tissues and concentrated in the synapses of neurons. Its primary function is not known, though it has been implicated as a regulator of synapse formation (Priller et al., 2006) and neural plasticity (Turner et al., 2003). APP contains several distinct, largely independently-folding structural domains which reside on the extracellular region or intracellular region. APP undergoes extensive post-translational modification including glycosylation, phosphorylation, and tyrosine sulfation, as well as many types of proteolytic processing to generate peptide fragments (De Strooper and Annaert, 2000). There are two predicted cleavages necessary to release Aβ from the precursor molecule. First the β-secretase cleaves the protein in the extracellular domain predominantly localised in the Golgi/TGN and endosomes, followed by the γ-secretase mediated processing in the transmembrane region and subsequent release of Aβ fragments (mainly Aβ1-40 and Aβ1-42) (see Fig. 1-6) during the endocytic/recycling step (Koo and Squazzo, 1994; Thinakaran and Koo, 2008). Available

data indicate the presence of a γ-secretase/Presenilin (PS) complex and enzyme activity in multiple compartments, including the ER, ER-Golgi intermediate compartment, Golgi, TGN, endosomes, and plasma membrane. Studies in non-neuronal and neuroblastoma cell lines suggest that Aβ is generated mainly in the TGN. Nevertheless, γ-secretase also exists as an intact complex on the plasma membrane which could form the Aβ fragments and release them in the extracellular space (Chyung et al., 2005). These fragments are endowed with a high propensity to aggregate, so that if they are produced in excess and/or if they are not properly degraded, they tend to progressively form oligomeric, multimeric and fibrillar structures (plaques) involved in the neurodegeneration. Soluble oligomers may be responsible for cognitive dysfunction in the early stages of the disease.

The size and distribution of the toxic oligomer may vary during the disease progression and can be as small as a dimer (Shankar et al., 2008) or as big as a dodecamer (Lesne et al., 2006). However, the aggregation and accumulation of Aβ culminates with the formation of extracellular plaques, which may be surrounded by oligomeric species co-localizing with the postsynaptic density where they exert their toxic effects (Koffie et al., 2009). Nevertheless, plaques formation could also be a strategy of the organism to neutralise their toxic effect.

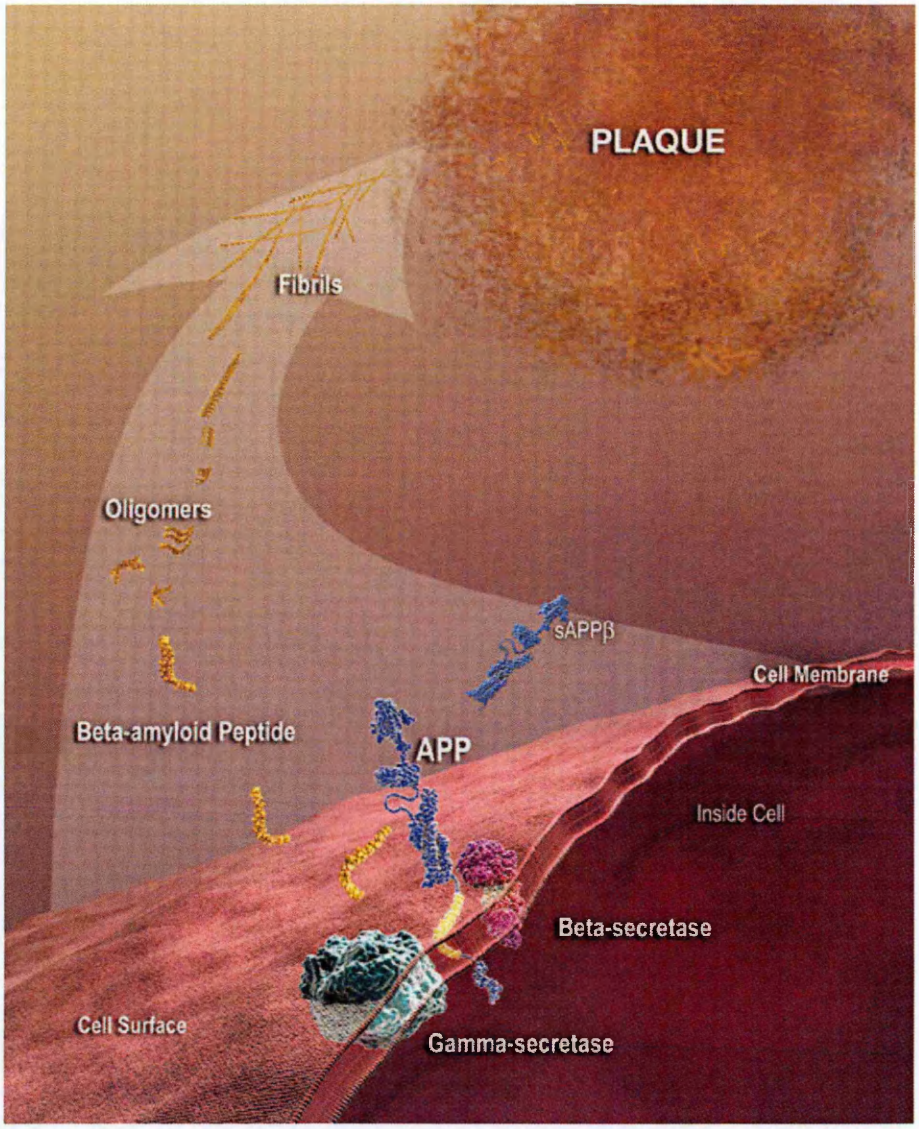

Fig. 1-6: From APP to beta-amyloid plaque in-vivo

The APP protein bound to a membrane is cleaved by γ- and β- secretase and the aggregation prone Aβ fragments are released into the extracellular space. Under this environmental condition the monomer can form oligomers which are thought to proceed to high ordered amyloid fibrils by monomer addition. Then the fibrils are deposited into plaques. (NIH, 2008).

1.2.2 Molecular and cellular processes of AD pathogenesis: What goes wrong?

The current model for AD pathogenesis (Fig. 1-7), based on the amyloid hypothesis, is that once Aβ levels reach a threshold in the brain interstitial fluid, a pathogenic cascade is initiated. Aggregation and accumulation of Aβ in the brain may result from increased neuronal production of Aβ (Citron et al., 1994), decreased activity of Aβ-degrading enzymes (Eckman and Eckman, 2005), or alterations in transport processes that shuttle Aβ across the blood–brain barrier (Bates et al., 2009). Aβ oligomers impair synaptic functions (Arendt, 2009; Shankar et al., 2008), whereas fibrillar amyloid plaques displace and distort neuronal processes (Grutzendler et al., 2007). Aβ oligomers interact with cell-surface membranes (Valincius et al., 2008) and receptors (Verdier et al., 2004), altering signal-transduction cascades (Fuentealba et al., 2004), changing neuronal activities (Salehi and Swaab, 1999) and triggering the release of neurotoxic mediators by microglia (Gonzalez-Scarano and Baltuch, 1999). Vascular abnormalities impair the supply of nutrients and removal of metabolic by-products, cause microinfarcts and promote the activation of astrocytes and microglia (Shi et al., 2000; Zhu et al., 2007). The lipid-carrier protein apoE4, a risk-factor in AD, increases Aβ production and impairs Aβ clearance (Kim et al., 2009). When produced within stressed neurons, apoE4 is cleaved into neurotoxic fragments that destabilise the cytoskeleton (Mahley and Huang, 2006) and, like intracellular Aβ (Reddy, 2009), impair mitochondrial functions (Nakamura et al., 2009). AD related proteins like tau and α-synuclein (Gallardo et al., 2008) can also self-assemble into pathogenic oligomers and can form larger intra-neuronal aggregates, displacing vital intracellular organelles (Crews et al., 2009; De Felice et al., 2008; Fink, 2006; Gendron and Petrucelli, 2009; Qin et al., 2007).

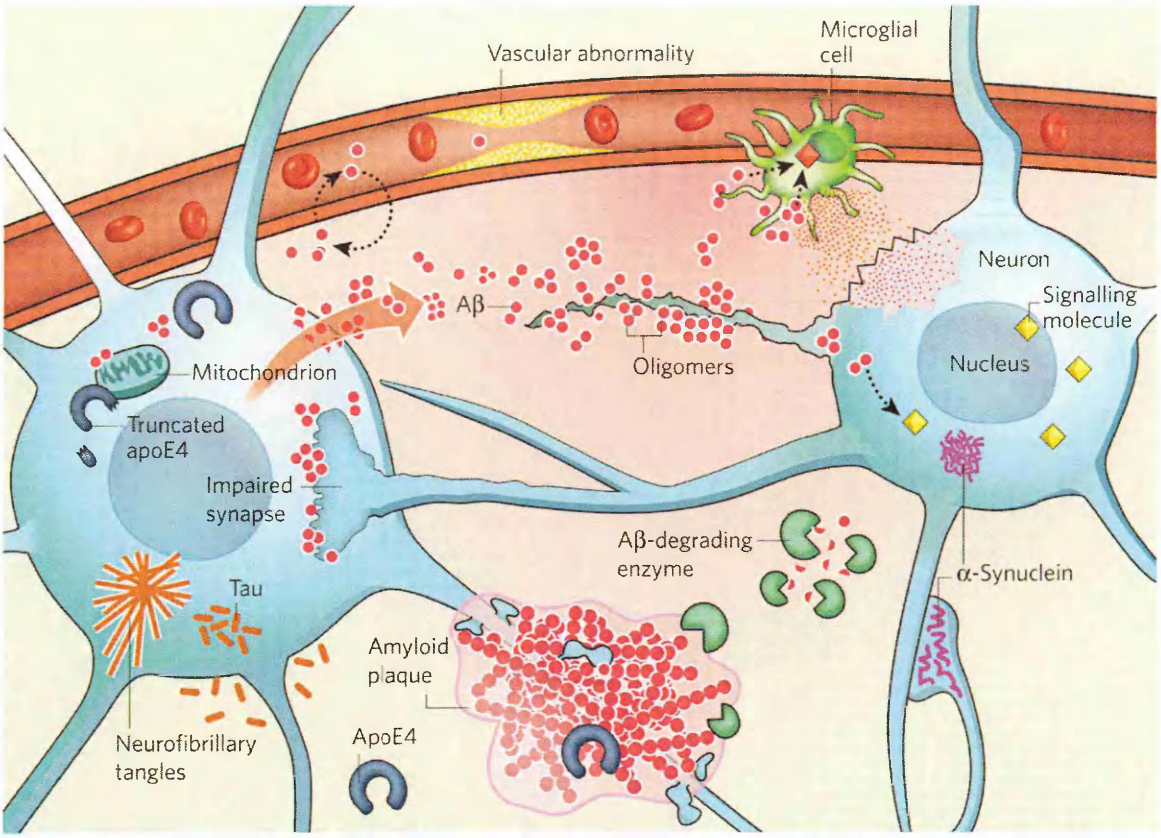

Fig. 1-7: Key players in the pathogenesis of AD (Mucke, 2009).

1.2.3 Kinetics of fibril formation in-vitro

It is thought that Aβ fibril formation follows a nucleation-dependent polymerization reaction. But the investigation of this process revealed a complexity in numbers and types of assemblies and pathways which can lead to on- and off-pathway aggregates depending on the condition of the polymerization reaction (Fig. 1-8).

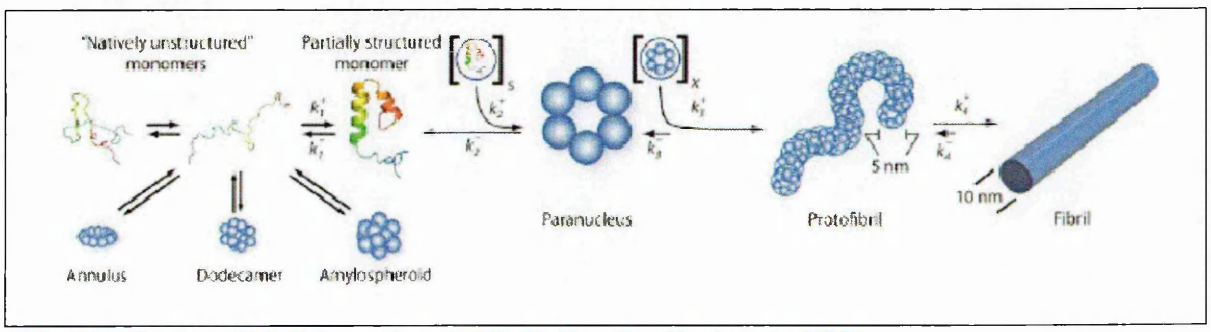

Fig. 1-8: Kinetics of fibril formation of Aβ1-42 (Roychaudhuri et al., 2009).

Aβ is an amphipathic peptide. The N-terminus is mainly polar, since 12 of the first 28 residues are charged at neutral pH. The remaining 12 (Aβ1-40) or 14 (Aβ1-42) side chains are apolar which allows the formation of micelles (Lomakin et al., 1996) or direct interactions with membranes. The turn forming residues A21–A30 are suggested to

nucleate monomer folding because of their solvent inaccessibility. This region is resistant to proteolysis and maintain this in the isolated decapeptide as well (Krone et al., 2008). That turn can be destabilised by amino acid substitutions that cause familiar AD, which correlates with accelerated Aβ oligomerization and higher-order assembly. In-vitro studies showed that Aβ1-40 and Aβ1-42 monomers adopted a predominantly α-helical structure in a membrane-mimicking environment (Coles et al., 1998) while a collapsed statistical coil is prevalent in aqueous solution (Bieschke et al., 2008; Danielsson et al., 2005; Gursky and Aleshkov, 2000; Klement et al., 2007) The monomer contains five relatively independent folding units, which are connected by four turn structures (Yang and Teplow, 2008). Molecular dynamics suggests that several monomeric conformers exist under physiological condition which are divided into two basins, comprising conformers with either substantial alpha-helix or beta-sheet (Yang and Teplow, 2008). Furthermore the addition of two hydrophobic amino acids I41 and A42 in Aβ1-42 shifts the conformational equilibrium towards beta-sheet structure. This is mediated by the increase of contacts within the C-terminus and the additional interaction between the C-terminus and the central hydrophobic cluster (CHC) (L17-A21) (Yang and Teplow, 2008), and could explain the higher aggregation propensity of Aβ1-42 and possibly explains the higher toxicity (Dahlgren et al., 2002). On the contrary, the N-terminus might be more important in stabilizing the monomer of Aβ1-40, thereby hindering the oligomerization. It was shown by NMR (Lim, 2006) and molecular dynamics (Yun et al., 2007) that the N-terminus of Aβ1-40 is more partially stabilised and more structured with a possible formation of beta-sheet structure spanning residue A2-F4. Furthermore, in Aβ1-40 this region is suggested to stay in contact with the CHC and could inhibit intermolecular interactions of the critical residues (histidines and L17VFFA21) (Lim, 2006).

The importance of the C/N-terminus of Aβ1-40 and Aβ1-42 in controlling the oligomerization has been revealed by experiments involving AD related amino acid

substitutions in the C-terminus and truncation of sequences in the N-terminus (Bitan and Teplow, 2004). The authors used photoinduced Cross-Linking of Unmodified Proteins (PICUP) to stabilise the metastable oligomers (Bitan et al., 2003a) which allowed the study of Aβ oligomerization pattern. The oligomerization patterns of the unmodified Aβ1-40 showed that the fragment exists as monomer, dimer, trimer, and tetramer and Aβ1-42 as pentamer, and the important hexamer units, termed paranuclei. Bernstein et al. confirmed these results and additionally suggested the formation of Aβ1-42 dodecamer as primary toxic species (Bernstein et al., 2009). All these metastable smaller oligomers are formed rapidly, and in equilibrium with the monomer. Native gel electrophoresis of un-crosslinked peptides revealed that Aβ1-40 forms unstable monomers, whereas Aβ1-42 forms stable trimers and tetramers prior to fibril formation (Chen and Glabe, 2006). Modification at position 22 (E22Q, E22G, E22K and D23N) led to higher order Aβ1-40 oligomers, but had little effect on the oligomerization patterns of Aβ1-42 (Bitan and Teplow, 2004). Furthermore, the removal of N-terminal residues N1–G9 in Aβ1-42 had no effect on its oligomer size distribution, whereas truncation of up to four N-terminal residues of Aβ1-40 produced higher-order oligomers. Interesting is also the fact that an antibody directed against residues 4-10 of Aβ1-42, inhibits both Aβ fibrillogenesis and cytotoxicity.(McLaurin et al., 2002).

The structure determination of these early oligomers is a difficult task. Recently Ono et al. reported a study in which specific Aβ1-40 oligomers have been stabilised structurally, fractionated in pure form, and then studied by using a combination of CD spectroscopy, Thioflavine T fluorescence, EM, atomic force microscopy (AFM), and neurotoxicity assays (Ono et al., 2009). These spherical oligomers (up to tetramer) exhibited order-dependent increases in β-sheet content, toxicity and fibril nucleation activity. This suggests that these assemblies are on the pathway of fibril formation, which is preceded by protofibril formation (Caughey and Lansbury, 2003). These study and the work of Chimon

et al. (Chimon et al., 2007) revealed a large conformational change between the unstructured monomer and the spherical oligomers while the transition from the oligomer to protofibrils and fibrils involves tighter packing of β-sheet.

Protofibrils in AD, were described as beaded chains, short, unbranched, β-sheet rich, and rod-like structure. Oligomers and protofibrils exist in equilibrium with each other. For Aβ1-42 pentamer or hexamer, the "paranucleus," was suggested to be the basic unit of the protofibril and that the beaded chains comprising protofibrils formed by the self-association of paranuclei (Roychaudhuri et al., 2009). Furthermore, structural differences between protofibrils and mature amyloid fibrils were determined by hydrogen-deuterium exchange-mass spectrometry (HX-MS) coupled with on-line proteolysis for Aβ1-40 (Kheterpal et al., 2006; Williams et al., 2005). It was shown that 12 of the backbone amino acids were protected from exchange in protofibrils and 22 in fibrils. The C-terminal segment 35-40 and the N-terminal segment 1-19 are highly exposed in both fibrils and protofibrils and the internal fragment 20-34 is highly protected in fibrils but much less in protofibrils. Interesting is the fact that the Thioflavine T and Congo-red sensitive β-sheet elements are already present in protofibrils, which are expanded into some adjacent residues upon the formation of mature amyloid. This suggests that protofibrils are on pathway of fibril formation and that the transition from protofibril to fibril involves substantial ordering of Aβ peptide inside the assembly.

This structural flexibility explains the polymorphism (Fandrich et al., 2009; Kodali and Wetzel, 2007; Wetzel et al., 2007) of fibril structures observed in electron microscope and atomic force microscope (Goldsbury et al., 2000). The reorganization and its resulting fibril structure depend on the precise details of growth. Petkova et al. have shown that fibrils formed under quiescent condition, differ in morphology and also have significantly different toxicities in neuronal cell cultures compared to non-quiescent condition (Petkova et al., 2005). Interestingly, the different structural motifs are conserved upon seeding

independent from the condition and are different in their toxic effect on neuronal cells. This finding prompted Paravastu et al. to investigate the structure of Aβ1-40 fibrils produced by seeded growing from fibrils extracted from brain tissue of deceased AD patients (Paravastu et al., 2009). They found that this fibrils formed from brain aggregates are different to the fibrils formed in-vitro. The determination of the fibril structure has been an unusually difficult task because Aβ preferentially form amyloid fibrils rather than protein crystals. Solid-state NMR studies have revealed that Aβ fibrils could comprise β-strands organised in a parallel, in-register fashion (Nelson and Eisenberg, 2006) or form parallel β-sheets between residue 12–24 and 30–40 connected by a turn involving residues 25–29 (Tycko, 2006). This is also determined to be the most likely structure when experimental X-ray diffraction patterns were compared to calculated diffraction patterns (Jahn et al., 2009). Recently the supramolecular structure of Aβ1-42 fibrils were probed by cryo-EM and real-space reconstruction method (Zhang et al., 2009). The findings suggests that 2 protofilaments wind around a hollow core and that, to the contrary of Aβ1-40 fibril models, the C-terminus forms the inside wall of the hollow core, which was supported by partial proteolysis analysis. Nevertheless the turn is still present in the monomer. In another model it was suggested that cross-β sheet pairing between two extended monomers which resembled the recently proposed steric zipper model (Sawaya et al., 2007) form the core of the fibril (Schmidt et al., 2009)

1.2.4 Other Aβ oligomers

The importance of the Aβ hexamer as a building block comes from the observation that at least four diverse assemblies, Aβ derived diffusible ligands ADDLs (Lambert et al., 1998), A*56 (Lesne et al., 2006),"globulomers," (Barghorn et al., 2005b) and "AβO" (Kayed et al., 2003) comprise multiples of this basic unit.

Even though, some controversy about the size of ADDLs exists in literature, it is now becoming clear that they are composed of two hexameric units (dodecamer) (Chromy et

al., 2003; Hepler et al., 2006). ADDLs were found to kill mature neurons in hippocampal slice cultures and are produced in vitro from Aβ1-42 under special solvent conditions (Lambert et al., 1998; Stine et al., 2003).

The 56 kDa "A*56" oligomer which is consistent with a dodecamer, was identified in SDS extracts from brains of Tg2576 transgenic mice.

A third type of dodecamer is the globulomer (a globular oligomer). This Aβ1-42 derived oligomer is formed in the presence of SDS close to the critical micelle formation concentration of SDS (Barghorn et al., 2005b). Protease digestion, antibody binding, mass spectrometry and NMR studies of globulomers (Yu et al., 2009) soluble forms have a mixed parallel and antiparallel β-sheet which are different to the structure of the monomer inside the fibril. Although the secondary structure of globulomers is mainly β-sheet, they are not ThT sensitive and do not form fibrils (Gellermann et al., 2008; Rangachari et al., 2007). This suggests that this oligomer is an off-pathway assembly. A 90 kDa larger species, the A oligomer, also has been produced in vitro. That assembly is consistent with that of an octadecamer.

1.2.5 Mutations in AD and early onset of the disease

Early-onset Alzheimer's disease is the term used for cases of AD diagnosed before the age of 65 (Miyoshi, 2009). It is uncommon and accounts for only 5-10% of the cases. Approximately half of them are Familial Alzheimer's disease (FAD), where a genetic mutation, mainly inherited in an autosomal dominant fashion, leads to the disease.

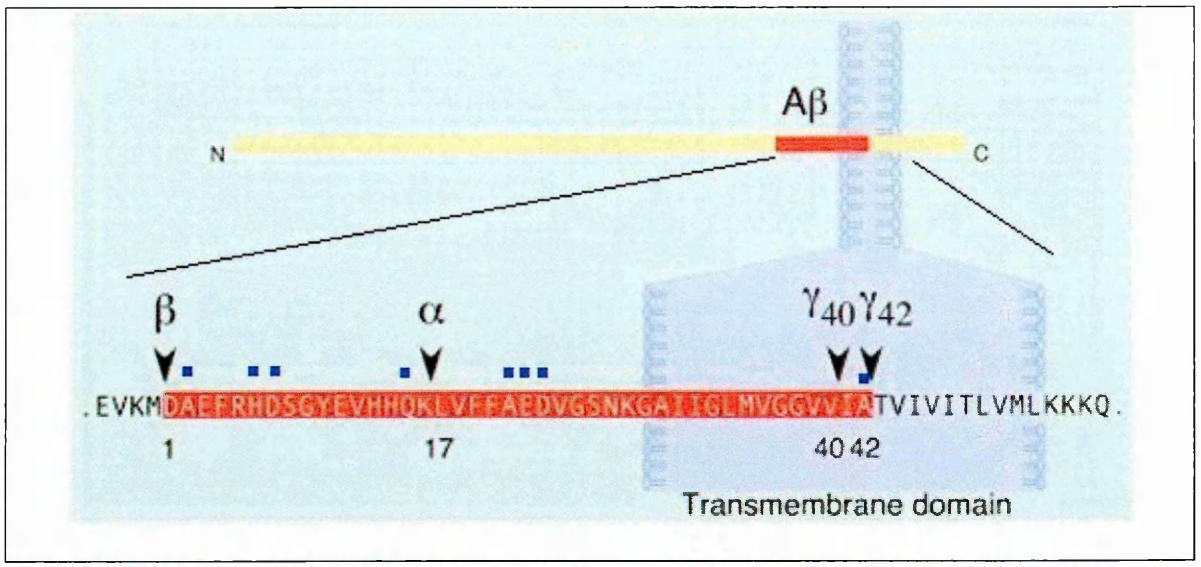

Fig. 1-9: The cleavage sites and loci of mutation of the Aβ sequence. (Thinakaran and Koo, 2008)

The blue dots indicate the amino acid were mutational variants were discovered.

Besides missense mutations in presenilins 1 and 2 gene, alteration of the APP gene has been linked to FAD (Fig. 1-9) (Goate et al., 1991; Levy-Lahad et al., 1995; Sherrington et al., 1995). Mutations in APP generally increase the ratio of the Aβ1-42/Aβ1-40, the amount of fragments produced (e.g. Swedish APP double mutation increases the overall production of Aβ by enhancing β-secretase cleavage) or increases the aggregation propensity of one of the fragments. Most intra- Aβ amino acid substitutions affect peptide self-association. For example, the Arctic mutation that causes an E22G substitution and early-onset FAD enhances the formation of protofibrils (Nilsberth et al., 2001) and fibrils of Aβ in vitro (Murakami et al., 2002) and the deposition of Aβ in vivo in the brains of transgenic mice (Cheng et al., 2004; Lord et al., 2006). The Dutch (E22Q), Italian (E22K), or Iowa (D23N) mutations have been shown to enhance the formation of protofibrils or fibrils from Aβ in vitro (Miravalle et al., 2000; Van Nostrand et al., 2001; Walsh et al., 1997) and produce parenchymal or vascular Aβ deposits in the brains of transgenic mice (Davis et al., 2004; Herzig et al., 2004). Taken together, the intra-Aβ mutations at position 22, 23 appear to enhance the deposition of Aβ by increasing the propensity of Aβ to aggregate whereas the terminal mutation enhance cleavage of Aβ fragments or change the ratio between Aβ1-40/Aβ1-42. A combination of these two properties is seen in recently

discovered recessive mutation in the N-terminus of Aβ (A2V) where the production of the Aβ fragments is increased and also the kinetics of fibril formation is accelerated (Di Fede et al., 2009). On the contrary, fibril formation was omitted and the formation of oligomers enhanced by the deletion of amino acid G22. These Aβ oligomers accumulate intracellular, cause endoplasmic reticulum stress-induced apoptosis in cultured cells (Nishitsuji et al., 2009) and are rich in β-sheet structure (Wang et al., 2009).

1.2.6 Surface-induced formation of Aβ assemblies

Surface properties such as hydrophilicity can influence the aggregation of Aβ (Kowalewski and Holtzman, 1999). Kowalewski et al. found that oligomeric Aβ1-42 formed mobile, nanoscale pseudomicellar aggregates on mica, and uniform, elongated sheets oriented along the crystallographic axis reminiscent of protofibrillar species of the graphite surface. This suggests that both hydrophilic and hydrophobic surface interactions at the cell membrane may influence aggregation and toxicity.

Besides interaction of Aβ with phospholipids (McLaurin and Chakrabartty, 1997), gangliosides (McLaurin et al., 1998) and cholesterol (Yip et al., 2001), membrane mimicking compounds like SDS have shown the influence on the assembly formation and toxicity Aβ aggregates (Barghorn et al., 2005b; Rangachari et al., 2007; Rangachari et al., 2006; Tew et al., 2008)

1.2.7 Metals in AD

Neurodegenerative diseases are associated to misbehaviour of the metabolism of metal ions. Although several biological transition metals can precipitate Aβ (Barnham and Bush, 2008; Ha et al., 2007), only copper and zinc, which are released during glutamatergic activity, have been found to directly bind Aβ in plaques (Dong et al., 2003; Opazo et al., 2002), which contain highly enriched concentrations of zinc, copper (Stoltenberg et al., 2005) and iron as ferritin complex (Quintana et al., 2006). There is clear evidence that metal ions mediate the oxidative stress mechanism of Aβ and form Reactive Oxygen

Species (ROS) such as hydrogen peroxide (H_2O_2) (Allsop et al., 2008). As a result marked oxidative injuries occur, that include protein DNA and RNA oxidations and lipid peroxidation (Butterfield et al., 2007).

Aβ has a strong positive reduction potential and displays high-affinity binding for Cu^{2+}, Zn^{2+}, and Fe^{3+} ions (Kawahara et al., 1997). Solution-state NMR and EPR have suggested that the three His residues in Aβ, (His6, His13, and His14), coordinate Cu^{2+}. The Aβ coordination of Cu and reduction of Cu^{2+} to Cu^{1+} leads to the generation of ROS. For instance, H_2O_2 is generated in the early phase of aggregation during protofibril or oligomer formation which later is converted to a reactive hydroxyl radical via Fenton chemistry (Allsop et al., 2008), which is accompanied by the oxidation of another moiety, such as cholesterol (Puglielli et al., 2005) or Aβ side-chains (Hureau and Faller, 2009). Electrospray ionization mass spectrometric analysis indicated the formation of methionine sulphoxide, methionine sulphone and related hydroxylated products which suggests that methionine 35 (Met35) could be a second centre of redox chemistry (Ali et al., 2005; Butterfield, 2003). Oxidation of Met35 in Aβ1-42 blocked paranucleus formation and produced oligomers indistinguishable in size and morphology from those produced by Aβ1-40 (Bitan et al., 2003b) and significantly reduced the rate of amyloid formation and alters fibril morphology (Hou et al., 2004).

1.3 Chemical synthesis of proteins

Solid phase peptide synthesis (SPPS) was first proposed by R.B. Merrifield in 1963 (Merrifield, 1963). Even though many proteins can be prepared by recombinant peptide synthesis, the chemical synthesis is a valuable tool. In particular, the formation of cytotoxic sequences or the incorporation of non-natural amino acids or other chemical building blocks is not possible without this technique. At present small proteins containing up to 60 amino acids can easily be prepared by linear SPPS. Longer peptides are prepared by the synthesis of small peptide fragments of the whole sequence and are later fused by fragment condensation (Chan et al., 2000). The principle of SPPS is shown in Fig. 1-10. For this a C-terminal unprotected amino acid is coupled to a linker who resides on a resin. Side chains and the Nα-amino function are protected by various groups. After the coupling the Nα-amino protecting group is removed and the next amino acid is attached to the sequence by peptide bond formation. The coupling is done eihter by ex-situ pre-activated Nα-protected amino (symmetric anhydride) or in-situ by activation of the C-terminus with guanidinium type coupling reagents (Marder and Albericio, 2004). In this way the whole sequence from the C- to the N-terminus is built in a stepwise manner, which will be cleaved from the resin in the end of the synthesis. Essentially two synthesis strategies are available. One is the by Merrifield proposed acid labile Boc/Bzl method and the other the base labile Fmoc/tBu, which uses orthogonal protection strategy. Furthermore, this procedure operates under milder conditions.

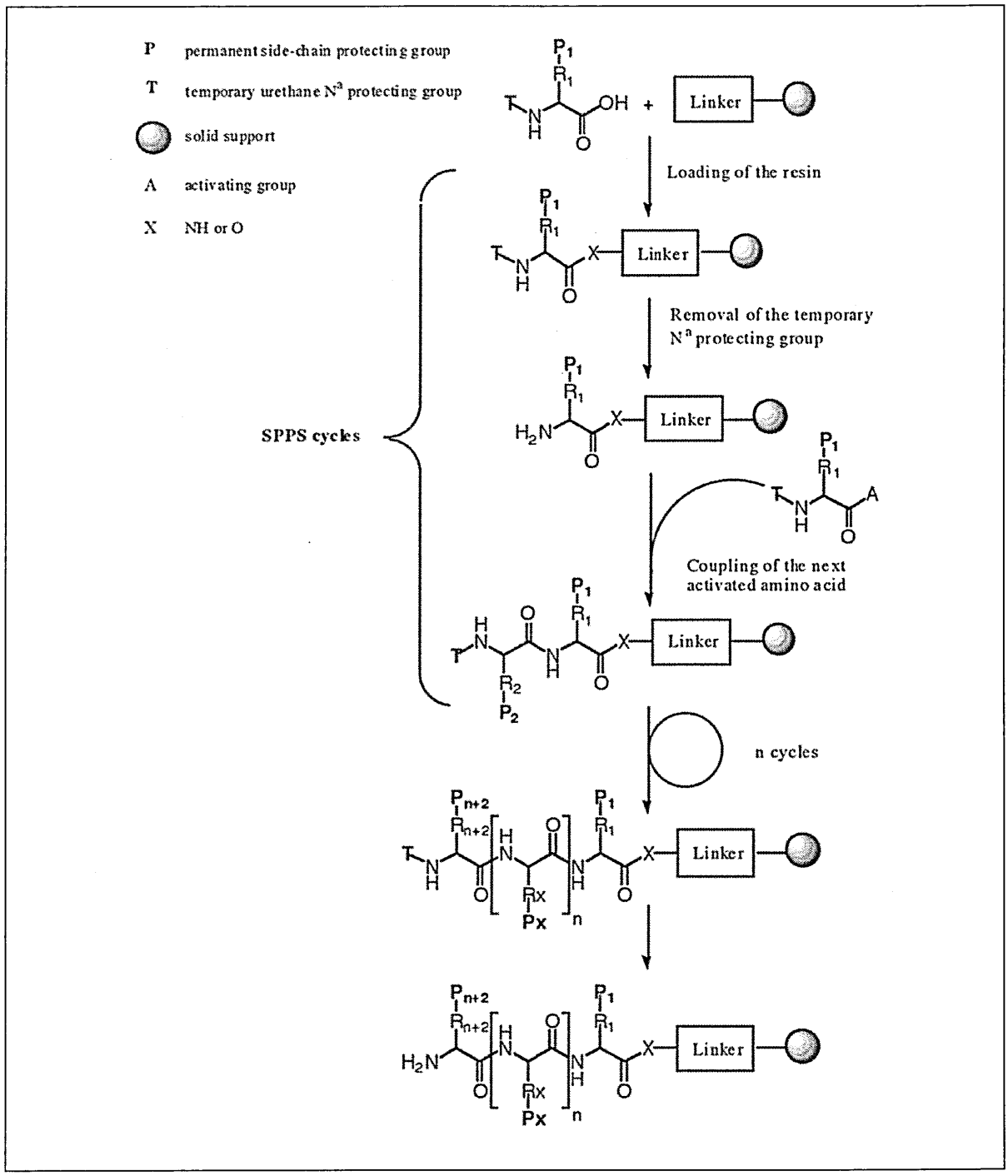

Fig. 1-10: Solid phase peptide synthesis (Amblard et al., 2006).

"Difficult sequence" has long frustrated chemists in their efforts to assemble peptides that contain such sequences by solid phase synthesis methods. Peptides containing β-sheet structures are thought to belong to this type of sequence. Possibly, these peptides are prone to form inter- or intra molecular interaction during the stepwise synthesis even in the presence of organic solvents. It is likely the formation of hydrogen bonds and the interaction between of hydrophobic side chain protection groups which are responsible for the poor salvation. As a result shrinkage of the resin, low reagent accessibility and the steric hindrance on the amino-terminus are observed. This could lead to incomplete acylation or cleavage of the Nα-protection group, which produces deletion or truncation sequences. This lowers the yield of the product or even makes the purification impossible. In the last 30 years progress has been made to overcome these problems.

Variation of the reaction condition made a lot of difficult sequences available to chemical synthesis. It was shown that changes in solvent composition, the use of chaotropic salts, variation of resin loading, more efficient reaction compounds (e.g. coupling and de-protection reagents) and elevated temperatures improve significantly the synthesis of difficult sequences (Tickler et al., 2004).

Problems are observed in the Fmoc chemistry as well as in the Merrifield methods. For instance, aggregation induced products formation which is reduced by in-situ neutralisation of the remaining Trifluoroacetic acid (TFA) after Boc-deprotection. This was later successfully translated to the Fmoc synthesis by washing the resin with an acidic solution just before the coupling step. This significant improvement could be due to the breakage of the amide hydrogen bonds. Nevertheless there is the risk that parts of the peptide and/or side chain protection groups are cleaved under this condition, which in turn reduces the purity and yield of the synthesis.

The observation that peptides containing Nα-alkyl-amino acids and Proline are often synthesised without difficulties led to the development of reversibly Na-alkylated amino

acids (Coin et al., 2007). Amide-protected building blocks, such as those shown in Fig. 1-11, can be used to improve the efficiency of Fmoc solid phase peptide synthesis of aggregation-prone sequences. Many of these building blocks are commercially available and are easily incorporated into the sequence during the automated peptide synthesis.

Fmoc-(FmocHmb)-AA-OH	Pseudo-Proline-Dipeptide	O-Acyl Isopeptide (depsi)
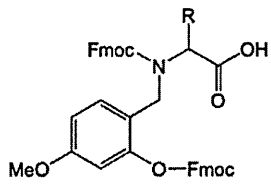	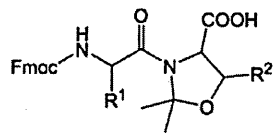	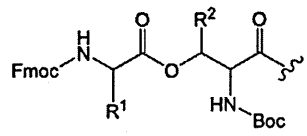

Fig. 1-11: Amide backbone modification strategies for the synthesis of difficult sequences.

These Na-alkylated amino acids are incorporated into the sequence instead of the non alkylated amino acids and reconverted into the native residue. For instance the 2-Hydroxy-4-methoxybenzyl (Hmb-) group disturbs the structure formation for the following six amino acids, improves in this way the salvation of the sequence and is removed from the sequence during the final TFA cleavage step.

Pseudoprolines developed by Manfred Mutters laboratory (Wöhr, 1995) are temporary cyclic protection building blocks for SPPS (Ser/Thr-derived oxazolidines or Cys-derived thiazolidines).They have similar to Proline the capability to disrupt secondary structure due to their restricted dihedral angles.

Another tool is depsipeptides. This new synthesis technique (the so called Depsipeptide-technique) requires, like the pseudoprolines, Ser/Thr/Cys to be present in the sequence. This technique has already been applied to Aβ1-42 (Sohma et al., 2007). As regards to the latter, in particular, the synthesis includes the formation of an ester bond between the side chain hydroxyl group of serine26 and the next incoming amino acid. Extreme care has to be taken in choosing the right experimental condition, since the presence of a strong base and the use of polar solvents lead to beta-elimination (formation of deletion sequences) and

chiral impurities of the final product. The native sequence of peptide is regained by an O-N intramolecular acyl migration step under neutral condition. Additionally to the capability to avoid the formation of secondary structures during the synthesis, it extremely improved the solubility of the peptide after the final cleavage step, since the depsipeptide remains stable as a TFA salt or under acidic condition. The resulting Depsi-Aβ1-42 is much more hydrophilic, with a 100-fold greater water solubility (15 mg/ml) compared to the native Aβ1-42 prepared by standard synthesis protocols (0.15 mg/ml) (Sohma et al., 2004b).

1.4 Disaggregation and peptide preparation

Many peptide preparations of Aβ1-40 can be contaminated with pre-existing aggregates (seeds) capable of acting as cytotoxic agents (Howlett et al., 1995), to accelerate the aggregation of the monomeric peptides (Evans et al., 1995), or as inhibitors of spontaneous aggregation (Wood et al., 1996). Numerous disaggregation methods have been described, which include filtration of dimethyl sulphoxide (DMSO) solutions (Evans et al., 1995), sequential, treatment with TFA and/or hexafluoroisopropanol (HFIP) (Bartolini et al., 2007; O'Nuallain et al., 2006; Wood et al., 1996; Zagorski et al., 1999), ultracentrifugation of aqueous solutions (Zhang et al., 2000), dissolution in basic aqueous solution followed by filtration or size exclusion chromatography (SEC) (Teplow, 2006). Disaggregation is a must, even if the experiment doesn't aim to investigate details of assembly kinetics and mechanism. This is due to the polymorphism in the fibril structure depending on the condition during preparation (Petkova et al., 2005; Tanaka et al., 2004).

Each method has potential advantages and disadvantages. One problem arises during the dissolution step of the peptide powder or peptide film in aqueous sodium hydroxide (NaOH) solution, since intense vortexing induces precipitation (O'Nuallain et al., 2006; Teplow, 2006). Bartolini et al. added acetonitrile (AcN) to the basic solution to circumvent this problem (Bartolini et al., 2007). They demonstrated that CD experiments designed to investigate the transition from random state to β-sheet were highly reproducible. Nevertheless, the velocity of the transition depended on the AcN concentration.

1.5 Aggregation inhibitors: A strategy in AD treatment

The available medications to treat AD fall into two classes, acetylcholinesterase inhibitors (donepezil, galantamine, rivastigmine, and tacrine) and N-methyl-d-aspartate (NMDA) antagonists (memantine). These drugs ameliorate the symptoms, but do not halt or reverse the illness. Many studies have postulated that the aggregation of Aβ in both soluble and insoluble forms in the brain is likely a key initiating factor in AD pathogenesis. Thus, controlling the aggregation process is a potential target. Great effort is undertaken to develop treatments which interfere with Aβ plaques and tau-based neurofibrillary tangles (Neugroschl and Sano, 2009). Amyloid-based therapies include γ-secretase inhibitors and modulators, BACE inhibitors, aggregation blockers, catabolism inducers, and anti-Aβ biologics (Fig. 1-12) (Barten and Albright, 2008).

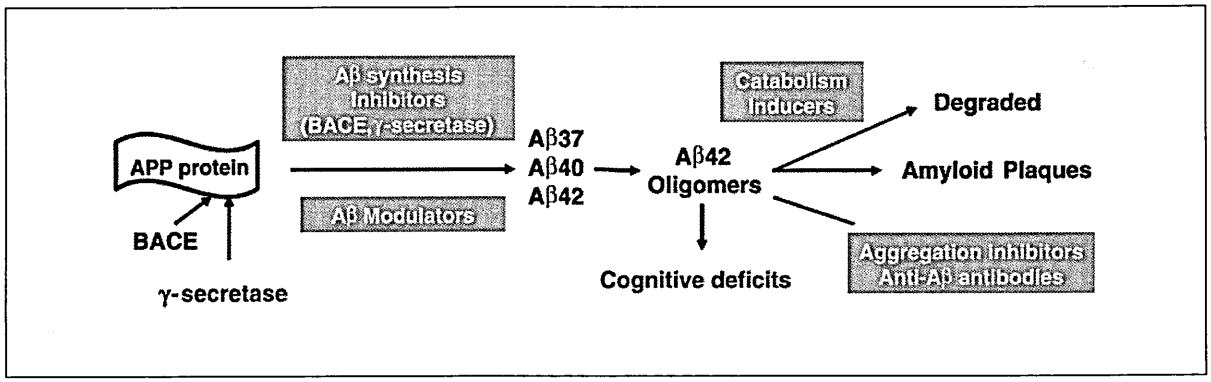

Fig. 1-12: Therapeutic strategies based on the "amyloid hypothesis"

A number of therapeutic strategies is currently being examined, both in the laboratory and in the clinic, which aim to reduce the amyloid load in the brain. These strategies can be broadly categorized as: (1) preventing or reducing the production of Aβ (pharmacological inhibitors of the enzymes responsible for APP metabolism), (2) direct or indirect targeting Aβ neurotoxicity, (3) preventing Aβ oligomerization and deposition, (4) enhancing Aβ degradation and (5) improving Aβ clearance from the brain across the blood-brain barrier (BBB) and into blood plasma.

There are numerous phases I and II clinical trials underway for a wide variety of new therapeutic approaches for the treatment of AD. Phase III clinical trials are in progress for γ-secretase inhibitors, an Aβ modulator, passive immunization of Aβ, and an Aβ aggregation inhibitor (Neugroschl and Sano, 2009).

Aβ aggregation inhibitor should stabilise a specific alloform (possibly the α-helical form) of the mainly disordered state of the monomer, resulting in complete blockage of oligomerization and fibril formation. Nerelius et al. showed for instance that compounds designed to interact with and stabilise the Aβ13–23 helix alter the aggregation properties of Aβ in vitro and reduce Aβ toxicity toward PC12 cells and hippocampal slice preparations (Nerelius et al., 2009). A second approach would be the stabilization of the less extended form of the Aβ monomer within the oligomer or in incoming monomers. But one requirement is that this strategy must not stabilise toxic oligomers, unless inhibitor binding blocks toxicity. Third, a complete destabilization of oligomers which are rich in β-sheet structure and higher in toxicity compared to monomer and fibrils could be a valuable strategy for inhibition of aggregation (Chimon et al., 2007; Roychaudhuri et al., 2009; Yu et al., 2009). And finally the dissociation of fibril could be used to decrease the amyloid burden in-vivo, but only if the formed assemblies are not toxic.

1.5.1 β-sheet binding compounds

Dyes like Congo red, chrysamine G, and Thioflavine S/T bind the cross-β-structure common to all amyloids (Fraser et al., 1992). Congo red attenuates fibrillogenesis, inhibits Aβ-induced toxicity, and reduces oligomeric Aβ production (Lorenzo and Yankner, 1994; Podlisny et al., 1995). Congo red possibly binds to the exposed N-terminal histidine residues (His13, His14) and influences in this way the fibrillogenesis (Inouye and Kirschner, 2000).

1.5.2 β-sheet breaker peptides

The determination of key residues important for aggregation led to the design of pentapeptide homologous of Aβ based on the hydrophobic residues of the CHC which inhibited fibril formation, by binding to Aβ40 to stabilise β-sheet structure (Esteras-Chopo et al., 2008; Tjernberg et al., 1997; Tjernberg et al., 1996). However, this so called "plaque busters" (Soto, 1999) are capable of self-associating into fibrils.

The potential for Proline residues to hinder β-sheet formation (Morimoto et al., 2004; Williams et al., 2004) led to the design of modified fragments of the CHC (LVFF to LVPP). This resulted in peptides which inhibit fibrillogenesis and disaggregate preformed fibrils in vitro (Soto et al., 1996)

Other inhibitors including the CHC recognition element, and additionally contained a disrupting element were probed. The inhibitor KLVFF-KKKKKK altered Aβ aggregation by altering aggregate morphology and kinetics, while protecting against Aβ-induced toxicity (Pallitto et al., 1999)

Because of the importance of hydrogen bonding in stabilizing β-sheet formation (Luhrs et al., 2005), the methylation of backbone amide nitrogen disrupted interstrand hydrogen bond formation and attenuated fibrillogenesis (Sciarretta et al., 2006). Alternatively, replacement of amide bonds with ester bonds also results in a monomeric, soluble peptide, which is capable of inhibiting aggregation and disaggregating preformed fibrils (Gordon et al., 2002). However, peptide inhibitors are not currently being pursued in clinical trials

1.5.3 Modulation of structural transitions

Several small molecules that inhibit the in vitro formation of amyloid fibrils from monomeric Aβ have been identified (Findeis, 2000; Hamaguchi et al., 2006; LeVine, 2007) Studies using quantitative measures of inhibition assembled from light scattering measurements, ThT fluorescence, or immunoassays have facilitated comparisons of inhibitory potential among different molecular structures (Dolphin et al., 2008; Ferrao-Gonzales et al., 2005; Howlett et al., 1999a; Howlett et al., 1999b; Ono et al., 2003; Reinke and Gestwicki, 2007; Simons et al., 2009). Most of these studies, however, have quantified the effect of small-molecule inhibitors on the overall extent of fibril formation without considering the high complexity and multitude of possible on-/off-pathways Aβ assemblies, like oligomers, protofibrils, and other soluble aggregates (LeVine, 2007; Necula et al., 2007b). Some small-molecule inhibitors selectively halt the formation of

mature Aβ fibrils from monomer without stopping the formation of soluble aggregates (Bohrmann et al., 2000) or the growth of preformed fibrils (LeVine, 2007). Alternatively, small-molecule inhibitors can promote fibril formation, inhibit ongoing fibril growth (Williams et al., 2005) or selectively inhibit different mechanisms of soluble aggregate growth (Moss et al., 2004). In addition, although some small molecules prevent both oligomer and fibril formation (De Felice et al., 2004; Howlett et al., 1999b; Necula et al., 2007b; Yang et al., 2005), other inhibitors halt the appearance of oligomers without altering mature fibril formation (Necula et al., 2007a) or, conversely, block the appearance of mature fibrils while permitting oligomer formation (Ferrao-Gonzales et al., 2005; Lashuel et al., 2002; Necula et al., 2007b). These qualitative studies suggest that small-molecule inhibitors of Aβ self-assembly can selectively act on various assembly pathways.

For example (−)-Epigallocatechin-3-gallate (EGCG) binds to natively unfolded Aβ, reduces ThT fluorescence, and promotes the assembly of large, spherical oligomers. EGCG redirects the aggregation to a disordered off-folding pathway that results in the formation of non-toxic amorphous aggregates which are unable to seed fibrillogenesis (Ehrnhoefer et al., 2008). Another compound is curcumin, the main constituent of the spice turmeric, whose extensive use is thought to account for the significantly lower prevalence of AD in the Asian Indian population (Ganguli et al., 2000). Curcumin inhibits fibril formation, extension, and destabilised preformed fibrils at nanomolar concentrations (Ono et al., 2004b). Furthermore it inhibits Aβ1-42 oligomer formation and toxicity in-vitro, and binds to plaques and reduces amyloid levels in-vivo (Yang et al., 2005).

1.5.4 Current clinical trials using aggregation modulators

The most promising compound in development was ionic compound 3-amino-1-propanesulfonic acid 3-APS, (also known as tramiprosate, homotaurine, and Alzhemed [Neurochem, Laval, Canada]. 3-APS was found to maintain Aβ in a non-fibrillar form, decreased Aβ deposition in transgenic mice, and significantly decreased the cerebral levels

of soluble and insoluble Aβ (Gervais et al., 2007). However, the phase 3 trial in the United States was reported as inconclusive, and the phase 3 trial in Europe was halted before the data were released. Currently another agent, scyllo-inositol, is in phase 2. It appears to bind oligomers of Aβ1-42, preventing them from damaging synapses (McLaurin et al., 2000; Sun et al., 2008b).

1.5.5 Tetracyclines (TCs): small compounds for AD treatment?

TCs have been shown to interact with assemblies of various non-sequence related proteins in peripheral and central amyloidosis in-vitro and in-vivo (reviewed by (Forloni et al., 2009) e.g. PrP^{Sc} and related fragments (Tagliavini et al., 2000), Aβ1-42 (Forloni et al., 2001), transthyretin (Cardoso et al., 2003; Cardoso and Saraiva, 2006), W7FW14F apomyoglobin (Malmo et al., 2006), amylin (Aitken et al., 2003), huntingtin (Smith et al., 2003) and α–synuclein (Ono and Yamada, 2006).

Various publications investigate the interaction of TCs with Aβ derived fragments in-vitro. Howlett et al. claimed that only RTC suppresses Aβ1-40 fibril formation effectively with an IC50 of 59 μM in a fibril-dependent immunoassay, whereas other compounds are less (OTC (34% of inhibition at 250 μM), TC (20% of inhibition at 250 μM)) or not effective at all (CTC, DMC, DC, MC) (Howlett et al., 1999b). Another study showed that TCs (TC and DC) not only inhibited the beta-amyloid aggregates formation but also disassembled the pre-formed fibrils of Aβ1-42 (Forloni et al., 2001). This capacity was determined by electron microscopy and quantified with ThT binding assay. The self-aggregation capacity was reduced by nearly 50% at a compound concentration of around 60 μM and 40% preformed fibrils were disassembled at 220 μM TCs concentration. Furthermore, the resistance of aggregates to trypsin digestion was reduced. The EC50 (effective concentration) for aggregation inhibition of TC determined via Thioflavine-T by Ono et al. was with 10 μM Aβ1-40 and 10 μM Aβ1-42 (Ono et al., 2004a) lower. TC showed also a greater potential in destabilization of preformed fibrils (EC50; 23 μM Aβ1-40 and 45 μM

Aβ1-42). Furthermore, the authors found that the extension of fibrils in a seeded reaction was suppressed. This suggests a direct interaction of TC with the β-amyloid structure. Support comes from the finding of Bartolini et al., where the slope of the exponential growth of β-sheet structures followed by CD was decreased in the presence of TC, but the lag phase did not change (Bartolini et al., 2007). An indirect method for the determination of binding potential of TCs was used by Inbar et al. (Inbar et al., 2008). They investigated the potential of molecules for their ability to associate with fibrils formed from synthetic Aβ peptides by monitoring their ability to inhibit the interaction of a monoclonal anti-Aβ IgG with these fibrils. OTC (IC50=144 μM), CTC (IC50=63 μM) and TC (IC50=8.2 μM) interfered with the binding of the antibody whereas DC and RTC didn't have an effect. Another study reported the use of X-ray fibre diffraction in characterizing the inhibition of Aβ fibrillogenesis (Kirschner et al., 2008). They investigated the effect of TC on the aggregation of Aβ (11-25) and Aβ (12-28) on the integral widths and integrated intensities of the two characteristic reflections at 4.7 Å and ~10 Å. They found that the volume of the β-crystallites is reduced in Aβ (12-28) and Aβ (11-25) using 6.93 mM TC but the coherent domain sizes along inter-sheet and H-bonding direction is not significantly altered (see Fig4 bottom in (Kirschner et al., 2008)). On the contrary, plaque formation by Aβ1-40 added to primary human macrophages was not impaired by addition of TC (Gellermann et al., 2006).

Presently, several studies are focused on the therapeutic potential of TCs, mainly MC in AD. Accumulation evidence suggests the neuroprotective effects of MC on AD models affecting various pathways, which underlines the potential for being an effective and safe AD therapeutics (Kim and Suh, 2009). It has been shown that MC reduces microgliosis, the expression of inducible nitric oxide synthase, caspase-1 activity, formation of interleukin 1b, metalloprotease activity, and production of cyclooxygenase and prostaglandins.

Table 1-2 Effects of Minocycline in AD (adapted from (Kim and Suh, 2009)).

APP transgenic mice:	suppress microglia production of IL–1β, IL-6, TNF-α (Seabrook et al., 2006) attenuate the increases in peIF2-α in hippocampus (Choi et al., 2007) attenuate cognitive impairment (Choi et al., 2007)
Adult human microglia:	downregulates pro-inflammatory cytokines (Familian et al., 2006; Rogers et al., 2002)
mu p75-saporin injected mice models	attenuates cholinergic cell loss, glial activation, transcription of downstream pro-inflammatory mediators (Hunter et al., 2004)
Aβ1-42 injected/infused rat models	inhibit neuronal cell death (Familian et al., 2007) decrease microglia and astrocyte numbers, COX-2 expression and 3-nytrosine (Familian et al., 2007; Ryu and McLarnon, 2006) attenuate the increases in peIF2-α in hippocampus (Choi et al., 2007)
Aβ 25-35 infused rat models	protect against alterations of somatostatin signalling pathways (Burgos-Ramos et al., 2008)

MC reduced also nitric oxide (NO) levels by inhibition of p38 activation (Lin et al., 2001). NOs and its derivative (reactive nitrogen species), also belonging to the group of ROS, are known to inhibit the mitochondrial respiration (Brown and Borutaite, 2006) which is thought to play an important role of mitochondrial dysfunction in the pathogenesis of AD, since NO levels are increased in PC12 cells and human embryonic kidney cells bearing the Swedish double mutation in the APP gene (Keil et al., 2004). Other TCs like TC have been found to decrease NO-levels as well (D'Agostino et al., 1998). In cultured rat cerebellar granule neurons treated with 6-hydroxydopamine, MC attenuated free-radical production and cell death (Lin et al., 2003), which could be realised by direct radical scavenging (Kraus et al., 2005). Nevertheless, the radical scavenging potential is greatest for MC and lowest for TC (MC>CTC>DC>>TC) which supports the finding that other pathways are affected by the compounds (D'Agostino et al., 1998; Kim and Suh, 2009).

1.6 Tetracycline

1.6.1 Nomenclature and structure

The Tetracyclines (TCs) are a group of structurally-related antibiotics and so named for their four ("tetra-") hydrocarbon rings ("-cycl-") derivation ("-ine"). They are a subclass of polyketides having an octahydrotetracene-2-carboxamide skeleton, substituted with many hydroxyl and other groups (Table 1-3).

Table 1-3. Chemical formula of various TCs.

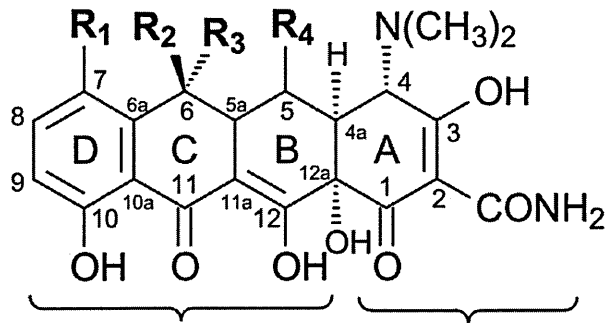

BCD-chromophore A-chromophore

Derivative	abbreviation	R1	R2	R3	R4	occurrence	
Tetracycline	TC	H	OH	CH3	H	n.o	
Oxytetracycline	OT	H	OH	CH3	OH	n.o.	
Chlorotetracycline	CTC	Cl	OH	CH3	H	n.o.	
Desmethylchlorotetracyline	DMCTC	Cl	OH	H	H	s.s.	
Doxycycline	DC	H	H	CH3	OH	s.s.	
Rolitetracyline	RTC	H	OH	CH3	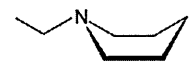	s.s.	
Minocycline	MC	N(CH3)2	H	H	H	s.s.	

Benjamin Mingo Duggar in Lederle Laboratries in Pearl River (US) discovered the first TC from a golden-coloured, fungus-like, soil-dwelling actinobacteria named Streptomyces aureofaciens in 1947 (Duggar, 1948). The substance was called Auromycine or also known as Chlorotetracycline (CTC). Terramycine was isolated in 1949 (Finlay et al., 1950) by

fermentation of the actinomycete, Streptomyces rimosus. The parent tetracycline (TC) itself was formed by catalytic hydrogenolysis of aureomycin in 1953 (Boothe et al., 1953), subsequently, this compound was prepared by cultivation of certain strains of Streptomyces albo-niger (Anderson, 1955). The first total synthesis of a TC derivative was done in 1962 (Conover et al., 1962). This compound is now called sancycline. Other members of the family with R2 or R4 = OH are much more difficult to synthesise because they are very sensitive to acid and base (Muxfeldt et al., 1979). This synthesis is linear, i.e. each step follows the previous one (D→A method); the authors did not report their percent yield, but if each of the 18 steps had produced an 80% yield, the overall yield would have been only 1.8%.

Because of the low yield and the high costs most TCs derivatives are normally produced from the fermentation products by a semi-synthetic route (Nelson et al., 2003). Although this approach has been somewhat effective, it is limited be the capacity of the TC skeleton to undergo chemical transformation (Martell and Boothe, 1967; Stephens et al., 1958). Recently Myers and co-workers report an efficient new pathway for the "total synthesis" of TCs with extraordinary flexibility, providing practical access to >50 TCs derivatives that would be difficult or impossible to prepare through the semi-synthetic approach (Sun et al., 2008a). This strategy involves the parallel preparation of the left (D ring) and the right (A and B ring) and the re-unification of these fragments close to the end of the synthesis, with concomitant formation of the central C ring (AB plus D method) (Charest et al., 2005; Sun et al., 2008a). Many of these new TCs would be very difficult or impossible to obtain through semi-synthesis. This finding could serve as a powerful discovery engine, but the clinical relevance of these derivatives remains to be seen.

1.6.2 Physical and chemical properties

Tetracycline is yellow, crystalline, odourless substance. Looking at the bonding properties of the ring carbon atoms of TC some statements about the conformational flexibility of the

molecule can be given. The aromatic D-ring is stiff. The flexibility of Ring B and C depends on the protonation of the 11, 12-β-dicarbonyl system and ring A is the most flexible. The conformation of ring A depends on the substitution with functional groups and their charges, as well as the capability to form H-bonds with functional groups on the BCD-chromophore. The latter is particularly true for the C4-dimethylamino group. The carbon atoms 4, 4a, 5, 5a, 6 und 12a are asymmetric and the molecules are separated by two characteristic chromophores: the A-chromophore and the BCD-chromophore. The UV-spectra of Tetracycline are pH dependant. The BCD-chromophore absorbs at 225, 285, 320 and 360 nm, whereas the A-chromophore absorbance is at 260 nm (Durckheimer, 1975). Hence the band at 275 nm is composed of the contribution of the different chromophores. OTC and TC have additionally a band at 360 nm, CTC at 370 nm, to which only the BCD-chromophore contributes (Dürckheimer, 1975). The free bases of the TCs make the molecule hardly soluble under physiological condition (1 mg/ml) (Durckheimer, 1975). TCs are amphoteric, because of the acidic groups and the basic dimethylamino-rest which let them form water-soluble, stable salts with bases and acids. Especially TC-Hydrochloride shows a high stability as a solid substance. The pH-value of the water solution is between 2-3 (Durckheimer, 1975). The free bases and hydrochlorides are well dissolved in alcohols and less soluble in organic solvents. TCs are instable in aqueous solution and are losing rapidly their antibiotic activity. The stability depends to a great extend on the pH-value and temperature and differs among the derivatives (Liang et al., 1998; Naggar et al., 1974a; Naggar et al., 1974b). Under acidic and neutral condition TC and OTC are more stable than CTC, whereas OTC is more stable under alkaline condition. The determination of the apparent acidity constants of TCs and the deduction of the macroscopic and microscopic pKa-values (Fig. 1-13) for the various functional groups is a valuable tool to predict the efficacy. The first deprotonation step of the cation, upon pH titration from pH 2 to pH 11, involves the tricarbonyl system composed of C1-C3 and Cam

(acid functional group **a**, pKa ~ 3.3). In a next step the β-keto-enol system at C11 and C12 is deprotonated (acid functional group c, pKa ~ 7.7) followed by a proton removal at the dimethyl ammonium group attached to C4 (basic functional group $\boldsymbol{bH^+}$, pKa ~ 9.6) (Colaizzi and Klink, 1969; Schmitt and Schneider, 2006; Schmitt et al., 2007). Duarte et al. allocated an additional pKa value of 12 to the phenol group at C10 atom (Duarte et al., 1999). Nevertheless, because of the varying substitution in the TC derivatives, the acidity constants of the molecules in a certain state of protonation can vary by several orders of magnitude depending on its actual conformation (geometry, tautomerism, hydrogen-bonding pattern).

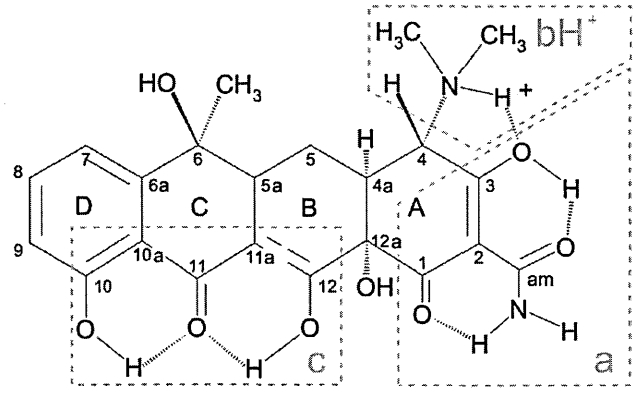

$$TcH_3^+ \rightleftharpoons TcH_2^0 + H^+ \rightleftharpoons TcH^- + 2H^+ \rightleftharpoons TcH^{2-} + 3H^+$$

Fig. 1-13: Acidic functional groups of Tetracycline a) C2 tricarbonyl system b) C4 Dimethylamino group (here bH+) protonated c) Keto-Enol-groupe of the BCD (Schmitt and Schneider, 2006).

NMR, CD and molecular dynamics studies suggested that two major conformations named "twisted" and "extended" (Fig. 1-14) exist in solution (Aleksandrov and Simonson, 2009; Lanig et al., 1999; Mitscher et al., 1968; Mitscher et al., 1972). These conformations differ in the relative positions of the carbon atoms C1-C12a and are governed by the various functional groups, solvent composition, metal complexation and pH (Mitscher et al., 1972). For instance NMR experiments combined with spectral data calculated using density functional theory suggest that tetracycline always prefers the extended conformation but that 5a,6-anhydrotetracycline exists in water as a mixture of the two conformers and in chloroform exclusively in the twisted conformation (Lanig et al., 1999). Schmitt et al.

confirmed the conformational changes during the pH titration by absorbance and fluorescence spectroscopy. Interestingly, they found that, if the crystalline material is dissolved directly at pH 2 or pH 11, the TC is in the extended conformation, but changes to twisted if the pH is changed from pH 2 to pH 11 (Schmitt and Schneider, 2006; Schmitt et al., 2007). Possibly the conformation influences the pharmaco-kinetic properties of tetracycline.

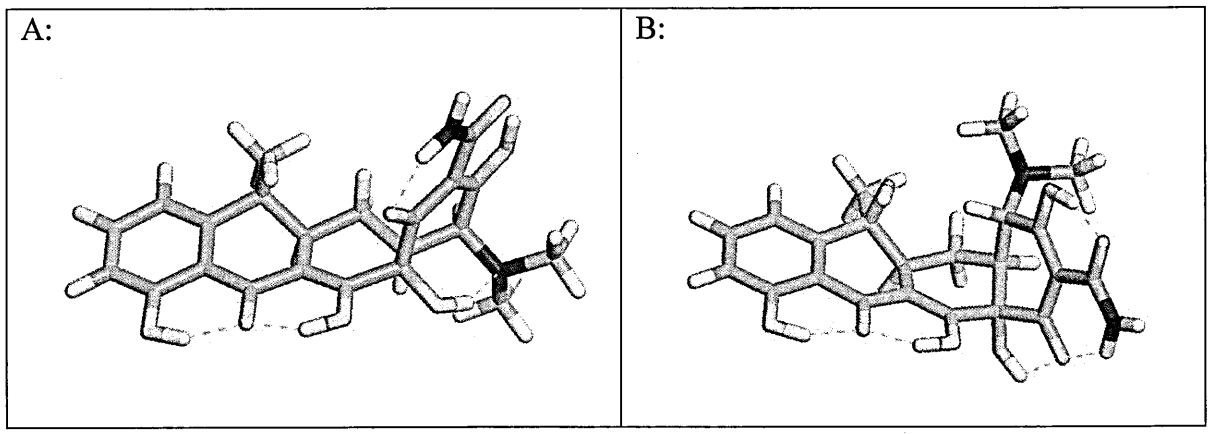

Fig. 1-14: The various structures of TCs A: extended B: twisted.

1.6.2.1 Complex formation

TCs are able to a reversible formation of antibiotic inactive complexes with anions and cations as well as with low- or high molecular substances (Durckheimer, 1975) (Table 1-4)

Table 1-4: Complexing agents for TCs (adapted from (Durckheimer, 1975).

Metal cation	Fe2+/3+, Cu2+, Ni2+, Co2+, Zn2+, Mn2+, Mg2+, Ca2+, Be2+, Al3+, Zr3+, Zr4+
anions	Phosphate, citrate, salicylate,p-hydroxybenzoate, saccharin anion
Natural compounds	caffeine, urea, thiourea, polyvinylpyrrolidone
Macro molecular substances	Serum albumin, lipoprotein, globuline, RNA

Whereas the hydrophobic TC, DC and MC scarcely form complexes, the hydrophilic compounds OTC, TC and RTC form a strong complex (Kuschinsky and Lüllmann, 1981). The stoichiometry ratio between the metal and the ligand (TCs) depends on the cation, its charge, and pH-value of the solution (Albert, 1953; Albert and Rees, 1956; Novak-Pekli et al., 1996). Below pH 3 no complexation is observed. The phenol-diketon-system of the BCD-ring binds a cation between pH 3 and 7.5. An additional cation can be bound between the dimethylamino-group and with respect to the former group cis-12a-Hydroxy-group above pH 7.5. In case of Anhydrotetracyline, 4-epi-tetracycline and iso-TC (involved in degradation and conversion of TC) are forming only a 1:1 complex (De Almeida et al., 1998; Durckheimer, 1975). OTC and metal cation form a chelat using ligand at 5 and 12a-Hydroxy-group above pH 7. The metal complex shows a characteristic UV spectra with a maxima at 275 nm and concentration dependant change between 370 nm and 390 nm. Wessels et al. found two isosbestic points during the Ca2+ titration, where the extinction coefficient doesn't change (Wessels et al., 1998). Furthermore, the TC fluorescence is sensitive to complexation (Schneider et al., 2003). That's why metals are

used for the qualitatively and quantitatively determination of the TC concentration. TC forms weak complexes with anions like phosphate and citrate, which increase the solubility of TC. The reversible binding capability of TC to macromolecules in blood and tissue is of great importance for efficacy and pharmacokinetic. Such equilibrium is quantitatively difficult to determine. TC binds to albumin, the constituent of the serum, as well as to the globulins and lipoproteins. The binding constant depends on pH-value and temperature. The effect of serum binding capability to the chemotherapeutic activity is up to date unknown (Durckheimer, 1975).

1.6.2.2 Rearrangement and Degradation

TC undergoes a series of rearrangement and degradation reaction depending on temperature and pH-value. There are distinct differences between the derivatives of TC (Halling-Sorensen et al., 2002; Soeborg et al., 2004). The conversion reactions are called isomerisation where the configuration changes but the chemical formula is the same. Isomerisation is in literature restricted to the alkaline conversion of TC to iso-TC and well distinguished to the epimerization and keto-enol-tautomerism. Besides the rearrangement the compound can be degraded by dehydration.

1.6.2.3 Epimerization

In weak acidic solution between pH 2 and 6 TC undergoes an isomerisation at C4 atom. This kind of configurationally changes, where more than one asymmetric C-atom is involved are called epimerization (Bryan et al., 1992). Epimerization follows a first order reaction mechanism. It is reversible and is catalyzed by phosphate, citrate and multivalent cations (McCormick et al., 1957). The equilibrium and the reaction velocity depend on the pH-value and the epimerization rate lies between 40% and 68%. Whereas below pH 1.5 no epimerization is observed, the epimerization rate increases with increasing pH-value (Hussar et al., 1968; Martinez and Shimoda, 1989; Remmers et al., 1963).

The epimerization products usually have a higher solubility compared to the parent compound and are more stable under alkaline and acidic condition (Brunner and Machek, 1962). Furthermore the configurationally changes have great impact on the antibiotic activity. Several publication described that the epimer has a by 90-99% lower antibiotic efficacy. This raises the question whether or not the epimer is active or the re-epimerization of the compound is responsible for this observation (Brunner and Machek, 1962; Hussar et al., 1968).

The epimers show a significant change in the UV-spectrum due to the chromophore A contribution. This difference was used to determine the amount of epimers in a solution by CD-spectroscopy (Brunner and Machek, 1962; McCormick et al., 1957).

1.6.2.4 Isomerisation

The alkaline treatment of TC leads to the C-ring opening by the hydroxyl-group at C6 attacking position 12 and the formation of phthalate structure (Brunner and Machek, 1962; Durckheimer, 1975). This reaction is irreversible. Whereas TC and OTC form isomers above pH 9-10, CTC forms the iso-CTC already at pH 7. These iso-TCs can rearrange to epimers under weak acidic condition.

The formation of iso-TCs is accompanied by the pH-dependant changes of the UV-absorption between 320-380nm (Kennedy et al., 1998). UV-absorbance of iso-TC is only present under alkaline condition and the fluorescence increases significantly and is used for analytical determination of TC (Blanchflower et al., 1989; Zhao et al., 1997).

1.6.2.5 Keto-Enol-Tautomery

TCs are able to form 64 distinct tautomeric forms depending on the pH-value (protonation state) and the polarity of the solvent. Duarte et al. demonstrated that the fully protonated state contains 9 structures (Duarte et al., 1999), whereas the equilibrium between these tautomers determine the real structure of the compound. Tautomeric rearrangement take

place on the C1-, C2- and C3-atom of the A-ring, on C10-, C10a-, and C11-atom of the CD-ring, and on C11-, C11a, and C12 atom of the BC-ring. Naidong et al. separate the first time tautomeric forms by chromatography and confirmed by NMR the changes in the C11-, C11a- and C12-atom (Weng et al., 1990). Basically the keto-enol-tautomerism is catalysed by acids and bases.

1.6.2.6 Dehydration

TCs containing a hydroxyl-group at C6-atom like CTC lose easily water below pH 1.5 and the C-ring gets aromatic (Durckheimer, 1975). This elimination reaction takes place because of the *trans*-position of the tertiary hydroxyl-group at C6 to the H-atom at C5a. This is an irreversible reaction second order. These formed Anhydro-TCs are able to form epi-Anhydro-TCs under weak acidic condition.

The changes in the BCD-ring upon dehydration affect the UV-absorption spectrum which shows a lower intensity in the wavelength range between 320 and 380 nm compared to the unmodified compound.

1.6.2.7 Pharmacology of the TCs

The different TCs derivatives show differences in enteral resorption, in plasma protein binding, elimination velocity, the expulsion pathway and their capability to form complexes (Zhanel et al., 2004).

CTC, TC, OTC and DMCTC are not fully absorbed and show low plasma protein binding (Schnappinger and Hillen, 1996; Zhanel et al., 2004). At variance the hydrophobic DC and MC show a full enteral absorption, a higher protein binding, a better diffusion in the tissue and a longer effective period (Zhanel et al., 2004). The complex formation capability can block the absorption and also leads to the accumulation of a potassium-phosphate-complex in the tissue which is containing an abundant amount of Ca2+ ions, as bones and teeth.

Other characteristics like half time and protein binding are summarised in Zhanel et al (Table VII)

2 Aim of the thesis

Two decades ago it was proposed that Alzheimer's disease was a consequence of the abnormal aggregation and deposition of the Aβ protein in the brains of affected individuals. Subsequent therapeutic approaches to halting the progression of the disease preventing the aggregation or oligomerisation, has attracted much attention. To date, while many compounds show effectiveness at inhibiting amyloid beta aggregation in vitro, all have failed to produce any promise of clinical efficacy. Nevertheless TCs have shown their potential as drugs for AD treatment. Besides of their possible anti-amyloidogenic effect, they are in general neuroprotective, interfering with various biochemical pathways in the brain. Since some inconsistency is observed among the scientific literature about the anti-amyloidogenic effect, the aim of the studies reported in this thesis is to further clarify the mechanism of action. This will be done as follows:

1) to investigate the lack of reproducibility of sample preparation and formation of amyloid structures by synthetic Aβ peptides, found in initial experiments and by review of the literature.

2) then to devise methods of preparation of the Aβ peptides in different well-characterised state, which can then be induced to aggregate (polymerise) to give a consistent product and with well-defined and reproducible kinetics.

3) to use a range of biophysical methods (SPR, AFM, CD etc) for the characterisation of starting materials and products in terms of structure of products, and conformational properties of the starting material.

4) to establish methods for making well-defined amyloid seeds and to use them for the kinetic study of the addition of Aβ monomers.

5) to examine the fluorescence of TCs and CD in the presence of amyloid peptides, and to evaluate the ability of TCs to monitor amyloid formation because of the structural changes of the compound.

6) to verify the possibility of TCs as inhibitors of in vitro amyloid formation, and to investigate the mechanism in terms of kinetics and structure.

7) to perform in vivo studies of plaque formation in APP/PS1tg mice to evaluate the magnitude of any inhibitory effect of the presence of a typical TC.

8) to seek a coherent explanation of inconsistencies in previous reports compared to the work of this thesis.

3 Material and Methods

3.1 Material

All the chemicals in this work were purchased from Sigma-Aldrich (Italy) and used as such. Variations are explicitly addressed. Standard amino acids were kindly provided by Flamma inc. (Italy). Aqueous solutions were prepared by using double distilled ultrapure water (Milli-Q, Millipore)

3.2 Peptide Synthesis

3.2.1 Automated peptide synthesis

The solid state synthesis (Merrifield, 1965) of Aβ fragments were mainly done on a ABI 433A automated peptide synthesiser (Applied Biosystems, Foster City, US). Fmoc group as a α–amino protecting group and the producer supplied FastMoc 0.10 mmol chemistry option was used to synthesise the peptide chain. All automated synthesis steps were done at room temperature.

The first amino acid were attached to the linker on a TentaGel-resin (0.26 mmol/g, Novabiochem) by the DIC/NMI method (Coin et al., 2008) in DCM (5 ml) for 1x1 h. For this 155 mg Fmoc-Ala-OH (5 eq, 0.5 mmol) in case of depsi-Aβ1-42, 77.4 µl DIC (5 eq, 0.5 mmol) and 31.7 µl NMI (4 eq, 0.4 mmol) were used. The loading was checked by quantifying the amount of Fmoc after the removal from the protected amino acid (Gude et al., 2002).

Despite the guest host depsi-Aβ14-24, which was synthesised on NovaPEG Rink amide resin (loading = 0.44 mmol/g, Novabiochem), the C- and N-terminus were free. The Fmoc group were removed in a 22% piperidine/DMF (v/v) solution for 10 min. The formation of the peptide bond was established using 10 fold excess of the reagent compared to the peptide chemistry (1 mmol) and reaction mixture containing either TBTU or HCTU (Novabiochem) as coupling reaction and DIEA were left for 9 min under continuous stirring.

The Depsidipeptide Boc-Ser(Fmoc-Gly)-OH (Novabiochem) and the ester bond formation between Boc-Ser-OH and next incoming amino acid in depsi-Aβ14-24 were manual introduced. The remaining amino acids were coupled with the automated synthesiser. The peptide bound to the dry resin was cleaved and de-protected with reagent R (Huang and Rabenstein, 1999) for 3 h. The peptide was precipitated into cold diethylether and washed for three times. Purification was done with semi-preparative HPLC (C4 Water Symmetry 19x150 mm) using the solvent system (solvent A: H2O + 0.1 TFA, solvent B: H2O/CH3CN 98:2 + 0.08 % TFA). Purity was determined under similar condition using an analytical C4 Waters Symmetry (4.6x150 mm) column. Finally, the molecular mass of the final products were analyzed with a MALDI-TOF mass spectrometer (Bruker).

3.2.2 Manual peptide synthesis

Manual peptide synthesis were done for the first amino acid coupling and the introduction of the depsi-dipeptide or the ester bond formation. For this the resin was put into a fritted polypropylene syringe. The dipeptide building block was dissolved in DCM containing DIC/HOBt. The completeness of the reaction was checked by the Kaiser-Test (Chan et al., 2000; Kaiser et al., 1970). In case of the guest-host system depsi-Aβ14-24 the ester bond between Boc-Ser-OH and the following amino acid was formed on the resin using the DIC/NMI method (Coin et al., 2007). Following are listed all the necessary steps for the manual solid state peptide synthesis.

3.2.2.1 Condition for the various steps of peptide synthesis

Table 3-1: Condition for first coupling to Rink amide resin using guanidium based reagents.

Fmoc-AA-OH	5 eq
TBTU, HBTU	5 eq
DIEA	10 eq
in DMF or NMP 1 x or 3 x 30 min on a stirring wheel	

Table 3-2: Condition for first coupling to NovaPEG resin and ester bond formation between Boc-Ser-OH and the following AA on the resin by DIC/NMI method.

Fmoc-AA-OH	5 eq
DIC	5 eq
NMI	4 eq
in DCM (with a minute amount of DMF to dissolve the AA) 1 x 3 h on a stirring wheel	

Table 3-3: Condition for coupling of depsi-Dipeptide by DIC/HOBt method.

depsi-dipeptide	2.5 eq
DIC	2.5 eq
2 h of pre-activation in DCM (with a minute amount of DMF to dissolve HOBt), reaction 2 x 2 h on a stirring wheel	

Table 3-4: Condition for Fmoc deblocking.

Piperidine	20 % in DMF (v/v)
1x5 min and 1x10 min	

3.2.2.2 Kaisertest (Kaiser et al., 1970)

This test recognises free primary amines and gives an easy qualitative measure about the completeness of the peptide bond formation. For this a small amount of resin is taken, and washed with ethanol. After 10 µl of every solution (80 % phenol in ethanol, KCN in water/pyridine, 6% ninhydrine in ethanol) of the Kaiser-Test kid (Fluka) is added, mixed and incubated at 120°C for 5 min. The resin beads and the solution turn dark blue when free primary amine is present.

3.2.2.3 Determination of resin loading

The loading was checked by quantifying the amount of Fmoc removed from 10 mg of resin beads weighted into a 1.5 ml polypropylene vial (Eppendorf) (Gude et al., 2002). After washing the resin with DCM the residual solvent was evaporated (concentrator 5301, Eppendorf) for 15 min. Then the resin was dissolved in DMF and left under continuous movement on a stirring wheel for 30 min. After this 20 µl of DBU was added affording a solution of 2% DBU/DMF (v/v) and left under stirring for other 30 min. 500 µl of the solution was diluted in 50 ml pure AcN. A reference solution is prepared in the same manner but without addition of the resin. The amount of Fmoc-group was quantified by absorbance measurement at 294 nm (extinction coefficient 8794 M-1cm-1) using a UV/VIS-spectrometer (Lambda 19, Perkin Elmer) in a 1 cm quartz cuvette.

3.2.3 Kinetics of native sequence formation

Around 1 mg/ml of depsi-peptide was dissolved in the clicking solution. The reaction was stopped by acidification pH 2 with aqueous 0.1 M HCl at various time points. This solution was injected onto a HPLC column (C4 Water Symmetry 19x150 mm) using the solvent system (solvent A: H2O + 0.1 TFA, solvent B: H2O/CH3CN 98:2 + 0.08 % TFA).

3.3 In-vitro binding and kinetics of fibril formation studies

3.3.1 Thioflavine T (ThT) fluorescence

3.3.1.1 ThT measurements

ThT measurements were done using the spectra fluorimeter LS 50 B (Perkin Elmer). For this the 10 µL of peptide solution was mixed with 400 µL of 50 µM of ThT in 50 mM phosphate buffer, pH 7.4. The dye was excited at 440 nm and the emission was taken at 480 nm.

3.3.1.2 In-situ ThT kinetic experiments

Every sample containing 20 µM of ThT was measured in triplicate and incubated on a plate reader (M200 Infinity, Tecan) in a 96 wells containing black plate with flat transparent bottom (Cornig). The plate was orbitally (5 mm) shaken for 10 s every 10 min and ThT was excitated 440 nm and the emission was measured at 495 nm.

3.3.2 Circular Dichroism (CD) analysis

Circular Dichroism experiments were mainly used to determine the secondary structure of the various preparations of Aβ fragments. This includes the investigation and reproducibility of the initial solution as well as the time dependant changes in secondary structure. The far-UV CD spectra (190–260 nm) scans were obtained on a J-810 spectropolarimeter (Jaso) at varying temperature which was maintained by a Pelletier heating system. The solution was put into a 0.1 mm path length quartz cell and the scan speed was chosen depending on response time and bandwidth as suggested by Kelly et al.

(Kelly et al., 2005) (Table 3-5). The buffer spectrum was subtracted and the raw CD values converted to mean molar ellipticity.

Table 3-5: Parameters for CD spectrum scan and timecourse experiment to monitor the changes at 215 nm.

Parameter	Setting	Parameter	Setting
Sensitivity	100 mdeg	Sensitivity	100 mdeg
Wavelength	260-190 nm	Wavelength	215 nm
Data pitch	0.5 nm	Data pitch	5 s
Scan speed	100 nm/min	Response	8 s
Response	0.5 s	Bandwidth	1 nm
Bandwidth	1 nm	Time	10 h
Accumulation	10		

The random state to β–sheet conversion was determined by repeated scans at various time points during the incubation. The β–sheet characteristic CD-values at 215 nm were then extracted from the scans and used for kinetic evaluation. In some cases however kinetic data were obtained by continuously measuring CD value exclusively at 215 nm (Table 3-5). In some experiments the magnetic stirrer incorporated in the pelletier heating system was used to move the solution with small magnetic bead (3 mm) in a 1 cm cuvette. Since the bead was relatively small compared to the cuvette diameter large values of agitation speed was used (up to 1330 rpm)

3.3.3 CD spectra of Doxycycline (DC) depending on pH

DC was dissolved in water to give a concentration of 20 mM. This solution was diluted into 500 ml of 20 mM Stenhagen buffer (20 mM citric acid, 20 mM boric acid and 20 mM phosphoric acid) to give 20 µM DC which were adjusted to the desired pH of two by adding either 10 M HCl or 1 M NaOH. In order to minimise the dilution effects, 1 M NaOH used as titration agents were added with a 100 µl Eppendorf pipette. The pH step width was $\Delta pH \sim 0.33$. After the stabilization of the signal when $\Delta pH/\Delta t < 0.01$/min

was reached, a sample of the solution was transferred to a 1 cm and the CD spectra taken (500 nm - 200 nm) at 25°C

3.3.4 Titration of Aβ assemblies with ligands (TCs) by following changes in the CD bands upon ligand binding

Since TCs are rich in the CD spectra any changes in the structure or perturbation of the electronic configuration due to binding should be visible. In these experiments the TCs concentration is changed whereas the concentration of the Aβ assembly is constant. For this two solutions are prepared, where one contains the Aβ (solution 1) and the other the ligand + Aβ fragment (various species) (solution 2). An example is given in following table (Table 3-6), where the concentration of the TCs concentration is assumed to be 200 μM:

Table 3-6: Pipetting protocol to determine the changes in the CD spectrum upon ligand titration.

Vol. Solution 1 (μl)	Vol. Solution 2 (μl)	Vol. sum (μl)	ligand concentration (μM)
100	0	100	0
100	25	125	40
100	50	150	66.67
100	75	175	85.71
100	100	200	100

3.3.5 Fluorescence Microscopy

Fibrils were formed under acidic condition at a concentration of 150 μM and diluted into phosphate buffer pH 7.4 in the presence of various concentration of TC, ThT or X-34 (Ikonomovic et al., 2006). A drop was put onto a cover glass and immediately observed under the microscope (Olympus). Two filters were used (F1: excitation 330-385 nm and emission detected at wavelength greater than 420 nm for TCs; F2: excitation 400-440 nm, emission >475 nm) for ThT and X-34.

3.3.6 Atomic force microscopy (AFM)

Sample was diluted with water to a final concentration of 10 μM and incubated for 0.5-2 min on a freshly cleaved mica disk. Then, the disk was washed with water and dried under gentle nitrogen stream. After, the sample was mounted onto a Multimode AFM with a

NanoScope V controller (Veeco/Digital Instruments, Santa Barbara, CA) operating in Tapping Mode using standard phosphorous doped silica probes (Veeco). The scan speed was 1 Hz.

3.3.7 Size exclusion chromatography (SEC)

SEC was done on an FPLC apparatus (Biologic FPLC system, Biorad) equipped with a precision column pre-packed with Superdex 75 resin, with a separation range of 3-70 kDa (GE Healthcare). The mobile phase flow rate was set at 0.5 mL/min and the elution peaks were detected at 214 and 280 nm UV absorbance. The mobile phase was 25 mM phosphate buffer (pH 7.4). The column was calibrated using insulin chain B (3.5 kDa), ubiquitin (8.5 kDa), ribonuclease A (13.7 kDa), carbonic anhydrase (29.0 kDa), ovalbumin (43.0 kDa) and bovine serum albumin (67.0 kDa). The void volume was determined with Blue dextrane 2000 (2000 kDa) and each peptide solution was injected at a final concentration of 20 μM in a volume of 100 μL.

3.3.8 Surface Plasmon Resonance (SPR)

The SPR apparatus used for these studies (ProteOn XPR36, Biorad) has six parallel flow channels that can be used to uniformly immobilise strips of six "ligands" on the sensor surface. The fluidic system can automatically rotate 90° so that up to six different analytes can be injected, allowing to monitor simultaneously up to 36 individual molecular interactions in a single run on a single chip (Bravman et al., 2006). Aβ1-42 monomers and fibrils (either sonicated or not) were immobilised in parallel flow channels of the same GLC sensor chip (Biorad) using amine-coupling chemistry, as previously described (Cannon et al., 2004). Briefly, after surface activation the peptide solutions (10 μM in acetate buffer pH 4.0) were injected for 7 min at a flow rate of 30 μl/min, and the remaining activated groups were blocked with ethanolamine, pH 8.0. The final immobilization levels were about 3200 and 2300 Resonance Units (RU, 1 RU=1 pg protein/mm2) for fibrils and monomers, respectively. A "reference" surface was always

prepared in parallel using the same immobilization procedure but without the addition of the peptide.

After the 90° rotation of the fluidic system, analytes (Aβ1-42 monomers, the anti-Aβ antibody 6E10, or Congo-Red specifically recognizing β structures) were then injected over immobilised Aβ1-42 species and reference surface, for 2-5 min at a flow rate of 30 µl/min. At the end of the injection, the dissociation reaction was followed for at least 10 min. The running buffer, also used to dilute analytes, was phosphate-buffered saline containing 0.005% Tween 20, pH 7.4 (PBST, Biorad). All these assays were done at 25 °C.

The sensorgrams (time course of the SPR signal in RU) were normalised to a baseline value of 0. The signal observed in the surfaces immobilizing the peptides was corrected by subtracting the response observed in the reference surface. Parallel injections of vehicle alone allowed correcting for binding-independent responses (i.e. drift effects). The resulting sensorgrams were globally fitted using at first the Langmuir equation modelling the simplest 1:1 interaction. Aβ1-42 fibril growth by monomers addition was fitted by a three-step conformational change model similar to that previously described for Aβ1-40 (Cannon et al., 2004). The nonlinear least squares data analysis program CLAMP was used for the optimization problem (Myszka and Morton, 1998).

3.4 Toxicity of Aβ assemblies

3.4.1 Preparation of primary hippocampal neurons

Hippocampus was dissected from 2 days old rat pups and incubated with 200 units of papain (Sigma Aldrich) for 30 min at 34°C, treated with trypsin inhibitor (Sigma Aldrich) and mechanically dissociated. Neurons were then plated on 96-wells plate pre-coated with 25 µg/ml poli-D-lysine and maintained in B27/neurobasal (Life Technologies, Gaithersburg, MD) supplemented with 0,5 mM glutamine, 100 U/ml penicillin and 100 µg/ml streptomycin. Aβ peptides were added to cells after 12 days in culture, when neurons are mature and differentiate.

3.4.2 MTT assay

Cell viability was analyzed by measuring the conversion of the yellow, water-soluble thiazolyl blue tetrazolium bromide (Sigma Aldrich, #M5655) to the blue, water-insoluble formazan. Data are presented as the percentage of survival relative to untreated control cultures. All experiments were repeated at least three times using indipendent culture preparations.

3.5 Treatment of APP/PS1tg mice with DC

The APP/PS1tg mice were treated at 15 months of age for 20 days with 10 mg/kg/ml of DC, intraperitoneally. The plaque deposit after DC treatment compared to a control experiment (physiological solution) was examined. APP/PS1tg mice were IP anesthetised with equithesin and intracardially perfused with 4% PAF and their brains removed and, after sucrose cryo-protection, frozen and stored at -80°C. Thirty μm brain sections were cut using a Leica cryostat and left free-floating in PBS 1X in 24-well plates. After the treatment with 1% H_2O_2 (5 minutes, RT) and blocking solution (10% NGS in PBS 1X; 1h at RT) the slices were incubated with the 6E10 primary antibody (1:500; Signet; O/N, 4°C). Primary antibody incubation was followed by that with anti-mouse biotinylated secondary antibody (1:200; Vector Laboratories) for 1h at RT. Immunostaining was developed using the avidin-biotin kit (Vector Laboratories) and DAB/H_2O_2 reaction.

4 Results

4.1 The initial state and sample preparation

A highly reproducible initial state is essential for conducting and comparing kinetic experiments. In this chapter we systematically changed the synthesis and preparation procedure to obtain a reliable stock solution of Aβ1-40 or Aβ1-42 which then is used to prepare various Aβ1-42 assemblies like initial state, oligomers and fibrils. These assemblies are then characterised by various physico-chemico procedures.

4.1.1 The improvement in reproducibility of the initial state CD spectrum by use of depsi-Aβ

First we wanted to analyze the structural properties of Aβ1-40 prepared by conventional SPPS. For this, CD spectra of different Aβ1-40 (synthesised by conventional SPPS) preparations were determined. The solution was prepared by dissolution of the peptide powder in 10 mM NaOH to give a stock solution concentration of 300 μM and vortexed to bring the peptide into solution. Then, the stock solution was diluted to give 30 μM of peptide in PB pH 7.4. Fig. 4-1 A shows five spectra from five different preparations. All the spectra show statistical coil structure but varied significantly from each other. To exclude that the variability comes from the variation in peptide concentration, the concentration independent ratio between the CD value at 205 nm and 215 nm was calculated. The value of the ratio for Aβ1-40 prepared by conventional SPPS is 1.9 with a standard deviation (SD) which demonstrates the irreproducibility of the initial state spectra (Fig. 4-1 B). Since extensive vortexing during the dissolution step could be responsible for the formation of precipitate which could be responsible for the changes in the initial state spectra (O'Nuallain et al., 2006; Teplow, 2006), acetonitrile (AcN) was added to the NaOH solution (50 AcN:50 20 mM NaOH) (Bartolini et al., 2007). Beside of the reduction of SD, also the ratio decreased to give 1.7 (Fig. 4-1 B) and no extensive vortexing was needed to bring the peptide powder into solution. Since AcN induces a-helix formation (Bartolini et al., 2007), another route of stock solution preparation without vortexing was needed. For this the peptide synthesis strategy was changed. The relatively new depsi-peptide technique was utilised (Sohma and Kiso, 2006).

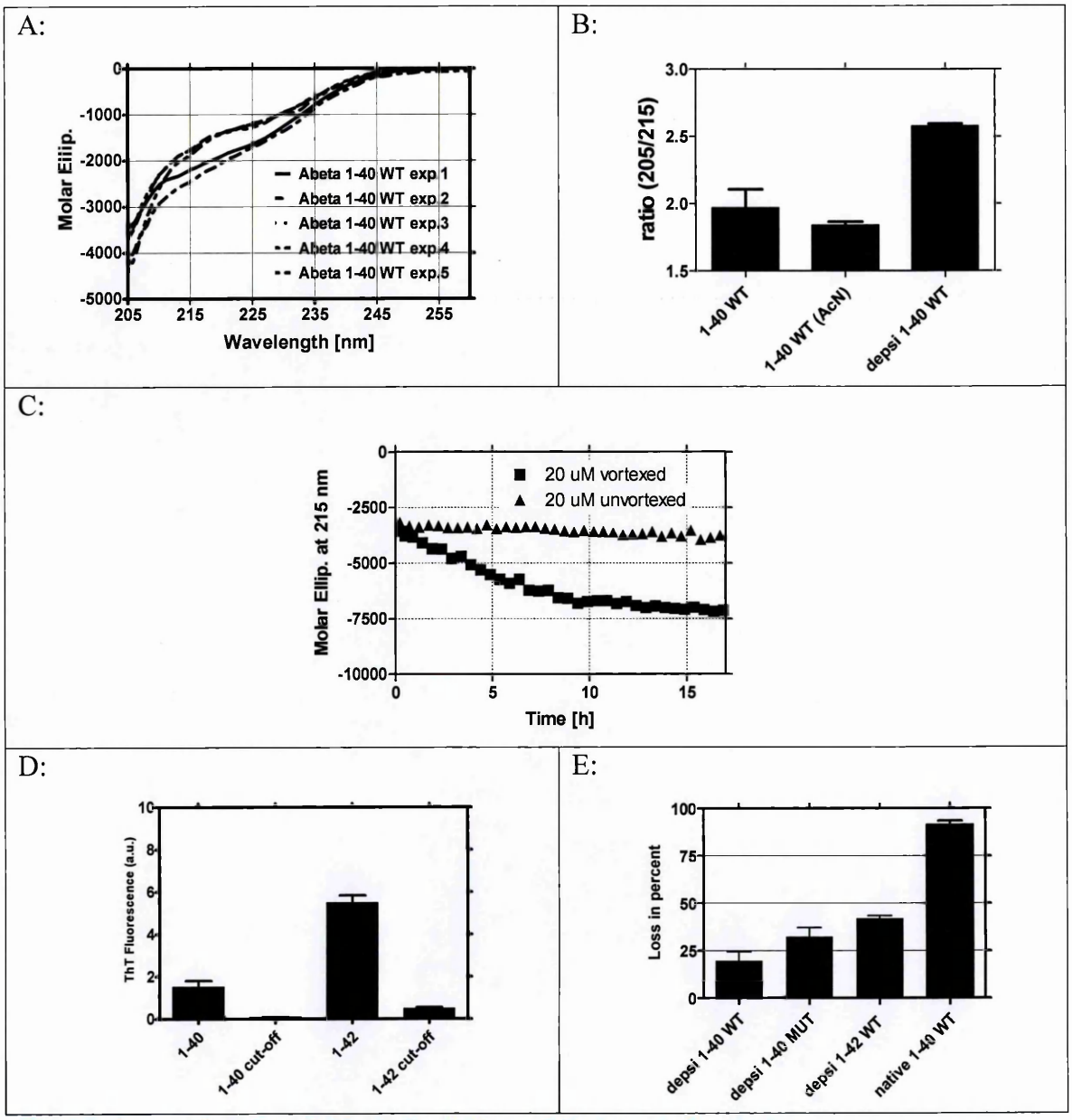

Fig. 4-1: Preparation of a reliable stock solution and the impact of vortexing

Panel A: Various CD experiments 30 µM Aβ1-40 synthesis by conventional SPPS in 50 mM PB pH 7.4 at 37°C to test the reproducibility of the initial state spectrum, for this the peptide powder was dissolved in 10 mM NaOH (peptide concentration 300 µM) and vortexed until full dissolution was reached, then the buffer was added and spectrum was taken. Panel B: Difference in the quality factor of three different preparations (peptide prepared by conventional peptide synthesis, column one = powder dissolved in 5 mM NaOH aqueous solution and column two = powder dissolved in 50:50 AcN:10mM NaOH and the depsi-Aβ1-40 dissolved in 0.02% water/TFA solution. Panel C: Comparison of the kinetic of β-sheet formation of in at 37°C, The extensive vortexed (5 min) or not vortexed high concentrated basic stock solution was diluted into 50 mM PB pH 7.4 to give 20 µM depsi-Aβ1-42 and incubated in 1 mm cuvette and the CD signal at 215 nm was monitored at 37°C. Panel D: ThT value of the depsi-Aβ1-40/1-42 stock solution (0.02% water/TFA solution) without and with the filtration through a 10 kDa cut-off filter. Panel E: Loss of material during the filtration of depsi-peptides and after the formation of the native sequence.

Especially notable is the fact that the ester bond increased the water solubility of Aβ1-42 by 100 times and furthermore blocked the aggregation of the peptide if kept under acidic condition (Sohma et al., 2004a). The native sequence is obtained by a pH shift at normally neutral pH.

Fig. 4-1 B shows an increase in the ratio to 2.6 and very low SD compared to the other two procedures. Like during the dissolution of the peptide powder in presence of AcN no vortexing was needed. To demonstrate that extensive vortexing is responsible for the irreproducibility or even formation of aggregates or precipitates, two different kinetic experiments were conducted where the changes of the β-sheet characteristic CD signal at 215 nm were monitored Fig. 4-1 C. Firstly a basic depsi-Aβ1-42 stock solution (300 μM) was prepared and diluted to 20 μM Aβ1-42 to give in PB pH 7.4 and incubated in a CD cuvette at 37°C. Secondly a 300 μM basic depsi-Aβ1-42 stock solution was extensively vortexed for 5 min and the kinetic was followed using the same sample condition like in the former experiment. Whereas the un-vortexed sample didn't show a significant change in the signal intensity, the vortexed sample immediately changes its value which indicates an immediate aggregation and β-sheet formation of the peptide.

After we had established the superiority of depsi-Aβ peptide over the peptide synthesised by conventional methods, all following experiments used the depsi-Aβ1-40 or depsi-Aβ1-42 where an ester bond is introduced between the Serine at position 27 and Glycine at position 26. Even though that the introduction of the ester bond in the turn of the monomer inhibits the intra molecular interaction which favour the aggregation, inter molecular contacts between two molecules which form fibrillar aggregates as well can't be excluded (Tuchscherer et al., 2007). Thioflavine T measurements show that a significant amount of fibrillar structure is present in the aqueous 0.02 % TFA solution (peptide is still in the depsi state Fig. 4-1 D) which is slightly higher for the more aggregation prone Aβ1-42 (5.5 AU) compared to Aβ1-40 (1.7 AU). Even though that these values are very low, any seed

present in the starting solution has an impact on the kinetic of fibril formation. That's why the aqueous 0.02 % TFA solution was filtered through a 10 kDa cut-off filter. For this, the peptide was dissolved in 0.02 % aqueous TFA at a concentration of around 1 mg/ml and was put on a cut-off filter (YM-10, Millipore). After the filtration was completed, the filter was washed with 100 µl with the same dissolution solution and filtered again. This was repeated once again. After, the concentration was determined and the loss of peptide during the procedure calculated. The ThT value was reduced for both Aβ variants (Aβ1-40 = 0 AU and Aβ1-42 = 0.5). Few amount of protein was lost during this procedure. In case of Aβ1-40 19.7 % and 42.15 % for Aβ1-42, which is very low compared to the nearly total loss of Aβ1-40 when filtered after the formation of the native sequence 91.5 % (Fig. 4-1 E).

The concentration of the stock solution was determined by measuring the absorbance at 280 nm of Tyrosine (ex. coeff. = 1280 $cm^{-1}M^{-1}$) putting the whole filtrate after cut-off filtration in 1 cm cuvette. Since the volume was not always sufficient, another technique was tried, where only a small amount of stock solution was utilised. Despite the use of the conventional colouring test (Bradfourd or BSA), the measurement of the absorbance at 214 nm was found to be a reliable method. For this the contributions of the amino acids to the absorbance and the peptide bonds were summed, like Kuipers et al. suggested (Kuipers and Gruppen, 2007) (Table 4-1).

Table 4-1: Extinction coefficient at 214 nm of various Aβ fragments based on the values suggested by Kuiper et al. (Kuipers and Gruppen, 2007).

Fragment	Extinction coeff. ($M^{-1}cm^{-1}$)
Aβ1-40 WT	75053
Aβ1-40 MUT	75064
Aβ1-42	76976
Aβ1-6 WT	15274
Aβ1-6 MUT	15285

The results obtained by measuring the absorbance at 280 nm (63.8 µM) or 214 nm (63.1 µM) of Aβ1-40 are nearly identical, only that the variability at 214 nm is slightly higher (Fig. 4-2).

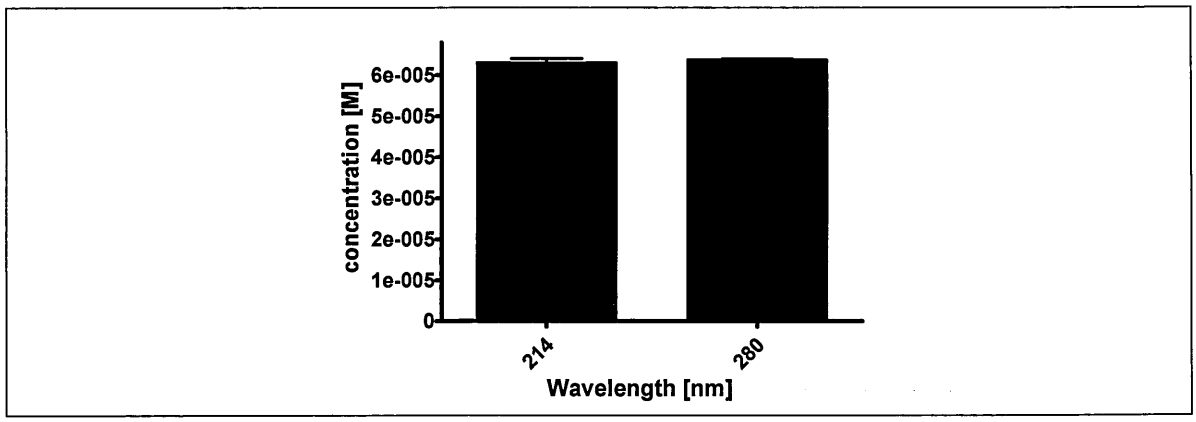

Fig. 4-2: Comparison of concentration determination of depsi-Aβ1-40 via absorbance measurements at 214 nm and 280 nm

Filtered Depsi-peptide in aqueous 0.02% TFA solution was put into a 1 cm cuvette and the absorbance was measured at 280 nm. To measure the absorbance at 214 nm 20 µl of the peptide solution were diluted in 700 µl aqueous 0.02 % TFA solution and the value taken when the stability of the value was reached after various homogenization steps by moving the solution with a 100 µl pipette.

4.1.2 The initial state of various Aβ fragments

Aβ1-40/1-42 are mainly unordered (statistical coil) structured peptides (Roychaudhuri et al., 2009). This was confirmed by measuring the initial state spectrum of the two sequences in PB pH 7.4 at 37°C (Fig. 4-3 A). Nevertheless the additional two amino acids in Aβ1-42 induce a small difference which is also visible if the ratio $CD_{(205\ nm/215\ nm)}$ between the fragments is compared (Aβ1-40 = 2.7 and Aβ1-42 = 2.3) (Fig. 4-3 B). This is probably due to the increase in β-sheet secondary structure of the monomer, which is demonstrated by the difference spectra between Aβ1-40 and Aβ1-42. The shape of the curve resembles a β-sheet spectra with a minimum at around 215 nm (Fig. 4-3 C).

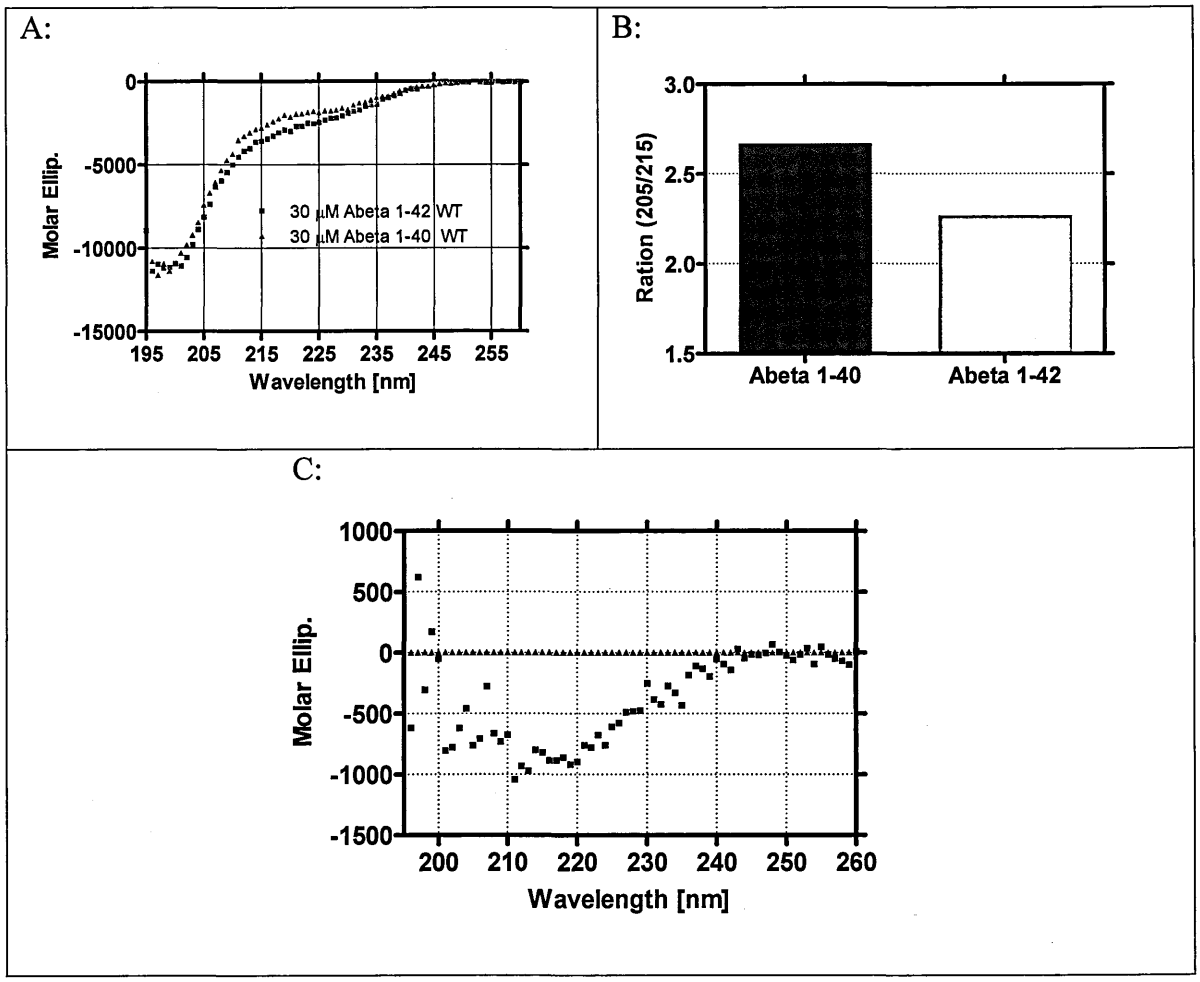

Fig. 4-3: The initial state of Aβ1-40 compared to Aβ1-42 in CD.

Panel A: Initial state CD spectra of 30 µM Aβ1-40/1-42 in 50 mM PB pH 7.4 at 37°C. Panel B: Ratio of the CD values at 205/215 nm for Aβ1-40/1-42. Panel C: difference spectrum CD (1-40)-CD (1-42).

Since mutations in a peptide sequence can alter the secondary structure of a peptide, the initial state CD spectrum of Aβ1-40 MUT of the recently discovered recessive mutation

(A2V) was measured. No such differences between the initial CD spectra were discovered, since both spectra Aβ1-40 WT and Aβ1-40 MUT (Fig. 4-4 A) and the two hexapeptides Aβ1-6 WT and Aβ1-6 WT of the N-terminus (termini free) (Fig. 4-4 B) are super-imposable. The hexapeptides contain a higher amount of unordered structure than the Aβ1-40 peptides, which can be seen by the maximum at 220 nm (Fig. 4-4 B).

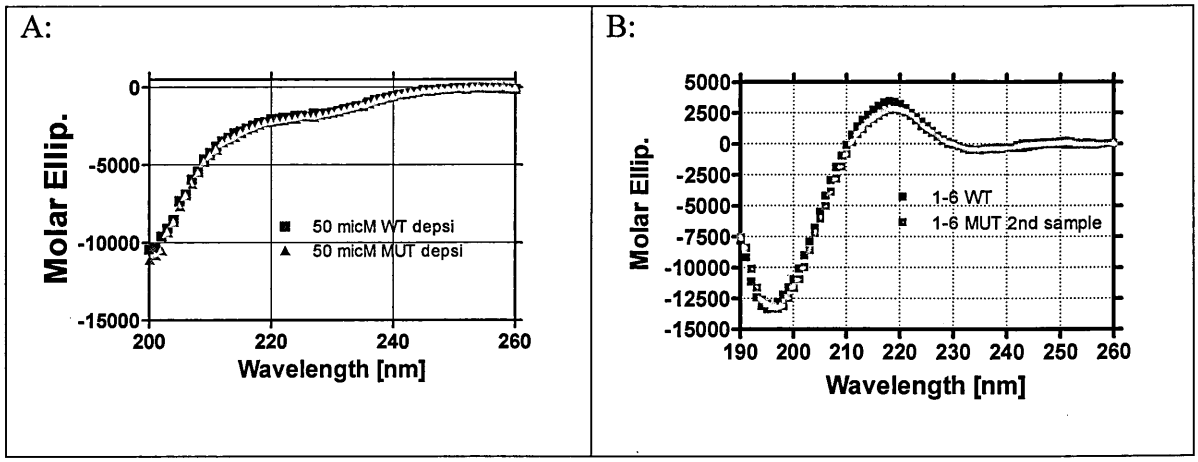

Fig. 4-4: The initial state of Aβ1-40 WT compared to Aβ1-40 MUT.

Panel A: CD spectra of 30 µM Aβ1-40 WT/MUT in 50 mM PB pH 7.4 at 37°C. Panel B: Comparison of the CD spectra of 200 µM Aβ 1-6 WT/MUT in 50 mM PB pH 7.4 at 37°C.

4.1.3 Native peptide formation: slightly basic condition permits the preparation of high concentrated Aβ stock solution

Normally the native sequence is obtained from the depsi-peptide at neutral pH. This takes around 2 h at room temperature or 15 min if the migration takes place at 37°C (Taniguchi et al., 2009). Drawback, especially in the case of Aβ1-42, is that, a stock solution concentration higher than 50 μM, the peptide immediately starts to form aggregates (Fig. 4-12 D). Since it is well known that basic condition stabilises and retards the Aβ peptide aggregation, we wanted to optimise the clicking condition by increasing slightly the pH, keeping in mind that hydrolysis of the ester bond could be an unwanted side reaction of this procedure. First we investigated the migration in 50 mM ammonium solution (Fig. 4-5 A) where after the indicated time points a aliquot was taken and acidified with some drops of 0.1 M HCl solution and separated by an analytical HPLC. Fig. 4-5 A shows the changes in the HPLC trace. The retention time increases by one minute for the native-Aβ1-40 (clicked) and the migration is completed after 30 min. The hydrolysis of the ester bond under basic condition produces two fragments which elute after 28 and 31 minutes (Fig. 4-5 B). The amount of these fragments is increased when 50 mM NaOH solution is used for the native sequence formation. Under this condition the purity of the peptide solution compared to the full length Aβ1-40 peptides drops under 95% (see Fig. 4-5 C). But most of the experiments require purity higher than 95 % we tried various ratios of the two bases. We found that the ratio smaller than 1:2 (NaOH to ammonium solution) is enough to gain the desired purity (see Fig. 4-5 C). Nevertheless, we used a ratio of 1:3 for the preparation of the native peptide sequence for all our experiments. Under this condition the migration is finished after 5 min at room temperature (Fig. 4-5 D). The fragmentation could be further reduced when smaller temperatures were used (e.g. on ice). But at the same time the incubation time must be increased since the migration kinetics is slowed down (data not shown). The exact procedures for sample preparation and native sequence formation taken from the results in the last paragraphs 4.1.1 - 4.1.3 are summarised in 7.3.

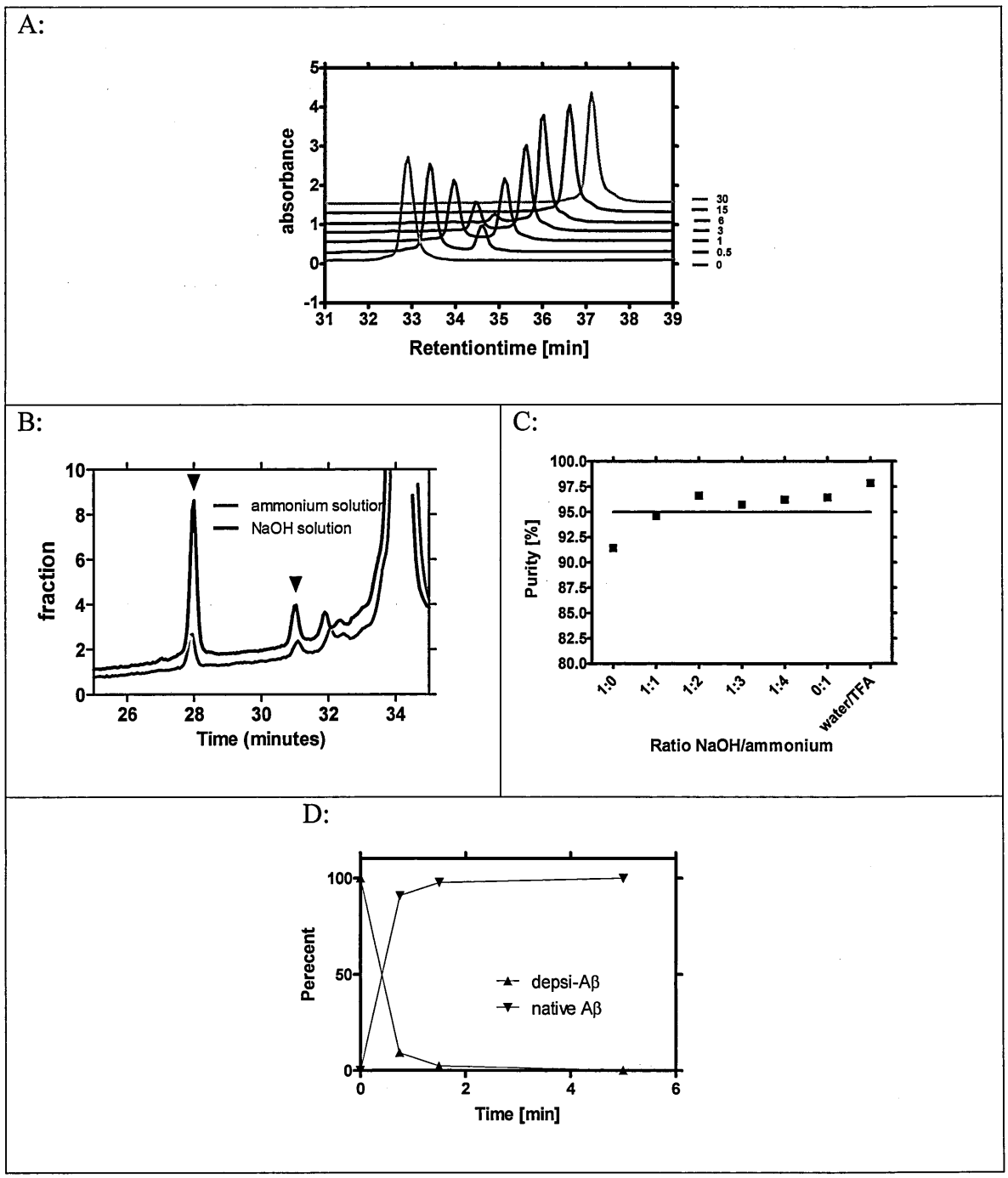

Fig. 4-5 Formation of the native sequence or the art of clicking.

The depsi-peptide Aβ1-40, originally in TFA 0.02%, was switched. Panel A: 50 mM ammonium solution, pH > 10.5 at RT. At the indicated time points, aliquots were taken and the switch reaction was stopped by dilution in 0.1M HCl solution. The amount of the various forms were determined by HPLC measurement, using an analytical C4 Waters Symmetry (4.6x150 mm) column (solvent A: H2O + 0.1 TFA, solvent B: H2O/CH3CN 98:2 + 0.08 % TFA). The area under peak was used to calculate the fractions of the different Aβ forms. Panel B: Formation of hydrolysis products in 50 mM ammonium solution or aqueous NaOH (50 mM) solution monitored by HPLC. Panel C: Purity in percent of the full length Aβ1-40 peptide solution depending on the ratio NaOH/ammonium solution. The purity was calculated determining AUC of Aβ1-40 peak compared to the overall area. Panel D: Timecourse of native peptide formation in 20 mM NaOH/ammonium (1:3) expressed in percent.

4.1.4 Preparation and characterization of specific Aβ1-42 assemblies (initial state, oligomers, fibrils)

The preparation of homogeneous peptide solution containing specific assemblies is essential for the investigation of the binding capacity of various ligands. For this we firstly prepared a solution, which was obtained shortly after formation, of native sequence with the aim to have the peptide at its very initial state. The other two solutions were prepared following the protocols described in the literature to obtain oligomers (Aβ derived diffusible ligands or ADDLs, (De Felice et al., 2008; Lambert et al., 1998)) or fibrils (Stine et al., 2003). We then used AFM, ThT, CD and SEC to analyze and compare the Aβ1-42 species present in these solutions. The results shown in Fig. 4-6 confirmed that the fresh peptide at its initial state was in random structure (CD), with negligible binding of ThT, no evident bigger assemblies by AFM and a single peak by SEC. The single peak in SEC at 30 min corresponds to a molecular weight of 12.3 kDa, which lies between the molecular mass of dimer and trimer of Aβ1-42 (Fig. 4-6 F). We also confirmed that the solution obtained by incubation of Aβ1-42 for 1-3 days at 37 °C under acidic conditions only contains well-structured Aβ1-42 fibrils (diameter = 3-4 nm) (Fig. 4-6E), with a very high ThT-signal (Fig. 4-6 D) and a characteristic β-sheet spectra in CD with a minimum at 215 nm (Fig. 4-6 B). SEC analysis indicated that most of the peptide was blocked by the filter at the top of the SEC column. Finally, the protocol developed to produce ADDLs (18h incubation in PBS, pH 7.4, at 4°C) actually resulted in a solution containing 2-3 nm aggregates and no evidence of fibrils or protofibrils. SEC highlighted the presence of a second minor peak appearing in the SEC void volume (>75 kDa) (Fig. 4-6 F), although the majority of the peptide is still in its initial state (Hepler et al., 2006). The small, but significant, ThT signal as well as CD spectra suggests that the few oligomers contain a similar structural motive like amyloid fibrils.

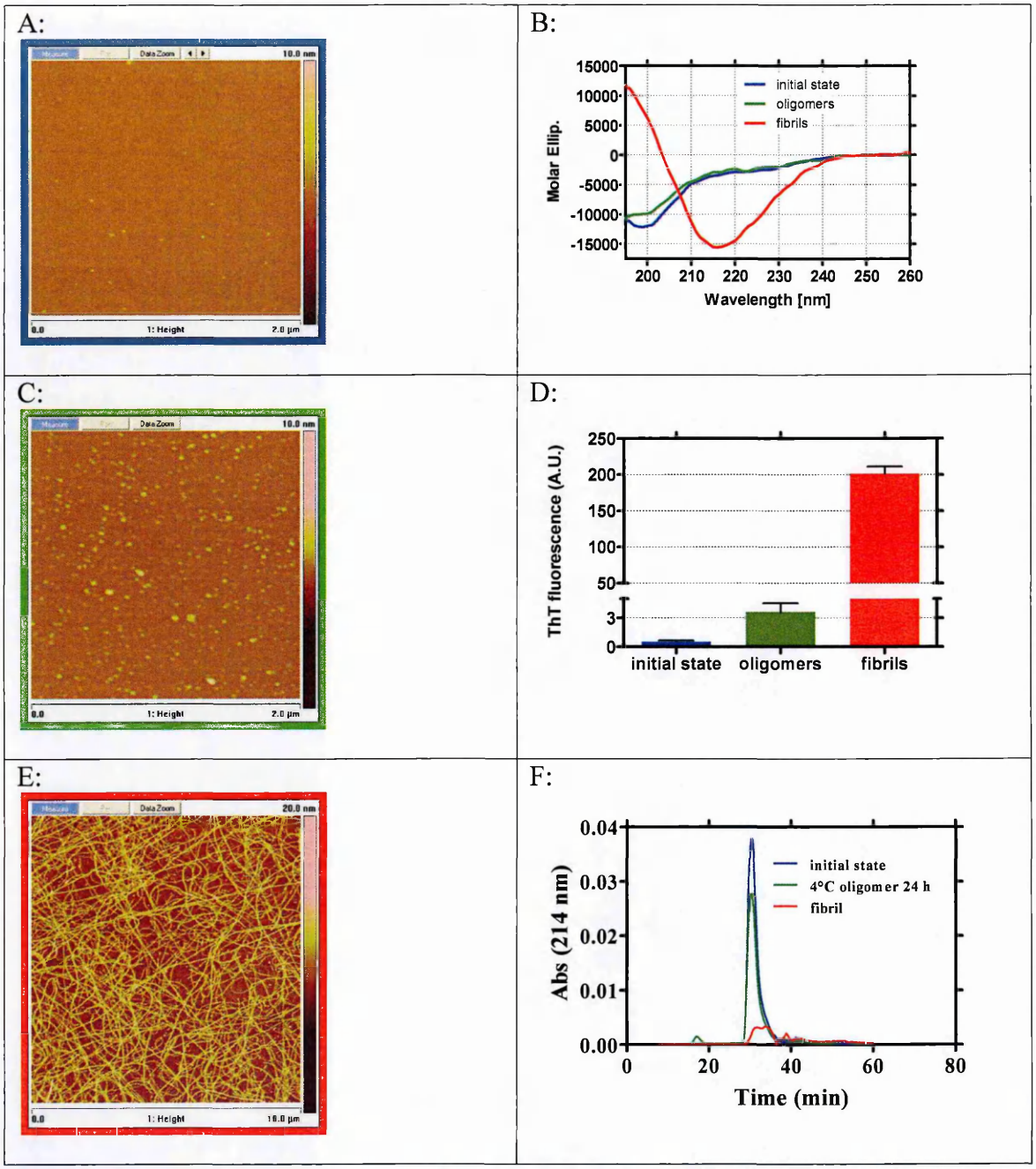

Fig. 4-6: Characterization of different species of native Aβ1-42 by AFM, CD, ThT, and SEC:

The acid solution of the depsi-peptide was switched to native $A\beta_{1-42}$ by raising the pH to > 10.5 for 15 min at 25°C. This solution was either: i) transferred to ice and used within 2h (initial state, blue); ii) diluted in 50 mM phosphate buffer pH 7.4 containing 150 mM NaCl to give 100 µM peptide and incubated at 4°C for 18 h (oligomers, green) or iii) diluted to give 100 µM peptide in 30 mM HCl (pH 2) and incubated at 37°C for 3 days (fibrils, red). Panel A, C, E: AFM analysis, the solutions were diluted to 10 µM in water, put on freshly cleaved mica and left there for 30 sec (fibrils) or 5 min. Samples were then washed with water, dried under N_2 and analyzed. Panel B: CD studies peptide solutions were diluted to a final concentration of 20µM and analyzed at 37°C. Panel D: ThT fluorescence was measured after addition of 50µM ThT to a solution containing 1 µM peptide (final concentration). The value for the "oligomeric" preparation was significantly different from that of the preparation at its initial state ($p<0.05$). Panel F: SEC, each peptide solution was injected at a final concentration of 20 µM.

Recently, it was proposed that the cellular prion protein (PrP^C) is the Aβ oligomer-receptor mediating Aβ-induced synaptic dysfunction (Lauren et al., 2009). Specifically, Aβ oligomers, prepared following the ADDL formation protocol but at a higher temperature (22°C), in hereafter following called 22°C oligomers, bound to PrP^C on the neuronal surface and inhibited long term potentiation (LTP) in hippocampal slices of wild-type (*Prnp*$^{+/+}$) but not PrP knockout (*Prnp*$^{0/0}$) mice. SEC indicated that, in this type of oligomer, most peptide was converted to high-molecular-weight aggregates (>75kDa; Fig. 4-7 A), which are spherical species and protofibrils confirmed by AFM (Fig. 4-7 B).

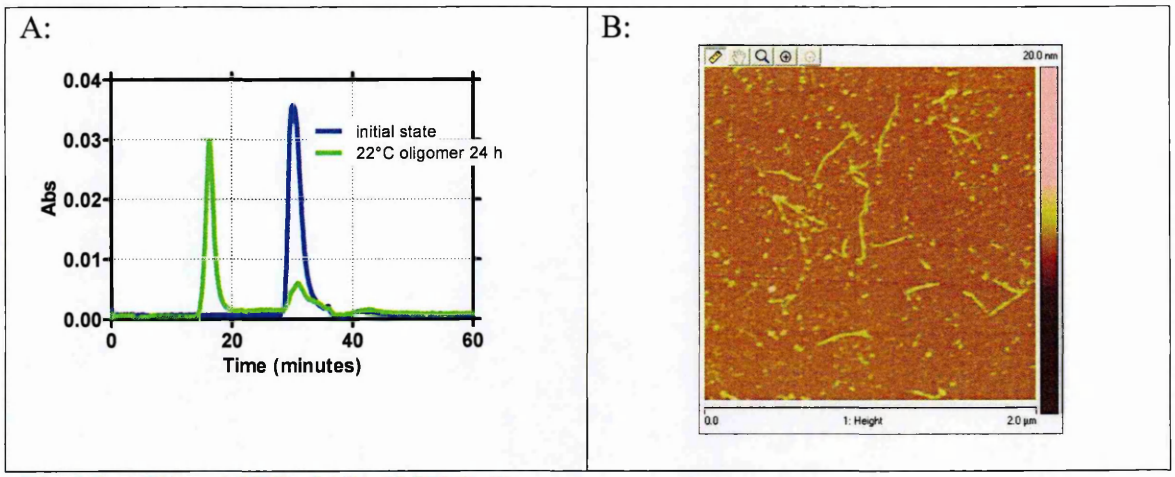

Fig. 4-7: AFM and SEC of Aβ1-42 22°C oligomers.

Panel A: SEC (running buffer 20 mM PB pH 7.4) of 20 µM off 22°C oligomer (green) and 20 µM initial state (blue). Panel B: AFM picture of the 22°C oligomer preparation (scan size 2 µm x 2 µm).

SPR showed that species present in the initial state and 22°C-oligomers solution of Aβ1-42 bind to the monoclonal antibody 6E10, which has an affinity to amino acid residues 1-17 of human β amyloid peptide, but did not bind to the pre-fibrillar oligomers detecting anti body A11 (Kayed et al., 2007; Kayed et al., 2003).

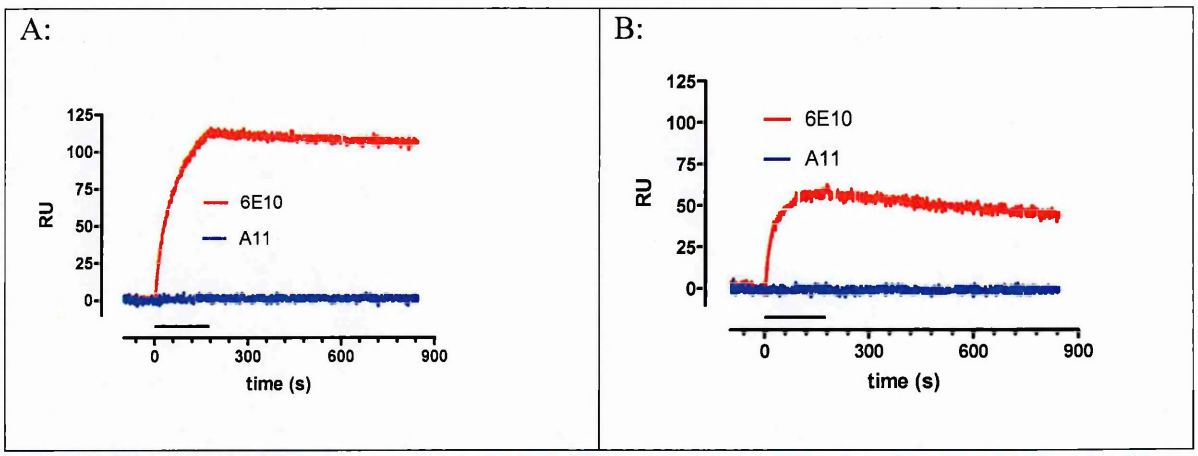

Fig. 4-8 Binding of Aβ1-42 monomers and 22°C oligomers to immobilised anti-bodies 6E10 and A11

Native stock solution samples were diluted to 1 µM in PBS and injected for 180 s and flown over the immobilized assemblies. Panel A: initial state. Panel B: 22°C oligomers.

The ligands can target different sites on the fibrils. To discriminate between fibril surface and fibril end binding we increased the amount of fibril ends by sonication. For this the fibrils grown under acidic condition were fragmented by a continuous ultrasound which was produced by a homogeniser.

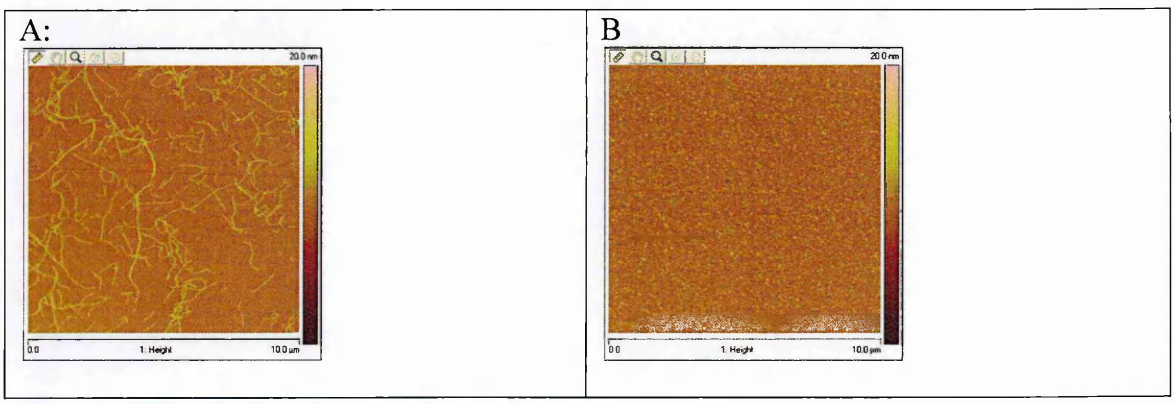

Fig. 4-9 AFM of fibrils before and after sonication

Fibrils formed under acidic condition (100 µM Aβ1-42 at pH 2 for 15 h). Panel A: Before the sonication. Panel B: After the sonication with a probe containing homogenizer probe (continuous ultrasound for five minutes at 10% intensity).

The ThT value of the sonicated fibrils (ThT = 198.2) were slightly higher than the un-sonicated fibrils (ThT = 190.5), indicating the binding to the fibril surface of the ligand.

4.1.5 Toxicity of the various assemblies on neuronal cells

To test the biological activity of these assemblies, we analyzed the effect of the various Aβ1-42 derived assemblies (initial state, ADDLs, 22°C oligomers, fibrils and sonicated fibrils) on rat hippocampal neurons grown in culture. Fully mature neurons (24 days) were treated with mixtures of Aβ1-42 assemblies at various concentration and incubated for 24 h. Fig. 4-10 A shows the concentration dependant cell toxicity of the initial state, ADDLs and 22°C oligomer solution. All show a similar IC50 of around 1 μM. The toxicity increased dramatically when the cells were treated with sonicated fibrils (IC50 around 0.02 μM) whereas the unsonicated fibrils only show a small deviation from the untreated sample, but more importantly no concentration dependence (Fig. 4-10 B).

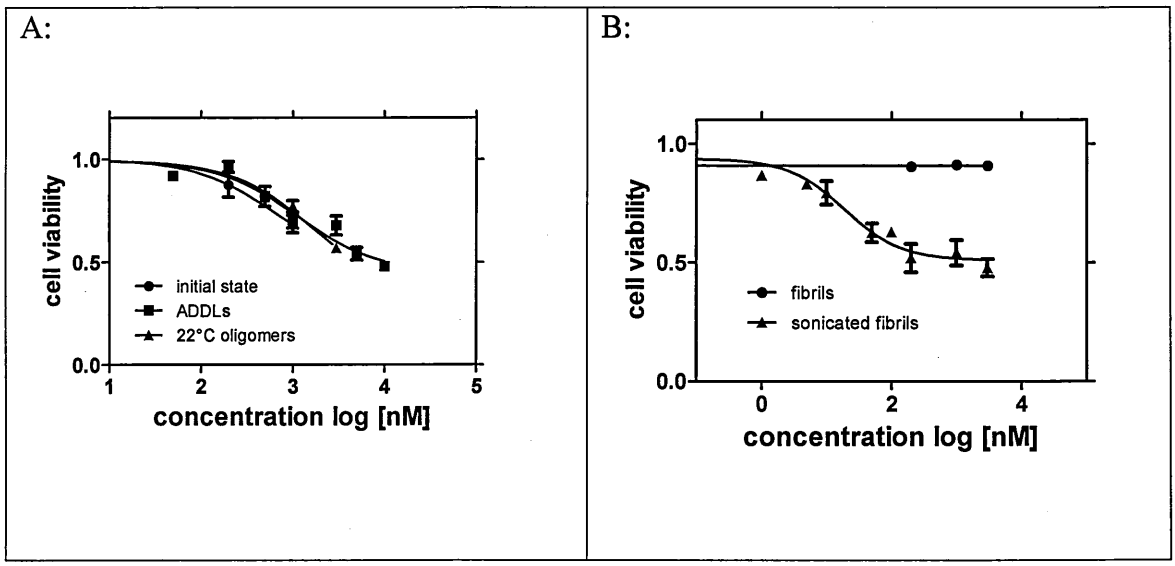

Fig. 4-10: Concentration dependent cell viability neuronal cells after treatment with various Aβ1-42 assemblies for 24h compared to the cells treated only with the buffer.

Hippocampus neuronal cells of rat pups were put on 96-wells plate and treated with β-amyloid peptides derived assemblies when neurons were mature and differentiated. Cell viability was then analysed by the MTT-assay. Panel A: cell viability of initial state, ADDLs, 22°C oligomers. Panel B: cell viability of fibrils (prepared under acidic condition) and sonicated fibrils.

4.2 Kinetics of fibril formation

The nucleated polymerization (NP) and nucleated conformational change (NCC) is characterised by an initial lag phase, followed by a progressive increase to a final plateau (Harper and Lansbury, 1997; Serio et al., 2000). The observed kinetic process depends strongly on the reproducibility of the initial state preparation and requires the total removal of seeds from the stock solution. Previously, it was shown that the use of depsi-peptides improved the reproducibility and eased the preparation of the aggregation prone Aβ peptides. In this chapter we will demonstrate that the depsi-peptides are a valuable tool for the study of the kinetics of fibril formation of Aβ peptides.

4.2.1 Sedimentation of aggregated assemblies during the CD experiments interfere with the secondary structure measurements under non agitating (quiescent) condition

First we investigated the kinetics of fibril formation of Aβ1-40 under quiescent condition. For this, 50 μM of Aβ1-40 in PB pH 7.4 at 37°C was prepared and divided to incubate one part in a 1.5 ml Eppendorf vial for ThT and AFM measurements and the other part in a 0.1 cm cuvette to determine the secondary structure by CD. We found that the overall CD intensity decreased without a visible formation of β-sheet structure (Fig. 4-11 A). Nevertheless, ThT (Fig. 4-11 D) measurement and AFM (Fig. 4-11 E) demonstrated that after a lag phase of 100 h, the fibril formation initiated until a plateau was reached after around 150 h. We hypothesised that sedimentation of aggregates could be the cause of this observation. This was confirmed by a decrease of the absorbance value at 214 nm which started at the end of the lag phase (Fig. 4-11 B). The secondary structure was followed throughout the decrease in absorbance (Fig. 4-11 C) and the spectra were normalised based on the modified values of the concentration. This should give an indication of the structure of the soluble species. As Fig. 4-11 C shows, the secondary structure represents mainly a statistical coil structure, similar to the initial state, with a minor increase in the negative intensity at 215 nm which is an indication for β-sheet formation. This could be due to the formation of oligomeric β-sheet containing assemblies, since the size of spherical aggregates observed by AFM increase over the 50 h time period (Fig. 4-11 E). Additional evidence that sedimentation is the reason for the low amount of detected β-sheet containing assemblies was seen by moving (shaking) the cuvette several times to ensure the homogenization of the solution. Fig. 4-11 A shows a significant increase in intensity at the negative band at 215 nm and the absorbance value increased slightly (Fig. 4-11 B). Nevertheless, the absorbance shows an overall decrease from that at the beginning of the incubation.

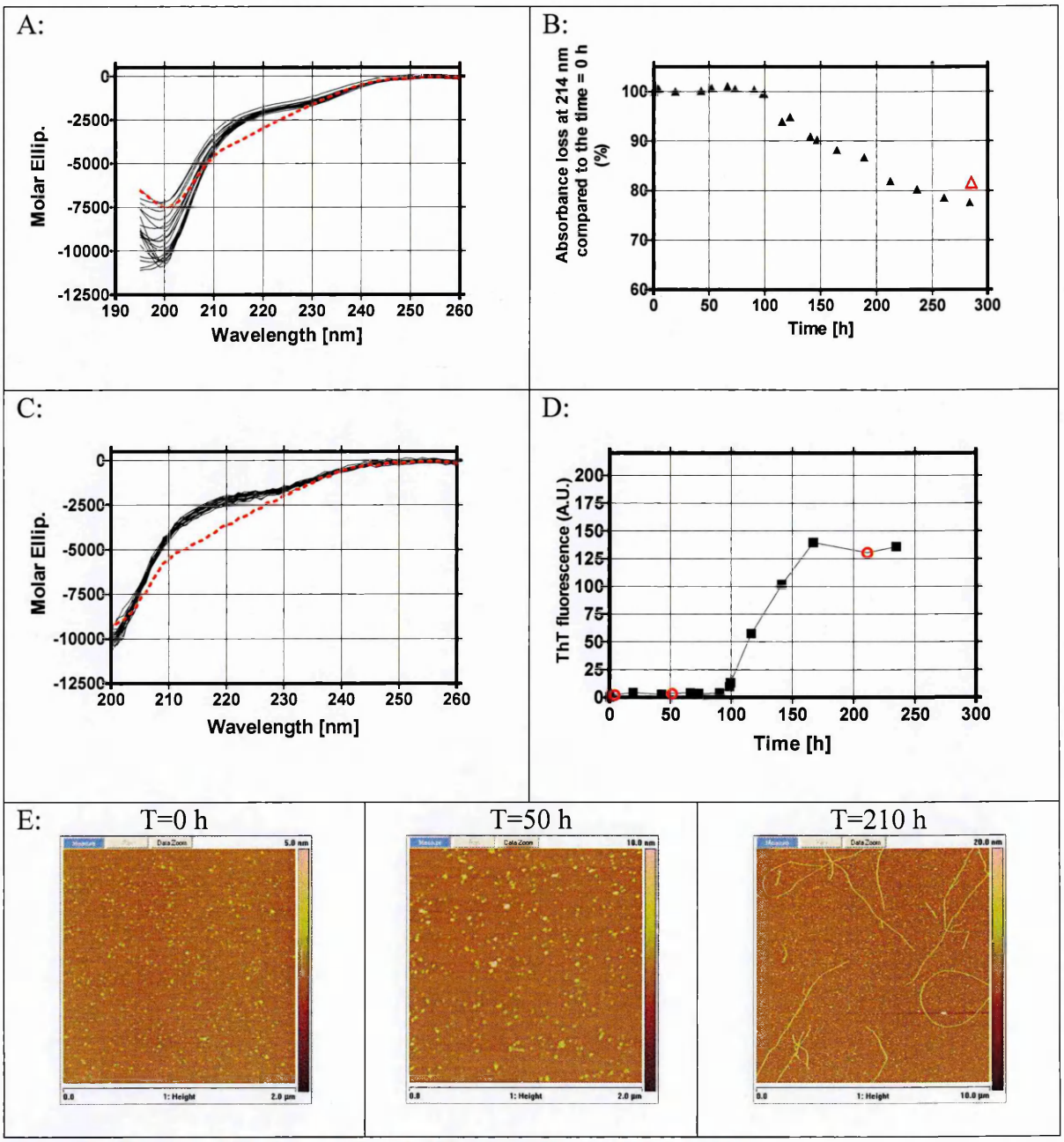

Fig. 4-11: Kinetics of fibril formation of Aβ1-40 under quiescent condition.

50 μM of Aβ1-40 in 50 mM PB pH 7.4 were incubated at 37°C under quiescent condition. Panel A: changes in the CD spectra during the incubation; red dashed spectrum was measured after the homogenization of the solution. Panel B: timecourse of absorbance measurements; red triangle characterizes the value after the homogenization of the solution. Panel C: determination of normalized spectra based on the changes in concentration; red dashed spectrum was measured after the homogenization of the solution. Panel D: Timecourse of fibril formation monitored by ThT. Panel E: AFM pictures of the peptide solution at different time points (marked in red in the ThT trace).

4.2.2 Kinetics of aggregation of Aβ1-42 and the impact of the variation in concentration

The more aggregation prone Aβ1-42 behaves similar like Aβ1-40. During the incubation of Aβ1-42 in PB pH 7.4 at 37°C under quiescent condition, aggregated assemblies tend to sediment during the incubation in a cuvette (Fig. 4-12 A). Nevertheless the increase in the negative band at 215 nm in the beginning of the incubation clearly demonstrated the formation of soluble β-sheet aggregates. The arrest of the intensity change at 215 nm after 25 h suggests the production of sedimentable β-sheet aggregates (Fig. 4-12 B). The movement after 280 h of the solution in the cuvette gave a pronounced β-sheet spectra (red curve, Fig. 4-12 A). The incubation of the same solution in a vial left for aggregation at RT (22°C) and followed by ThT measurements showed that, after a lag phase of 70 h and the exponential growth of ThT-sensitive species until 150 h after the start of the incubation the final plateau is reached (Fig. 4-12 C). Interesting is the fact that ThT sensitive assemblies are present even during the lag phase. Since the kinetics of aggregation is concentration-dependent we wanted to find conditions which permit us to study the kinetics in a reasonable time but still representing the features of NP (nucleated polymerization). We found that by increasing the peptide concentration to 100 μM, the peptide readily forms β-sheet species as demonstrated by the immediate increase in the CD signal at 215 nm (Fig. 4-12 D).

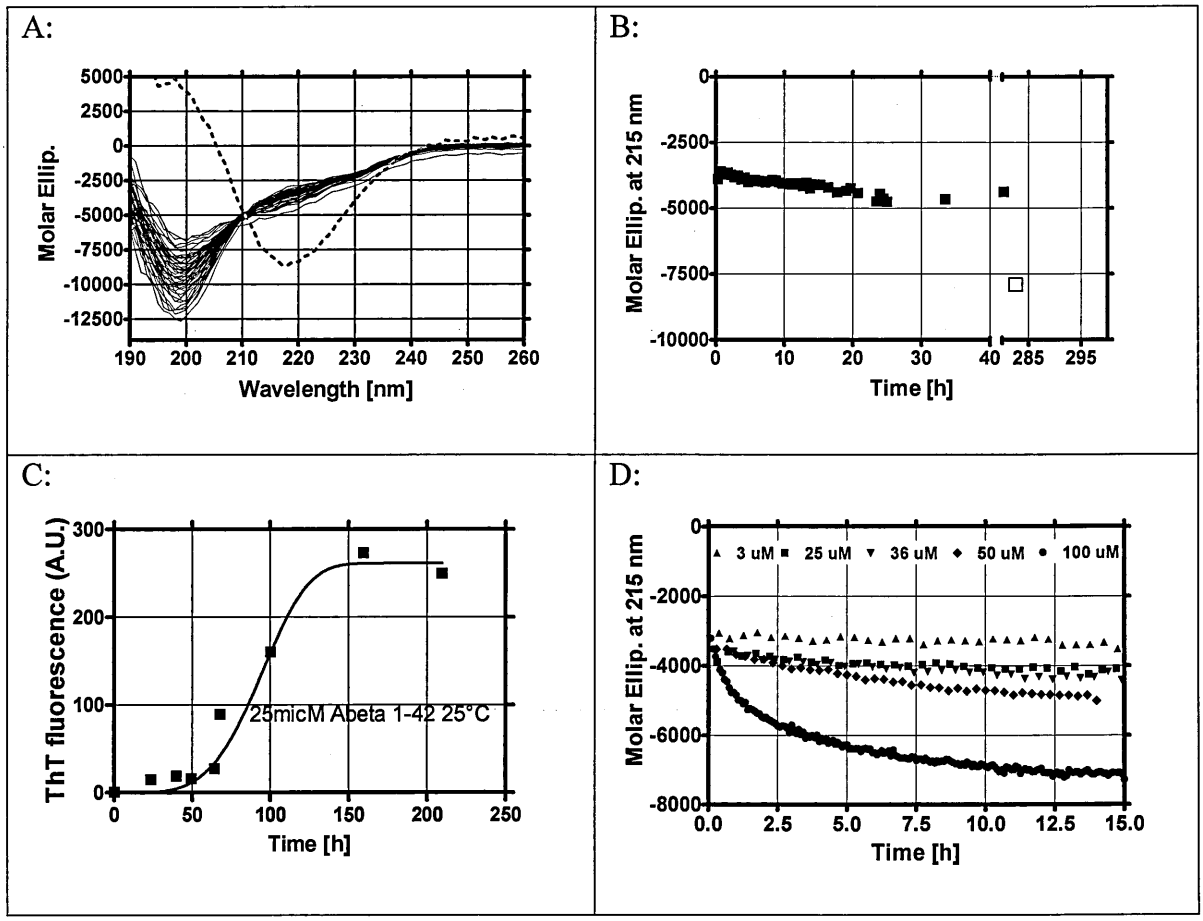

Fig. 4-12: The kinetics of fibril formation of Aβ1-42 under quiescent condition.

Panel A and B: 25 μM of Aβ1-42 in 50 mM PB pH 7.4 were incubated at 37°C under quiescent condition in CD cuvette. Panel A: changes in the CD spectra during the incubation; red dashed spectrum was measured after the homogenization of the solution. Panel B: timecourse of CD value at 215 nm; red open box characterizes the value after the homogenization. Panel C: 25 μM of Aβ1-42 in 50 mM PB pH 7.4 were incubated at 22°C under quiescent condition in Eppendorf vial. Panel D: concentration dependant changes of the CD value at 215 nm. Aβ1-42 was incubated in 50 mM PB pH 7.4 at 37°C in cuvette under quiescent condition.

4.2.3 Stirring-induced alignment of amyloid fibrils revealed by CD

Since high concentration reduces the lag phase in the CD experiment and peptides tend to sediment under quiescent condition, low peptide concentration and stirring could be the appropriate answer to the problem. To test this we incubated 3 μM of Aβ1-42 in a 1 cm cuvette under continuous stirring at 1330 rpm. We found that under this condition the lag phase is about 70 h and the plateau is reached after 100 h (Fig. 4-13 A). However, the final spectra did not resemble a typical β-sheet spectrum (Fig. 4-13 B). The shape of the CD spectrum does not compare to any secondary structure spectra possible. We hypothesised that this is due to a stirring-induced alignment of the fibrils (Adachi et al., 2007). This was confirmed after we switched off the stirring apparatus. Under this condition we obtained a spectrum which showed a pronounced β-sheet secondary structure (Fig. 4-13 C). Fibrils formed under this condition immediately align even at the lowest possible stirring velocity (Fig. 4-13 D). Turbulent stirring was tried to avoid the alignment, but this led to the formation of visible aggregates or precipitate (data not shown).

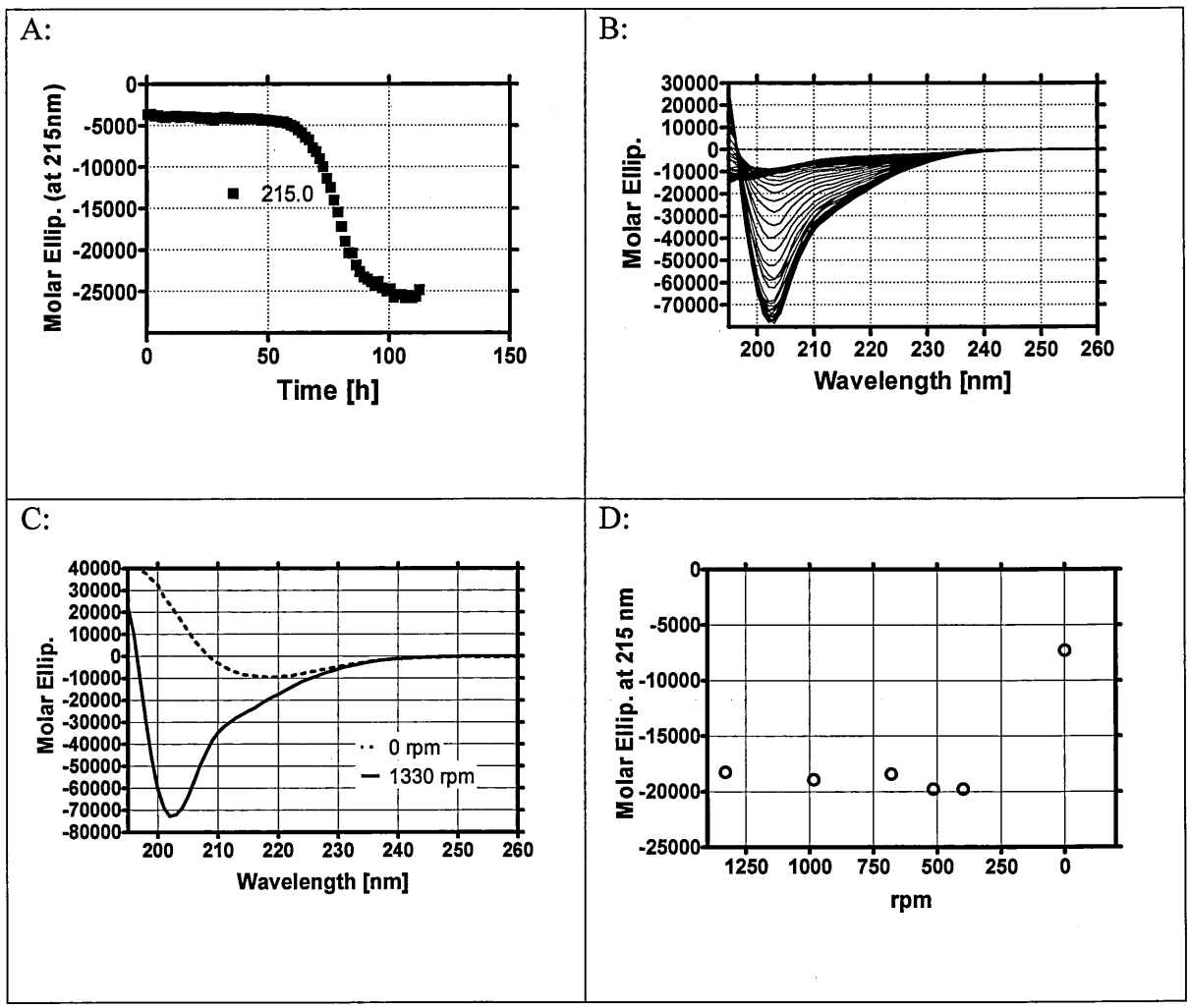

Fig. 4-13: Stirring induced alignment of β-sheet assemblies determined by CD.

The changes in the secondary structure 3 μM of Aβ1-42 in 5 mM PB pH 7.4 at 37°C was followed by CD by incubating the solution in a 1 cm cuvette under continuous stirring at 1330 rpm. Panel A: The timecourse of the CD value at 215 nm. Panel B: The changes in CD spectra during the timecourse of aggregation. Panel C: comparison between the spectra with and without stirring of the solution at the end of the incubation period. Panel D: CD value at 215 nm in dependence of the stirring velocity in rpm.

4.2.4 Determination of optimal condition for the kinetic experiments

In addition to the concentration and temperature dependence of the kinetics of fibril formation, the pH can also influence the kinetics. As demonstrated in 4.1.4, Aβ1-42 exclusively forms fibrils at acidic pH. Preliminary data suggested that, at neutral pH the lag phase is absent at high peptide concentration (data not shown). However, at low peptide concentration, the peptide undergoes an unordered coil to β-sheet transition with an iso-dichroic point at 206 nm observed by CD spectroscopy (Fig. 4-14 A). Fig. 4-14 B shows the time-course of this transition, investigated at either 25°C or 37°C. A lag phase of about 5 hours was apparent at the lower temperature, whereas it significantly decreased to < 2h at 37°C. The results were highly reproducible as shown by the very low SD values obtained from the results of three different experiments. Additionally, an increase in temperature augmented the velocity of the rate of fibril elongation (Fig. 4-14 B).

Following the changes of ThT fluorescence during the incubation of Aβ peptides on a plate reader with periodical shaking is another popular technique (Hortschansky et al., 2005; Klement et al., 2007). We demonstrated that 10 μM Aβ1-42 aggregates faster than 50 μM Aβ1-40 under the same condition (Fig. 4-14 C). The single experiment was done in triplicate and the small SD in the half time of aggregation, which was 27.5 h and 16.2 h for Aβ1-40 and Aβ1-42 respectively, again proved the high reproducibility (Fig. 4-14 D).

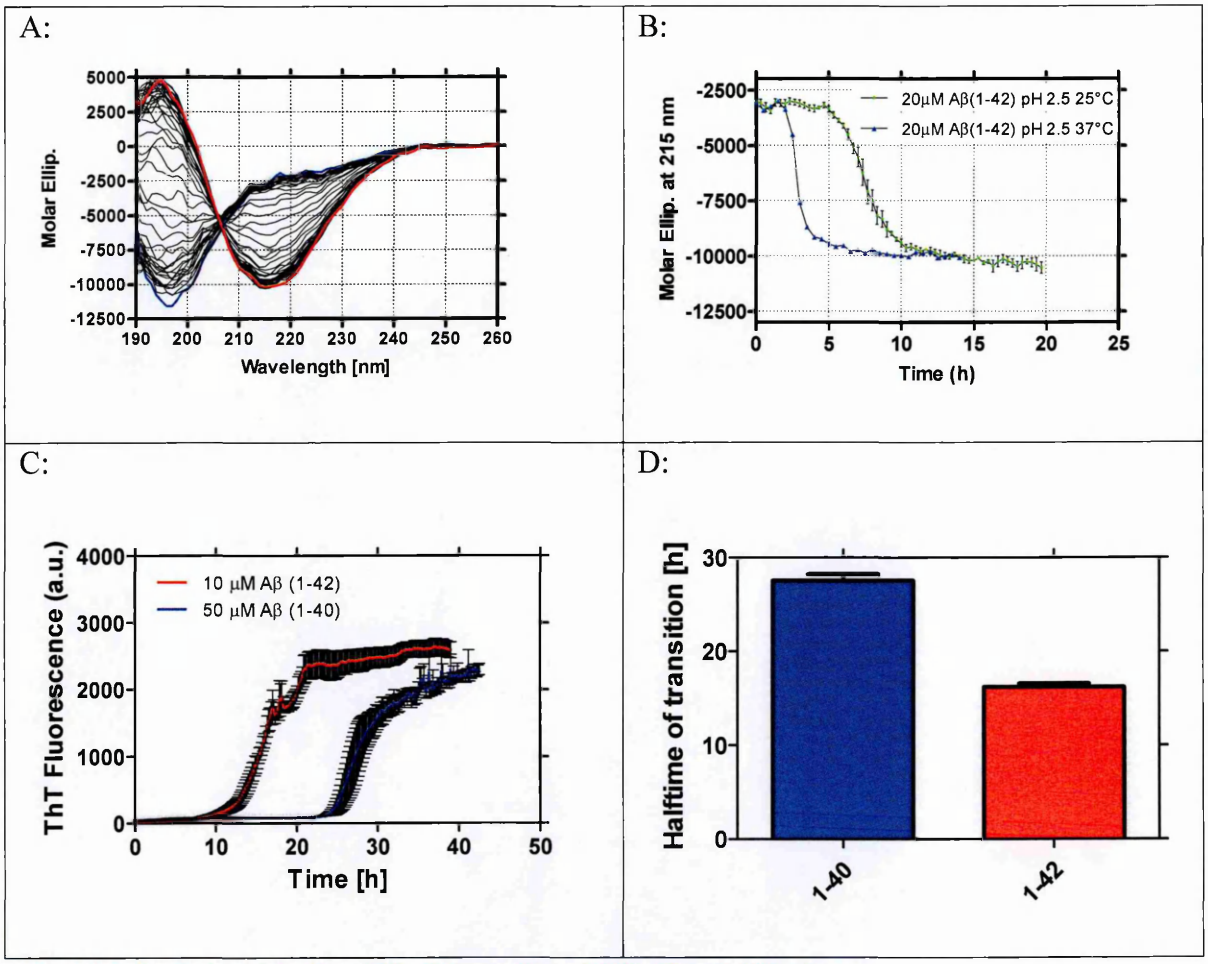

Fig. 4-14: Optimised kinetics of fibril formation of Aβ1-42 and Aβ1-40.

Panel A: Aβ1-42 readily forms β-sheet-containing species. Aβ1-42 stock solution was diluted in acidic buffer (Stenhagen buffer, pH 2.5) to 20 µM and incubated at 25°C. CD spectra were obtained every 20 min. The blue trace was taken at t=0 h and the red trace at t=20 h. The transition to β-sheet is associated with the increase of the negative value at 215 nm. Panel B: Kinetics of formation of β-sheet containing Aβ1-42 species at pH 2.5; effect of temperature. Data at 37°C are means±SD of the results from three independent experiments. Panel C: Kinetics of fibril formation of Aβ1-40/ Aβ1-42 (50/10 µM) incubated on a plate reader in 50 mM PB pH 7.4 at 37°C. Polymerization was accelerated by periodical plate shaking every 10 min. Panel D: Halftime of transition. Data are means±SD of three traces of the same experiment.

4.2.5 Analysis of Aβ1-42 fibril elongation by Surface Plasmon Resonance

Probing the binding of Aβ monomers to preformed fibrils by SPR gives valuable insights into the elongation phase of the kinetics of aggregation. For these studies we immobilised Aβ1-42 fibrils, either sonicated or not, on the sensor chip. Aβ1-42 monomers were immobilised in parallel as internal control whereas a sensor surface was left empty for referencing. No decay of the SPR signal was observed when flowing buffer for 30 min over just-immobilised Aβ1-42 fibrils (data not shown) indicating that no depolymerisation occurred at variance with the slow linear decay observed with immobilised Aβ1-40 fibrils (Cannon et al., 2004). Fig. 4-15 shows the results obtained by injecting three different concentrations of Aβ1-42 monomers (1-3-10 μM). No binding was observed during the flow of Aβ1-42 monomers on the reference, empty, surfaces (not shown). Aβ1-42 monomers showed a marked and dose-dependent binding to fibrils - but not to monomers – which under our experimental conditions never reached plateau. Very good reproducibility was observed when repeating peptide injections over the same sensor surface without intermediate regeneration steps (see the replicates in Fig. 4-15).

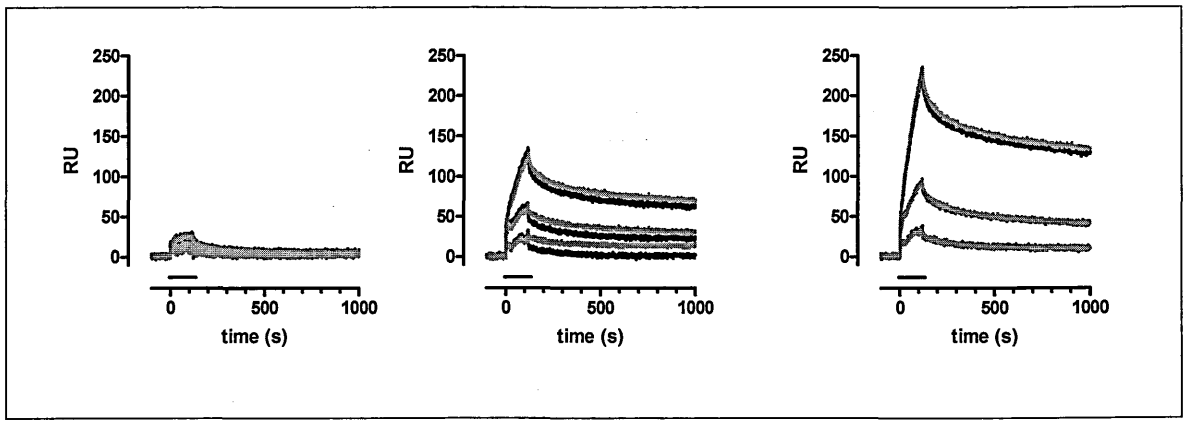

Fig. 4-15: Aβ1-42 fibril elongation investigated by SPR:

Aβ1-42 monomers, fibrils and sonicated fibrils (from left to right) were immobilized on three parallel strips of the same sensor chip, with similar immobilization levels. Figures show the corresponding sensorgrams, i.e. time course of the SPR signal expressed in Resonance Units (1 RU = 1 pg protein/mm^2), each of them normalized to a baseline value of 0. As regards Aβ1-42 monomers, the black and grey sensorgrams indicate the results of two consecutive injections without any intermediate regeneration step. These sensorgrams could be fitted well according to the conformational change model.

The multiphase dissociation could be well fitted by a triple exponential function, with a plateau indicating that a significant fraction of the binding is likely irreversible. These features are consistent with the dock-and-lock model of fibril elongation (Esler et al., 2000), in which the "locking" step is due to sequential conformational changes, each increasing the affinity of the monomer for the fibril until a condition of irreversible binding is reached. Accordingly, the sensorgrams could be adequately fitted by a complex equation modelling the "dock-and-lock" mechanism ("conformational change" or "three steps" model), as previously described for Aβ1-40 (Cannon, Williams et al. 2004). The results of this analysis are shown in Table 4-2 and indicate that the initial binding step between Aβ1-42 monomers and Aβ1-42 fibrils has an apparent Kd of 44 μM.

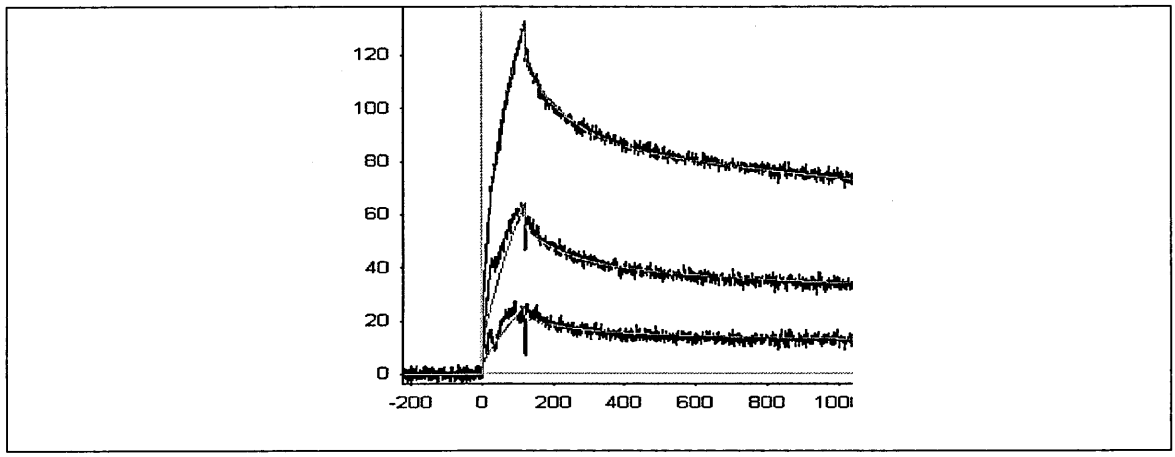

Fig. 4-16 Global fitting of the sensorgrams obtained injecting Aβ1-42 monomers (three concentrations) over immobilised Aβ1-42 fibrils:

Representative sensorgrams obtained in a single run, injecting the three concentrations of $A\beta_{1-42}$ monomers at the same time. The three sensorgrams were analyzed together (i.e. global fitting) using the nonlinear least squares data analysis program CLAMP (Myszka and Morton 1998) and using a three-step conformational change model (Cannon, Williams et al. 2004). The fittings are shown in red.

Table 4-2: The kinetic parameters obtained in three independent runs, identical to the one shown here, are indicated in Table. The table reports the mean±SD of the kinetic parameters in three independent runs. The data for $A\beta_{1-40}$ are from Cannon et al. (16) and are shown here for comparison.

	$A\beta_{1-42}$	$A\beta_{1-40}^{*}$
k_1 (M^{-1} s^{-1})	$9.1 \pm 1.3 \times 10^{3}$	$6.6 \pm 1.5 \times 10^{3}$
k_{-1} (s^{-1})	$4.0 \pm 1.9 \times 10^{-1}$	$8.1 \pm 1.4 \times 10^{-1}$
k_2 (s^{-1})	$4.7 \pm 1.9 \times 10^{-2}$	$6.4 \pm 0.4 \times 10^{-2}$
k_{-2} (s^{-1})	$2.9 \pm 0.6 \times 10^{-3}$	$4.4 \pm 0.4 \times 10^{-3}$
k_3 (s^{-1})	$4.4 \pm 0.2 \times 10^{-3}$	$4.6 \pm 0.2 \times 10^{-3}$
k_{-3} (s^{-1})	$5.9 \pm 0.8 \times 10^{-4}$	$4.3 \pm 0.3 \times 10^{-4}$

4.2.6 Investigation of the kinetics of aggregation of a guest-host system Aβ14-24 permits the incubation at neutral pH under quiescent condition

Since reasonable results of the kinetics of fibril formation of Aβ1-42 using CD under quiescent was so far only obtained at acidic pH, we wanted to have smaller Aβ fragment which showed similar features of nucleated polymerisation at neutral pH, similar to the full length sequence at acidic pH. Recently Camus et al. described a guest-host peptide that can be used for in vitro mechanistic and screening studies aimed at discovering aggregation inhibitors that target highly amyloidogenic sequences (Camus et al., 2008).

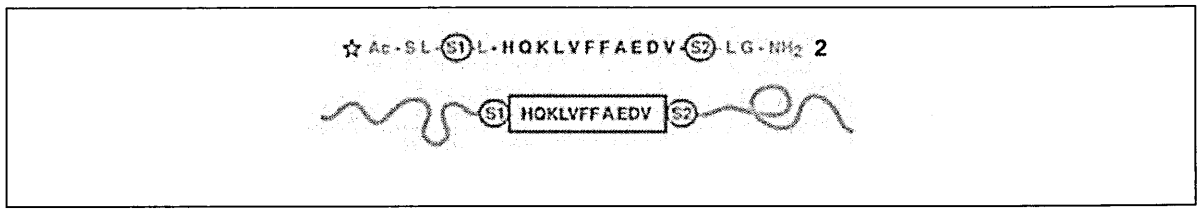

4-17: Design principles of host–guest switch-peptides that are derived from Aβ14-24 (guest) which contains two switch elements at the N and C termini, separating the guest sequence form the β-sheet formation favouring host sequence (SL-motif)(Camus et al., 2008).

We also prepared the guest-host peptide containing the hydrophobic core of Aβ residues 14-24 with click elements (depsi-bond) at the N and C termini to investigate the usability as a reliable tool to design kinetic experiments of high reproducibility at neutral pH.

After dissolving the peptide in 10 mM PB pH 7.4 at 37°C to give 172 µM, the peptide secondary structure of the initial state is mainly in random state. Nevertheless, under these conditions (neutral pH), the native sequence of the peptide is formed and the aggregation is triggered which is characterised by a random to β-sheet transition with an apparent iso-dichroic point at 209 nm (Fig. 4-18 A). The iso-dichroic point disappears during the progression of polymerization, the final spectrum is not a pure in β-sheet secondary structure and a loss in overall intensity in the CD spectrum is visible. This is again due the sedimentation of ordered aggregates which is indicated by the fact that after an initial increase (light scattering), the absorbance value at 214 nm decreases (sedimentation) (Fig. 4-18 B) and the CD intensity at 214 nm reaches a plateau which represents only the structure of the soluble species in the solution.

Nevertheless, the highly reproducible kinetic data (Fig. 4-18 C) show a characteristic lag phase which is with 0.6 h three times smaller at 37°C compared to 25°C (Fig. 4-18 C). Decreasing the peptide concentration from 176 μM to 82 μM extended the lag phase from 2°h to 8 h at 25°C (Fig. 4-18 E).

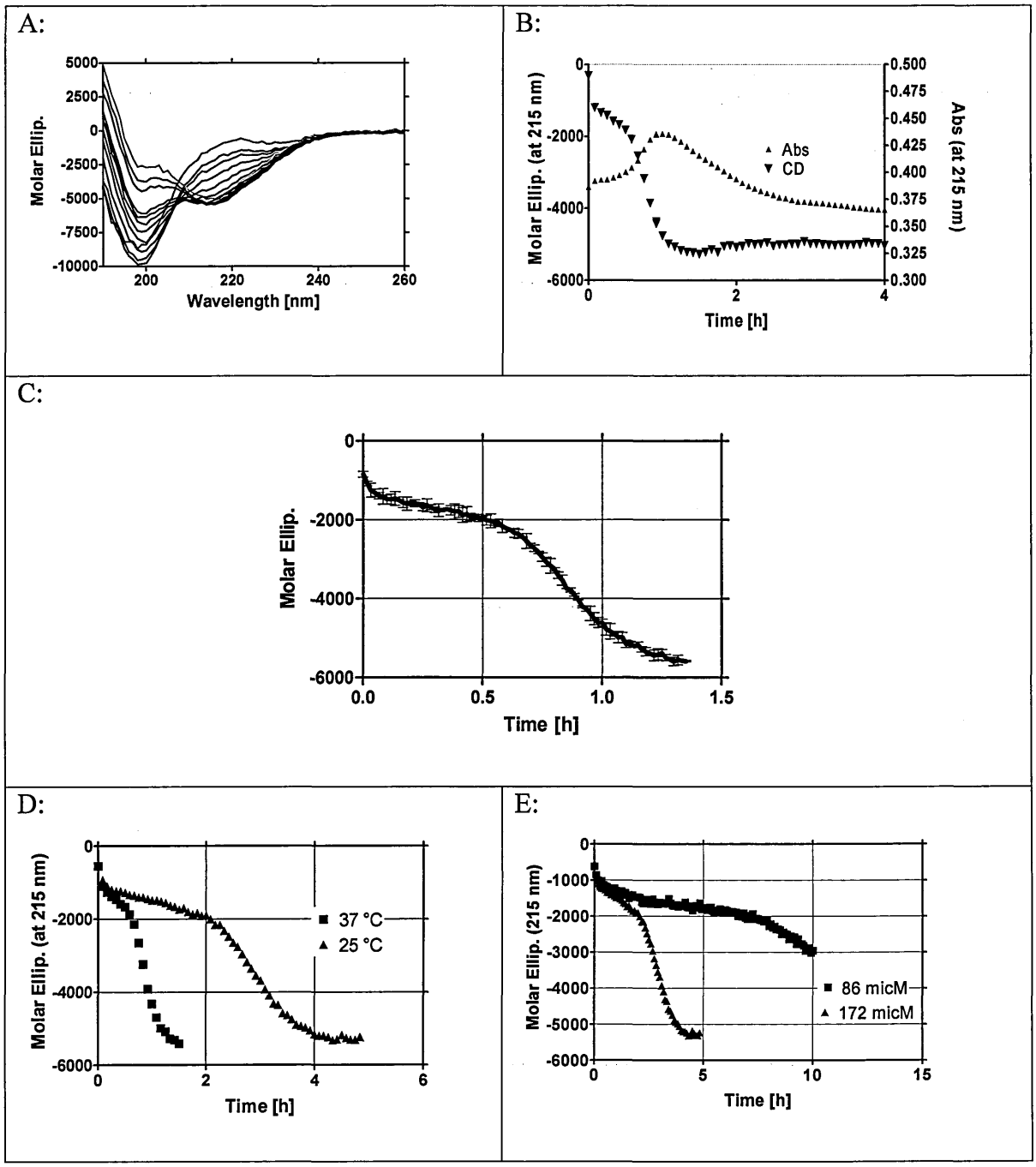

Fig. 4-18: The kinetics of fibril formation of Aβ14-24:

Aβ14-24 peptide powder was dissolved in 10 mM PB pH 7.4 put into a 0.1 cm cuvette. Panel A: CD spectra of the random structure to β-sheet transition of 172 µM Aβ at 37°C. Panel B: timecourse of the transition from Panel A, monitoring CD signal at 214 nm and its corresponding absorbance values. Panel C: Reproducibility of the kinetics run in triplicate under the same condition as in Panel A. Panel D: timecourse of the transition at different 25°C and 37°C. Panel E: timecourse of the transition at 86 µM and 172 µM at 25°C.

To further investigate the properties of the model peptide, we determined the aggregate induced change in the ThT signal during the incubation in PB pH 7.4 at 22°C and the structures formed in the end of the polymerization. The aggregates are short, needle-like and fibrillar (Fig. 4-19 A), and the characteristic ThT fluorescence develops at the end of the transition (60 minutes: Fig. 4-19 B). Aggregates formed during the lag phase are ThT sensitive and the characteristic fibril elongation with a final plateau is observed.

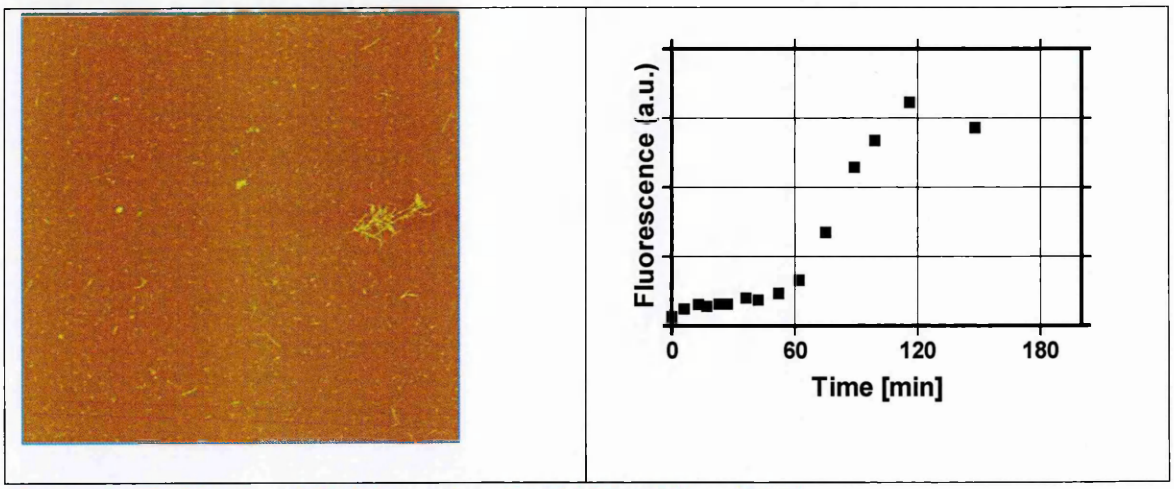

Fig. 4-19: The kinetics of fibril formation of Aβ14-24: AFM and ThT.

Fibril formation of 86°μM Aβ14-24 peptide in 10 mM PB pH 7.4 incubated at 37°C. Panel A: AFM picture in the end of the transition (10x10 μm). Panel B: Changes of the ThT during incubation.

This model peptide is subsequently used to investigate the changes to the lag phase and initial kinetics of fibril formation in the presence of anti-amyloidogenic compounds by CD.

4.2.7 Differences in the aggregation propensity of Aβ1-40 MUT (A2V) compared to Aβ1-40 WT

The finding that the A2V mutation in the Aβ fragment of APP strongly boosts Aβ production (Di Fede et al., 2009) raises the question if only the higher amount of Aβ peptides is responsible for the early onset of the disease in patient. We set out to investigate the kinetics of aggregation to clarify this point. Theoretical consideration based on the software tool Zyggregator and mutational studies suggested that the mutation at position two increased the fibrillar and the generic aggregation propensity (Kim and Hecht, 2008; Meinhardt et al., 2007).

The kinetics of aggregation was followed by in-situ ThT experiments using a plate reader. We confirmed that the mutation A2V in the Aβ sequence greatly enhanced the rate of fibril formation. Fig. 4-20 A shows the two traces of the transition of 50 μM Aβ1-40 WT/MUT in PB pH 7.4 at 37°C. The length of the lag phase is around 25 h for Aβ1-40WT and 12 h for Aβ1-40MUT but the elongation rate is similar for both variants (Fig. 4-20 A) and mainly long unbranched fibrils are present in the MUT sample after the transition (Fig. 4-20 B).

Furthermore, kinetic studies confirmed the usefulness of the cut-off filtration of the aqueous 0.02 % TFA Aβ stock solution since the values for the halftime of transition increased and the SD values decreased (Fig. 4-20 C), which underlines the relevance of the removal of preformed aggregates during storage and peptide work up after the synthesis. This has to be done for sequences which are thought to be less prone to aggregate Aβ1-40WT and even more for sequence with higher aggregation propensity like Aβ1-40MUT or Aβ1-42.

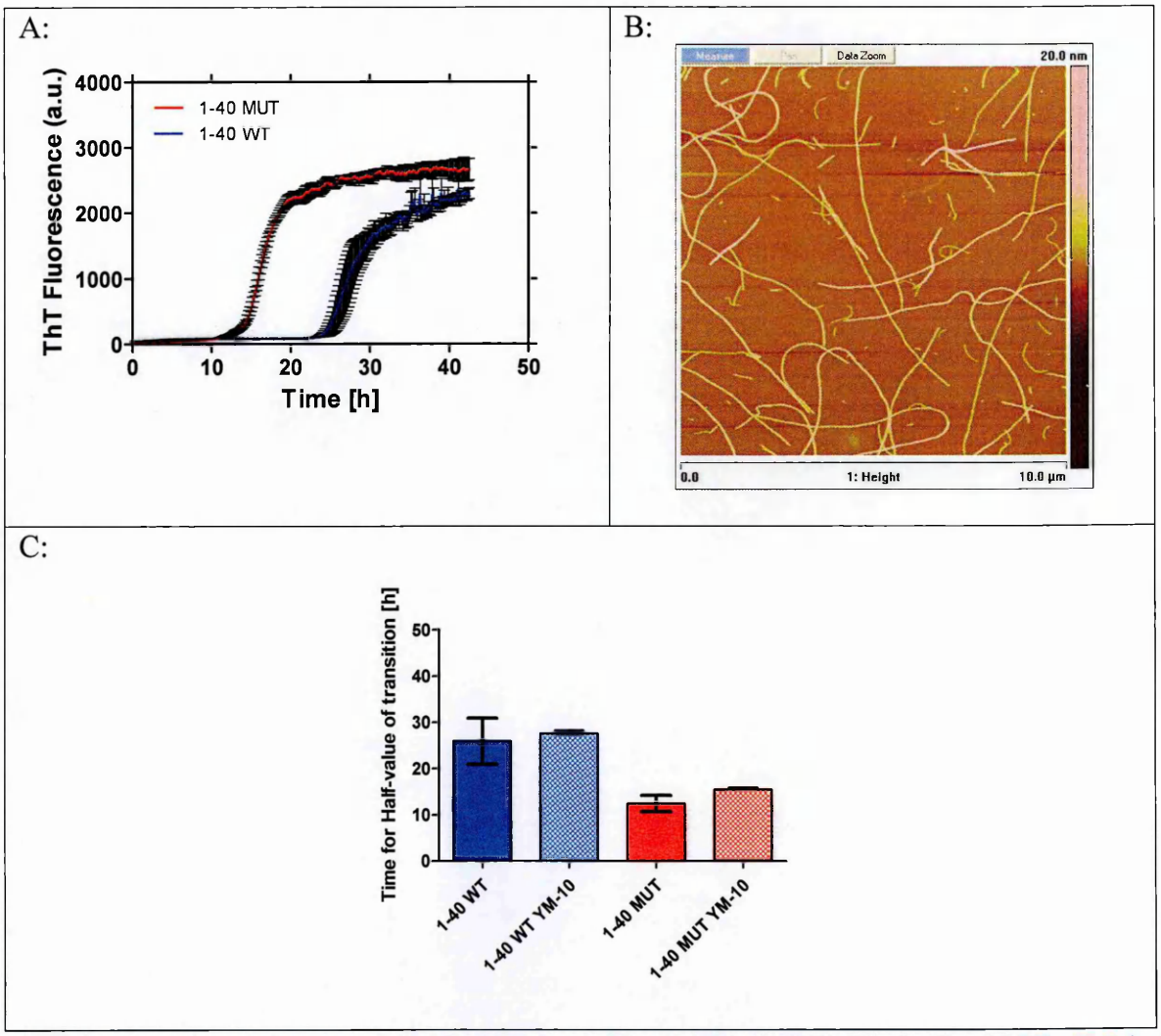

Fig. 4-20: In-situ ThT kinetics of fibril formation of 50 µM Aβ1-40 WT/MUT in 50 mM PB pH 7.4 at 37°C.

Samples were shaken every 10 min and done in triplicate. Panel A: The time dependent changes in ThT values during the incubation of Aβ1-40 WT (blue) and Aβ1-40 MUT (red). Panel B: AFM scan of Aβ1-40 MUT in the end of the transition (10x10 um scan). Panel C: The halftime of transition of Aβ 1-40WT and Aβ 1-40MUT before and after the cut-off filtration (10 kDa).

4.3 Tetracycline and the synthetic Aβ fragments

In this chapter, the previous findings are examined in the light of the interaction with TCs of the various assemblies and the influence on the kinetics of fibril formation of the different Aβ fragments. We concentrated our investigation on TC and DC since these are the derivatives that have been mainly used in in-vitro studies (Bartolini et al., 2007; Forloni et al., 2001; Howlett et al., 1999a; Inbar et al., 2008; Ono and Yamada, 2006).

4.3.1 Solubility of TC and the changes of the CD spectra depending on the pH

Many molecules have been proposed to exhibit an anti-amyloidogenic effect (Necula et al., 2007b). For most of them the mechanism of action is unknown. Recently, for some of the compounds, a unifying mechanism of compound self aggregation was proposed (Feng et al., 2008). These compound aggregates are thought to be localised to preformed fibrils and prevented new fibril formation by a possible non-specific interaction with the monomer (Lendel et al., 2009). The formation of these colloids was tested by centrifugation and flow cytometry which resulted in the determination of critical aggregation concentrations (Coan and Shoichet, 2008). Since TCs are amphiphilic in nature (Forloni et al., 2009) we determined the absorbance of TC after centrifugation of various concentration of TC in PB pH 7.4 at 22°C. After centrifugation at 16 000 g for 1 h the absorbance of the supernatant were measured. Fig. 4-21 shows that the linearity breaks down after the concentration reaches 2 mM, which is much higher than any concentration used to demonstrate the anti-amyloidogenic effect and could determine the solubility limit of the compound under this condition.

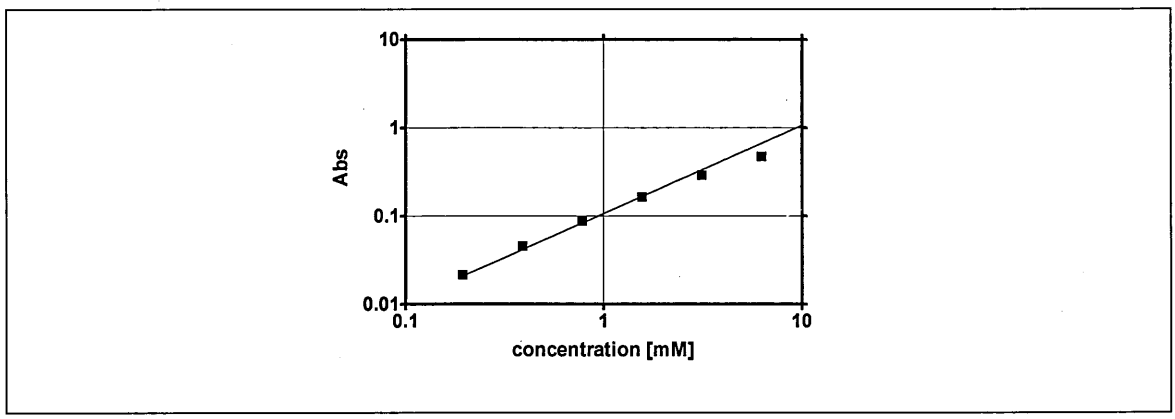

Fig. 4-21: The solubility of TC.

50 mg of TC was diluted in 1 ml of water. This solution was diluted to give up-to 50 mM in 50 mM PB pH 7.4 to give various concentrations. The sample was left for 1 h in the dark at 22°C. After the samples were centrifuged for 1 h at 16000g, the supernatant was taken and the absorbance was determined at 360 nm.

The CD technique will be extensively used to investigate the kinetics of fibril formation in presence of various compounds. However, the TCs show a pronounced optical activity in the wavelength region for peptide secondary structure determination. In addition the absorbance spectra changes depending on the pH of solution (Schmitt and Schneider, 2006). We wanted to know to what extend pH influences the CD spectra of the TCs DC. Fig. 4-22 A and B show the high pH dependency of the CD spectra, and the corresponding absorbance spectra.

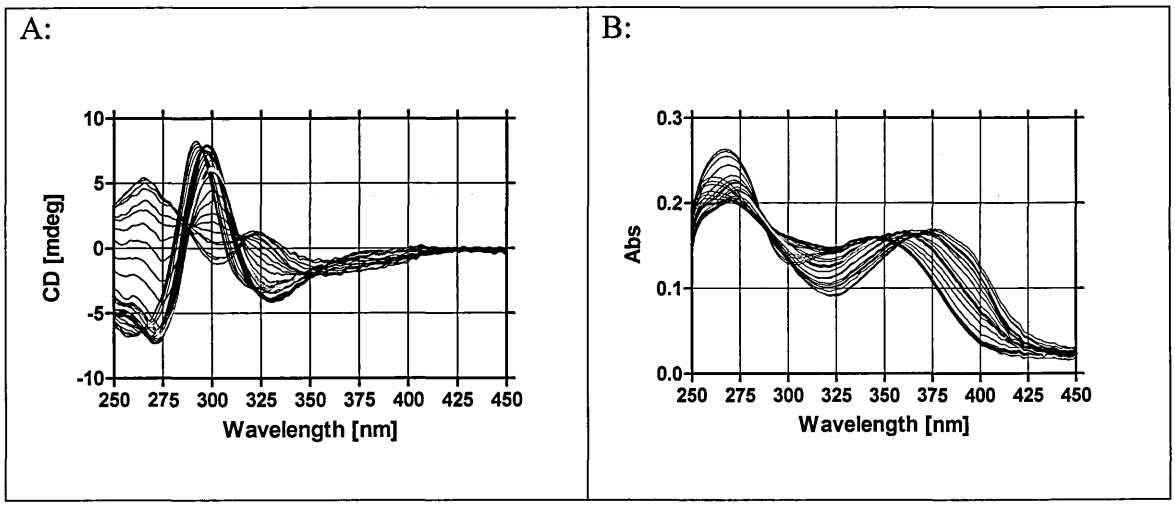

Fig. 4-22: pH dependent changes in Doxycycline CD spectrum and absorbance spectrum.

20 µM DC was dissolved in 20 mM of 500 ml Stenhagen buffer initially at pH 2. The pH value was monitored with pH meter. The pH (2-12) was changed with a 0.1 M HCl solution by 0.25 pH units. 2 ml of this solution was put in a 1 cm cuvette and the CD spectra were taken. The red curve indicates the spectra at pH 7.4. Panel A: CD spectra. Panel B: absorbance spectra.

4.3.2 Binding of tetracycline to Aβ fibrils

Since TC has been reported to bind the fibrils with an EC50 of 8.7 μM (Inbar et al., 2008), we used SPR, CD and fluorescence spectroscopy to investigate the binding of TC to preformed fibrils. The fibrils were prepared under acidic condition and immobilised on the SPR chip or diluted to 10 μM for the CD and fluorescence measurements in PB pH 7.4 at 25°C. None of three methods showed evidence of binding (Fig. 4-23). First we wanted to detect any changes in the CD spectra due to binding of TC to fibrils, but no deviation from the linear concentration-dependent increase of the CD value at 288 nm was observed over a large concentration range. The SPR was used to investigate interaction of the compound with immobilised species. First the compound was injected for 180 s at various concentrations (data not shown). Since this was not successful, the compound was flowed constantly with the running buffer over the various species. But even under this condition TC didn't show any binding capability (Fig. 4-23 C). The sensitivity of SPR was determined to be sufficient since, in a corresponding experiment CR (Congo Red) showed a binding curve with apparent Kd of 4.5 μM (Fig. 4-23 D) to fibrils. Moreover CR demonstrated its high selectivity for amyloidogenic structures since it didn't bind to ADDLs and monomers Fig. 4-23 D). Unexpectedly, ThT did not show the usual association curve during the injection and dissociation curve during the dissociation. Only a fast increase and decrease of the signal was observed (Fig. 4-23 E) which is characteristic for a bulk effect due to the variation of the refraction index of the solution in the presence of the compound or due to electrostatic interaction. A similar picture is drawn by fluorescence spectroscopy. TC does not show specific features which are indicative of fluorescence changes upon binding. Moreover the fluorescent variant of CR, X-34 and as expected ThT showed fluorescence emission from interaction of the dyes with species due to binding (Fig. 4-23 F-G).

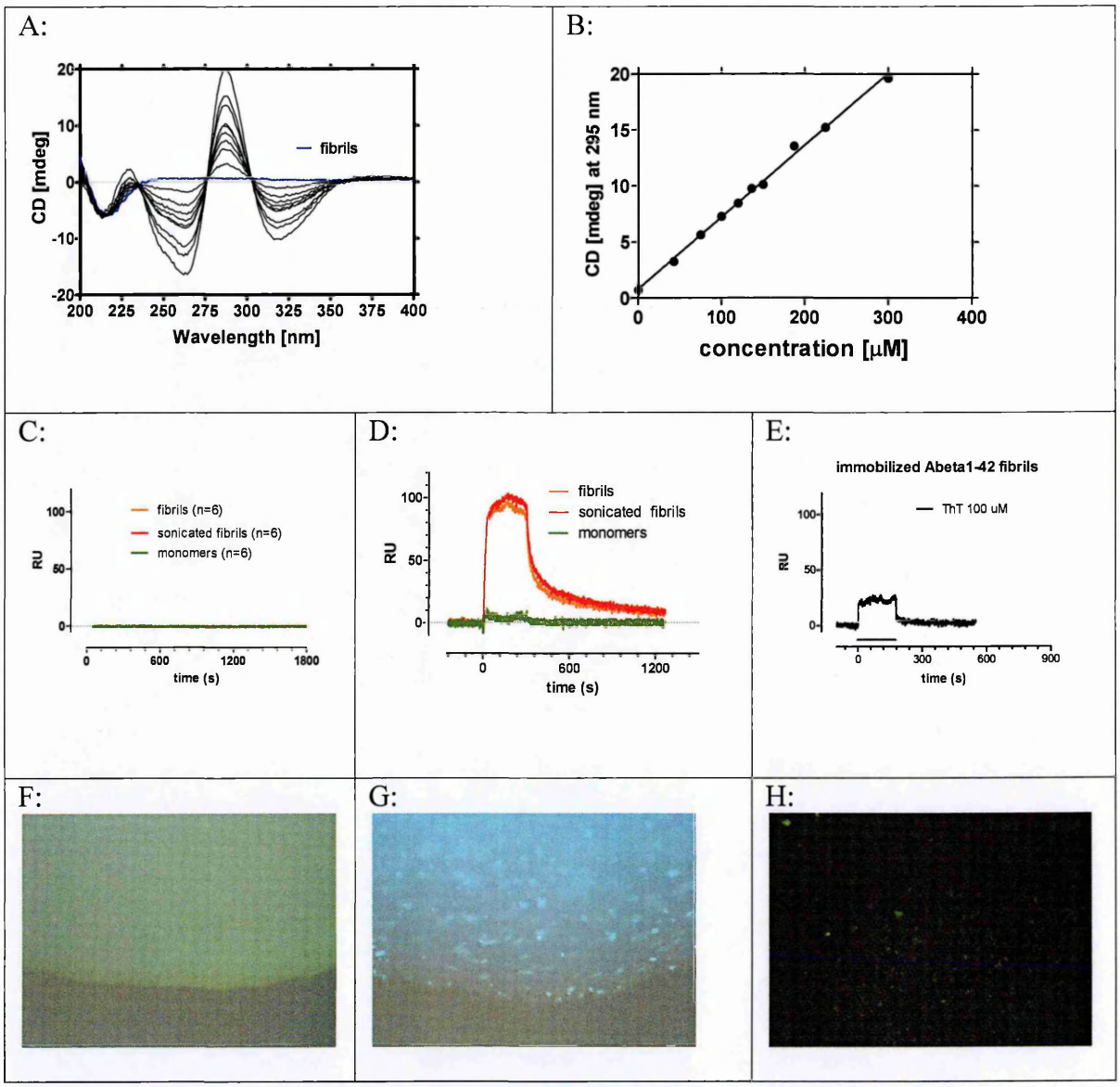

Fig. 4-23: Binding of TC to fibrils investigated by CD, SPR and fluorescence spectroscopy.

Panels A, B: Titration experiment; Ab1-42 fibrils prepared under acidic condition were diluted to 10 µM into 50 mM of PB pH 7.4 and the CD spectra was measured for varying TC concentrations. Panel B: concentration dependant changes of the CD signal at 288 nm. Panel C: 30 µM TC in PBS was flown for 30 min over immobilized fibrils and monomers. Panel D: 3 µM CR to the immobilized species (fibrils, sonicated fibrils, monomers). Panel E: 100 µM ThT in PBS were injected to bind to immobilized fibrils 180 s. Panel F-H: Fluorescence spectroscopy (20x) of 15 µM fibrils in 50 mM PB pH 7.4 buffer containing 100 µM TC (F) X-34 (G) and ThT (H).

4.3.3 Tetracycline and the kinetics of fibril formation

Since no apparent binding was measured, we examined if TC is able to alter the kinetics of aggregation. For this following experimental set-ups were used: 1. **in-situ ThT** on plate reader (Aβ1-40 in PB **pH 7.4** at 37°C in presence of varying concentration of TC) 2. Changes of **CD** signal at 215 nm during the aggregation of Guest-Host-System Aβ14-24 in the presence of 300 μM TC and DC in PB **pH 7.4** at 37°C and 3. Changes of **CD** signal at 215 nm during the aggregation of Aβ1-42 in the presence of 100 μM TC in 50 mM Stenhagen buffer **pH 2.5** at 25°C.

In all three experiments no change of the lag phase and elongation rate was observed (Fig. 4-24). Only the final plateau in the in-situ ThT experiment decreased with increasing compound concentration (Fig. 4-24 A). But no difference in kinetic parameter are observed after the normalization of the traces to the final value under the assumption that most of the monomer is polymerised and the differences in the final value is due to different ThT sensitive structural motives. Moreover, the kinetics of random to β-sheet secondary structure was not altered based on the invariance of the kinetic traces in the CD experiments compared to the control under neutral (Fig. 4-24 C) and acidic condition (Fig. 4-24 C). To investigate the elongation rate of monomers to fibrils, which was shown to be varied in the presence of TC, we determined the binding curve of monomers to preformed (sonicated) fibrils immobilised on a SPR chip in the presence of 100 μM TC. An important feature of the experimental design is the fact that the compound was already present in the running buffer before the monomer was injected to ensure the saturation of potential binding sites (even that no binding was seen in the previous binding studies, see 4.3.2). Nevertheless, Fig. 4-24 E confirms that the elongation rate is not altered in presence of TC.

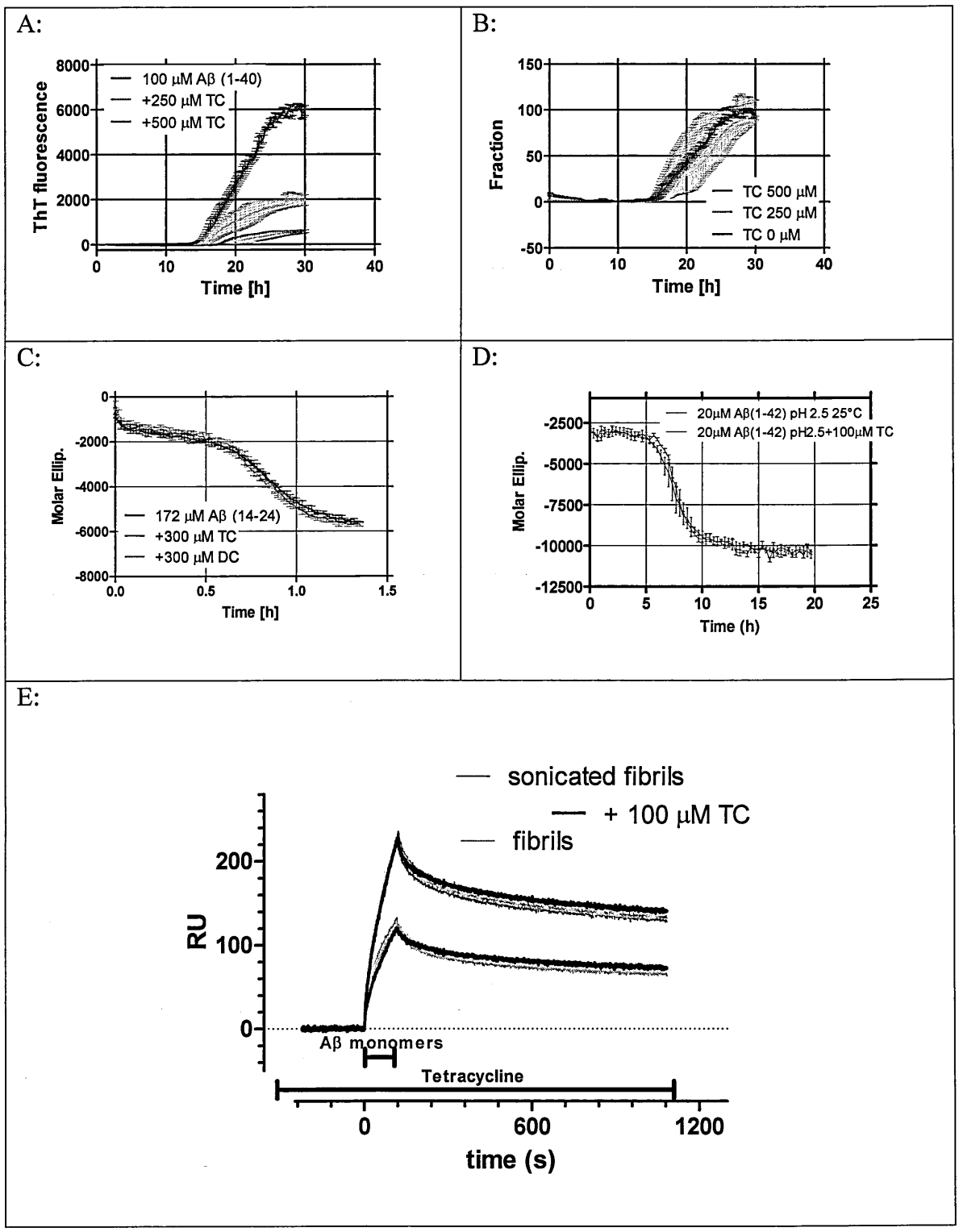

Fig. 4-24 TCs and the kinetics of fibril formation.

Panel A: In-situ ThT kinetic of 100 µM Aβ1-40 in 50 mM PB pH 7.4 at 37°C without and in presence of 250 µM or 500 µM TC done in triplicate. Panel B: Normalized date of Panel A. Panel C: CD transition monitored at 215 nm of 172 µM Aβ14-24 in 50 mM PB pH 7.4 at 37°C without and in presence of 300 µM TC or 300 µM DC. Panel D: CD transition monitored at 215 nm of 20 µM Aβ1-42 in 50 mM Stenhagen buffer 2.5 at 25°C without and in presence of 100 µM TC. Panel E: fibrils and sonicated fibrils were immobilized on an SPR chip and 100 µM TC constantly flown over. 10 µM of Aβ1-42 initial state solution in PBS were injected and the results were compared to results obtained without the presence of TC in the running buffer (see 4.2.5).

4.3.4 Stability of Tetracycline

TCs are known to be unstable under various condition which is mainly covered by pH (neutral to basic) and temperature (Durckheimer, 1975). The extent to which these interfere with the values obtained by in-situ ThT and CD during the kinetics of fibril formation is subject of this section. The changes of the CD and absorbance spectra of TC at neutral pH in PB at 37°C were investigated. Under these conditions a significant decrease of the absorbance value in the BCD ring characteristic band is observed (Fig. 4-25 A). The changes are even larger for the CD spectra where nearly all the characteristic features are lost (Fig. 4-25 B). It has to be noted that during the decomposition the absorbance at wavelength higher than 430 nm and at least up to 500 nm increased. The process takes about 60 h at 37°C and accelerated by increasing temperature to 20 h or 2 h at 60°C or 90°C respectively (Fig. 4-25 C) .

Recently it was argued that destabilizing reaction could be catalyzed by proteins as well (Necula et al., 2007b). We confirmed that the presence of 100 μM Aβ1-40 in PB pH 7.4 at 37°C destabilised 250 μM RTC to a greater extent than a solution only containing the compound (Fig. 4-25 D).

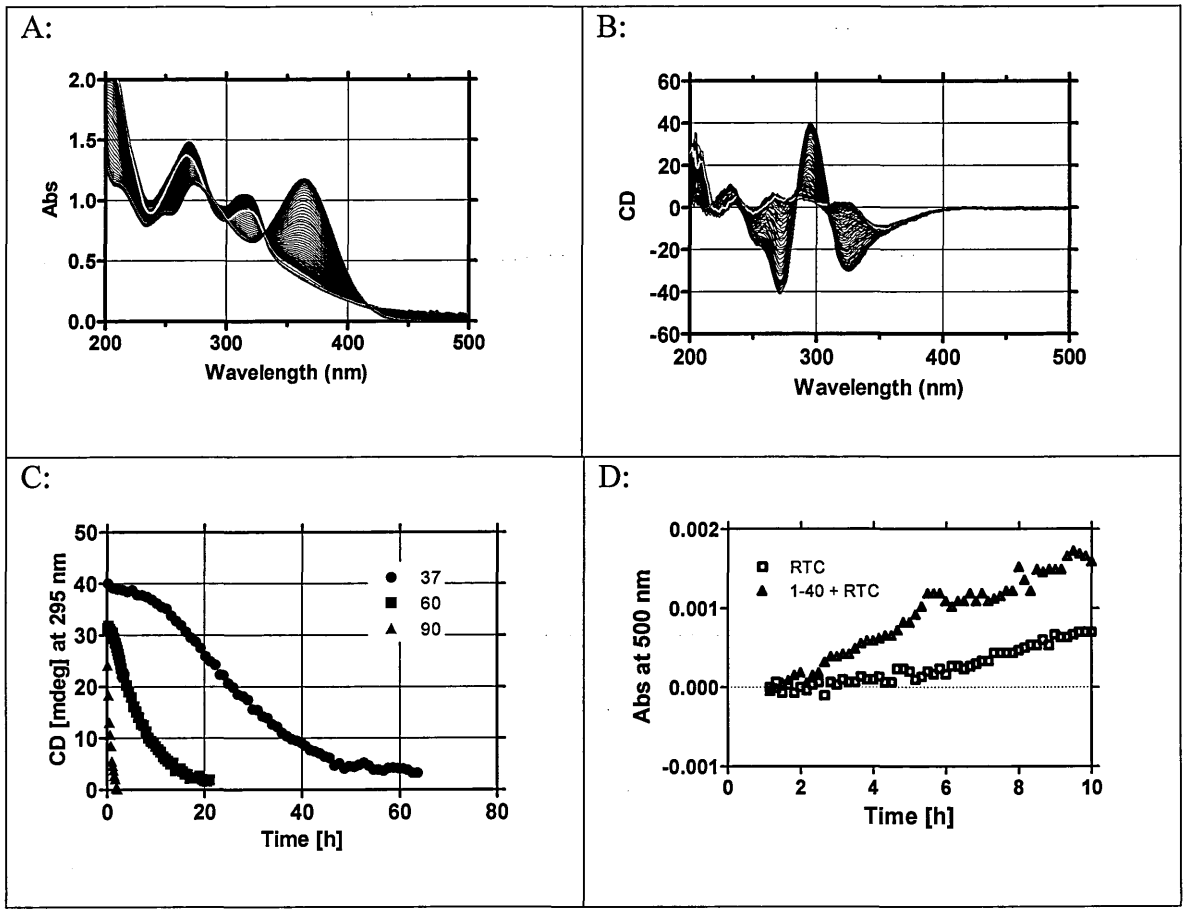

Fig. 4-25: The decomposition of TC.

Panel A: Changes in the absorbance spectra of 700 µM TC in 50 mM PB pH 7.4 at 37°C (blue trace = initial spectrum, red trace = final spectrum). Panel B: Changes in the CD spectra of TC under condition like in Panel A (blue trace = initial spectrum, red trace = final spectrum). Panel C: Loss of CD signal at 295 nm due to the decomposition of TC during the incubation under the same condition like in Panel A only the temperature was varied. Panel D: Kinetic experiment similar to the in-situ ThT experiment only ThT was not present. The changes of the absorbance value at 500 nm due to the decomposition of 250 µM RTC were determined without and in presence of 100 µM Aβ1-40 in 50 mM PB pH 7.4 at 37°C.

4.3.5 The influence of the Tetracycline instability upon CD and ThT measurements

This site reaction makes it extremely difficult to interpret kinetic data. Fig. 4-26 shows the absorbance change at 500 nm during the time course of the kinetic of 100 µM Aβ1-40 in PB pH 7.4 at 37°C without and in presence of 250 µM RTC. As already mentioned, the absorbance value changes immediately due to the decomposition of RTC. Nevertheless, the lag phase is unchanged compared to the control experiment (arrow Fig. 4-26).

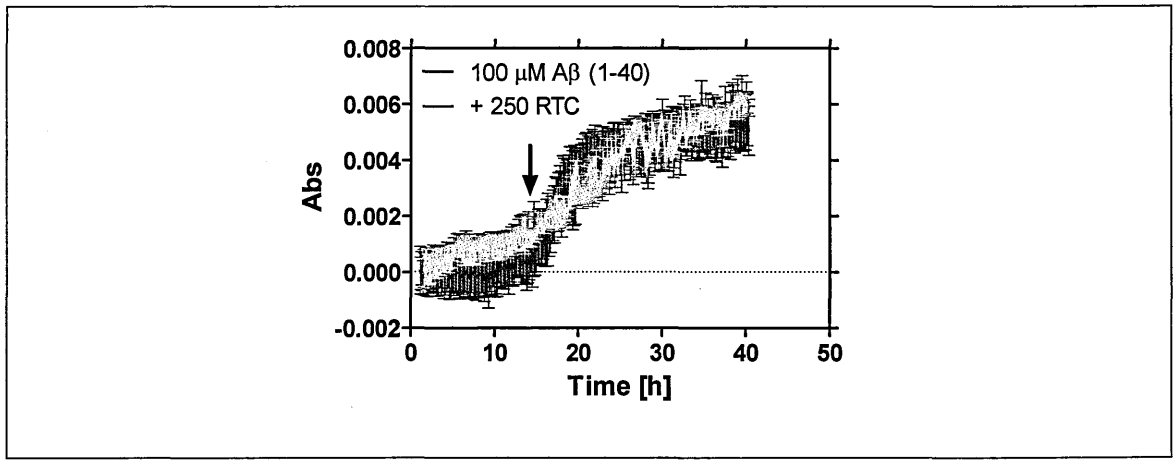

Fig. 4-26: Turbidity changes at 500 nm of Aβ1-40 during fibril formation in either presence of absence of RTC.

100 µM Aβ1-40 were incubated in 50 mM PB pH 7.4 with and without the presence of 250 µM RTC. The conditions are the same as for the in-situ ThT experiments except that no ThT was added to the solution.

How does the decomposition influence the outcome the kinetic results? Since the decomposed TC exhibits a significant absorbance increase at the ThT specific 482 nm emission wavelength (Fig. 4-27 A), we were concerned that these effect could interfere with the results of the ThT measurement. We used preformed fibrils prepared under acidic condition and determined the ThT value by varying the concentration of fresh or decomposed TC. Fig. 4-27 B clearly shows that decomposed TC lowers the ThT value in a concentration dependent manner with an EC50 of 3.7 µM whereas fresh TC leaves the ThT-value nearly unchanged. That this decrease is not due to the disaggregation of the fibrils was demonstrated by the use of a peptide (fibril) free glycerine/50 mM PB pH 7.4 system which increases the ThT fluorescence at 482 nm similar to that observed to amyloid bound ThT because of the high viscosity of the solution (Stsiapura et al., 2008). Fig.

4-27 C confirmed that decomposed TC reduces the ThT fluorescence at higher concentration whereas the effect by fresh TC is not so pronounced. CD, the other used technique to study the kinetics of fibril formation is influenced as well. Fig. 4-27 D shows the changes in the CD signal at 215 nm during the decomposition of TC in PB pH 7.4. The values are up to 20 h relatively stable and increase thereafter. Nevertheless the presence of TC in the solution increases the noise level. This finding suggests that the duration of ThT and CD kinetic experiments should not exceed 10 h or 20 h respectively.

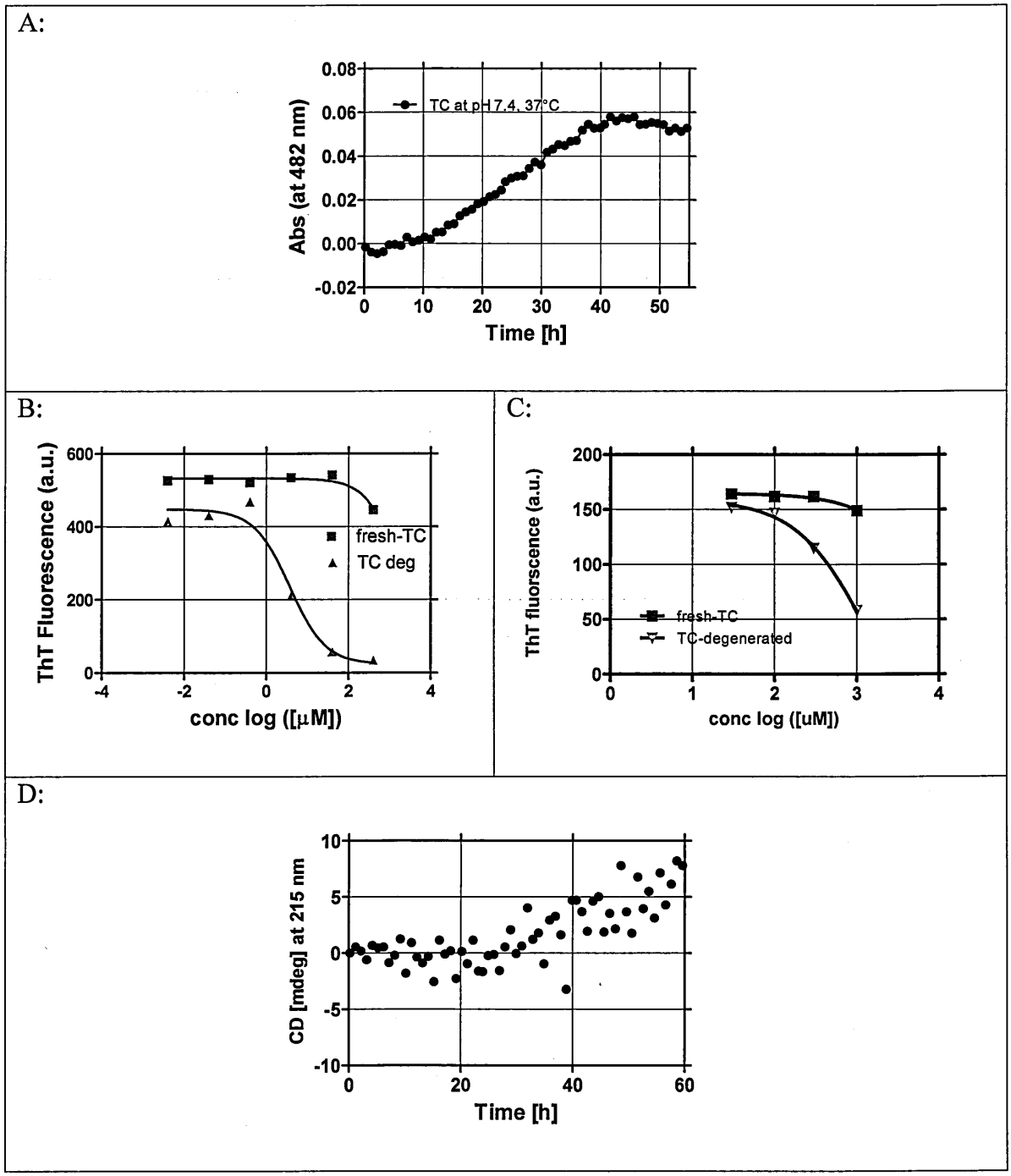

Fig. 4-27: The decomposed TC influences the ThT fluorescence and the CD measurement.

Panel A: The change of the absorbance value at 482 nm during the incubation of 700 µM TC in 50 mM PB pH 7.4 at 37°C. Panel B: Fluorescence measurement of fibrils (prepared under acidic condition) at varying concentration of fresh and decomposed TC in 50 mM PB pH 7.4. Panel C: Fluorescence measurement of fibrils (prepared under acidic condition) at varying concentration of fresh and decomposed TC in 50:50 Glycerine/50 mM PB pH 7.4. Panel D: The change of the CD value at 215 nm during the incubation of 700 µM TC in 50 mM PB pH 7.4 at 37°C.

4.3.6 No disaggregation of preformed aggregates

Several publications reported that TC is able to disaggregate preformed fibrils (Forloni et al., 2001). This was mainly done by EM and ThT measurements (Forloni et al., 2001; Ono et al., 2006b). Here we investigated the changes of the CD value at 215 nm and the ThT value upon incubation of amyloid containing samples in the presence of 300 μM TC in PB pH 7.4 at 37°C. In one experiment, 50 μM of Aβ1-42 fibrils (prepared under acidic conditions) and in another 50 μM Aβ1-42 aggregates (22°C oligomers) were incubated for up to 10 h in the presence of 300 μM TC. No changes in CD and ThT intensity were observed over this period of time (Fig. 4-29).

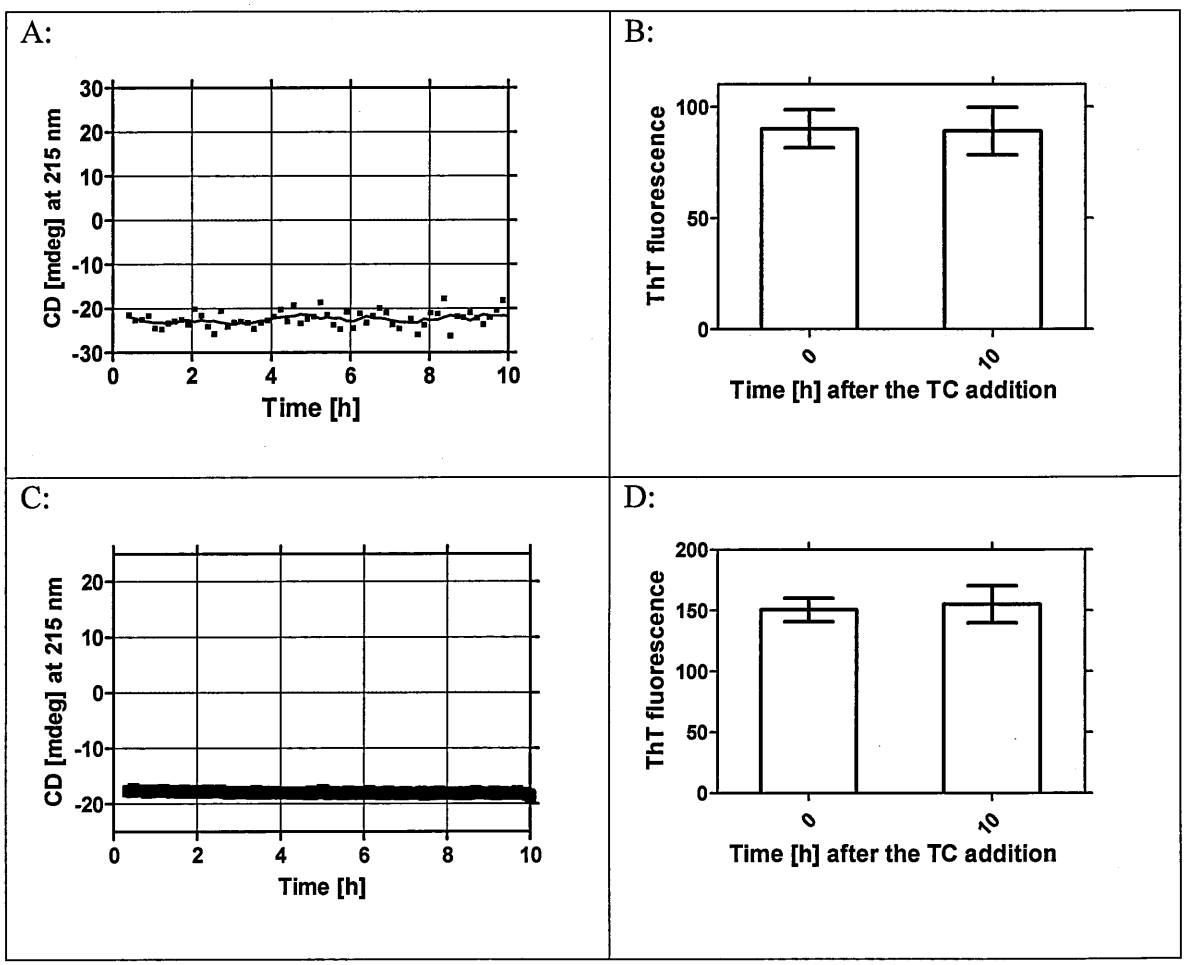

Fig. 4-28: No disaggregation of fibrils and 22°C oligomers by CD and ThT.

Fibrils prepared under acidic condition were diluted into 50 mM PB pH 7.4 to give 30 μM Aβ1-42 fibrils which were incubated in the presence of 300 μM TC at 37°C. Panel A: Time course of CD values at 215 nm. Panel B: ThT value of samples from the solution in Panel A;

22°C oligomers were diluted into 50 mM PB pH 7.4 to give 30 μM Aβ1-42 fibrils which were incubated in the presence of 300 μM TC at 37°C. Panel C: Time course of CD values at 215 nm. Panel D: ThT value of samples from the solution in Panel C.

4.3.7 DC does not reduce the plaque load in an animal model

Recently it was shown that DC is capable of disrupting TTR CR-positive amyloid deposits and decreases standard markers associated with fibrillar deposition in a transgenic mouse model for mimicking the transthyretin amyloid deposition in-vivo (Cardoso and Saraiva, 2006). To study the effect of DC on amyloid deposits in-vivo, we used Aβ fragment overproducing APP/PS1tg mice whose phenotype shows a greatly enhanced formation of plaques compared to normal APP mice (Fig. 4-29 E). After 15 month of plaque deposition, the mice were treated with DC or with physiological solution for 15 weeks. The amount of plaques, which were estimated by investigation of immunostained brain slices, did not show any reduction of the deposits in treated mice (Fig. 4-29 A, C) compared to the control mice (Fig. 4-29 B, D).

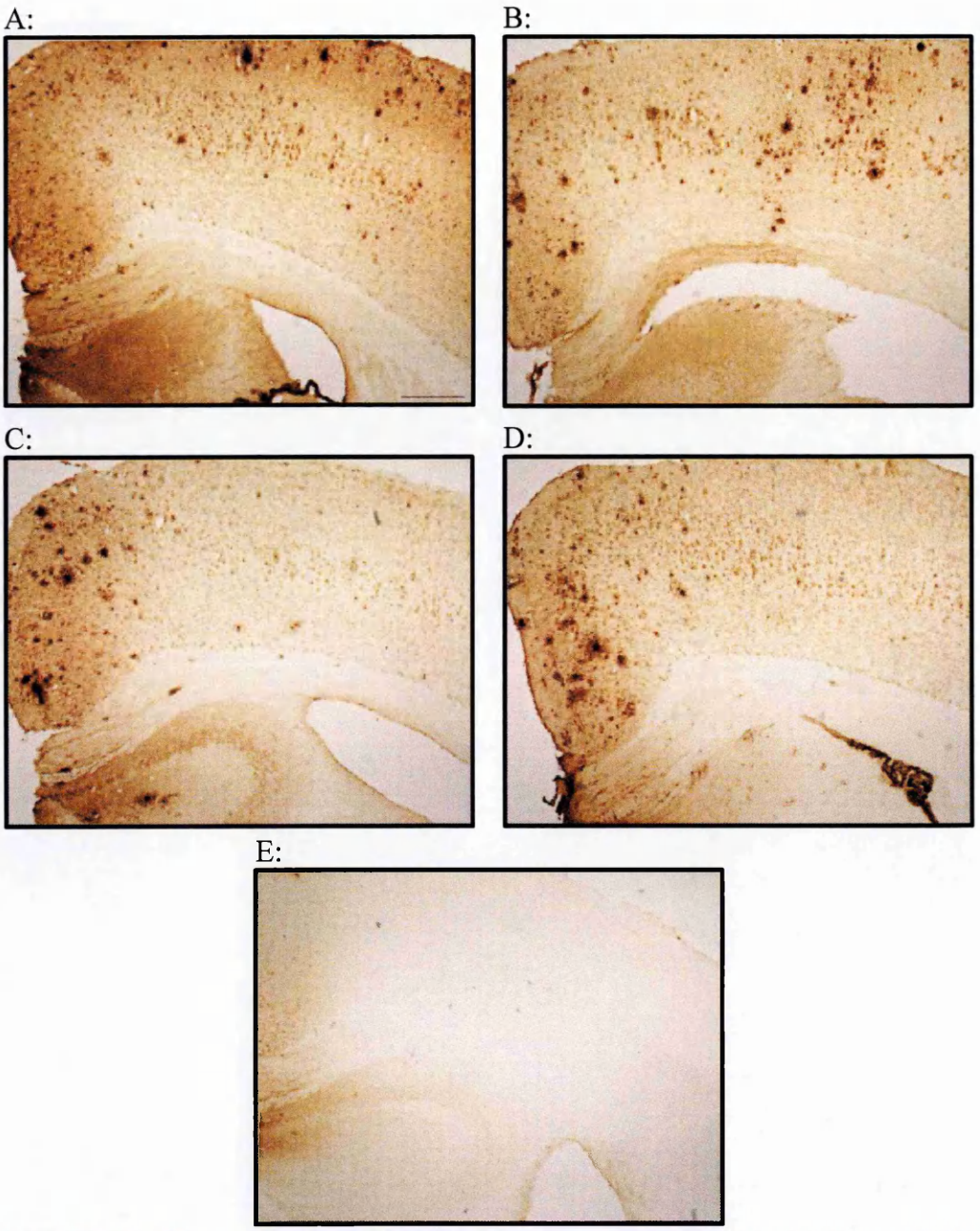

Fig. 4-29: No differences in amyloid plaque deposition after doxycycline treatment of APP/PS1tg mice.

15 month old APP/PS1tg were treated with 10 mg/kg DC or physiological solution for 20 days, after this the mice were sacrificed and the brains were removed, brain slices prepared and stained with 6E10 antibody and immonostained. Panel A, C: untreated. Panel B, D: treated animals. Panel E: normal mouse brain.

5 Discussion

The studies in literature investigating the effect of TC as anti-amyloidogenic compound are not consistent. Whereas some in-vitro studies by ThT fluorescence, EM spectroscopy and CD suggested that low concentrations of the compound reduce the formation of amyloid during incubation (Bartolini et al., 2007; Forloni et al., 2001; Hamaguchi et al., 2006) or disaggregate fibrils (Forloni et al., 2001; Hamaguchi et al., 2006), other studies did not see a pronounced effect under similar conditions (Gellermann et al., 2006; Howlett et al., 1999a). To clarify this discrepancy this project has further investigated the effect of TC upon binding to carefully characterised and well-defined preformed assemblies of various Aβ related model peptides, and possible effects on the kinetics of fibril formation.

5.1 Refinement of peptide preparations for kinetics of fibril formation

The importance of the preparation of reliable stock solution of self aggregating peptides is well known (O'Nuallain et al., 2006; Teplow et al., 2006). Initial studies using Aβ1-40 synthesised by classic peptide synthesis showed a great variability in the initial state secondary structure (Fig. 4-1 A), as monitored by the concentration-independent ratio between the CD values at 205 and 215 nm (Fig. 4-1 B). This was due to the requirement for extensive vortexing during peptide solubilisation (Fig. 4-1 C) and could be reduced by adding AcN as a co-solvent during peptide dissolution (Fig. 4-1 D) as suggested by Bartolini et al. (Bartolini et al., 2007). However, AcN also induces changes in secondary structure which in turn alter the kinetics of fibril formation (Bartolini et al., 2007). The highly soluble depsi-peptides, which are stable under acidic condition, (Coin et al., 2007; Dos Santos et al., 2005; Sohma and Kiso, 2006), have proven to be a valuable alternative, since the peptide powder readily solubilises without extensive vortexing (Fig. 4-1 D). Normally the native sequence is obtained by O-N acyl migration ("click") at neutral pH at room temperature in 2 h (Sohma et al., 2005). This can be reduced to 15 min if the temperature is increased to 37°C (Taniguchi et al., 2009). This is not always applicable, since published protocols especially for the formation of Aβ1-42 oligomers (ADDLs) and

fibrils (acidic pH) require high peptide concentration (Dahlgren et al., 2002) which would induce immediate rapid β-sheet formation at neutral pH (Fig. 4-12 D). A mixture of 5 mM NaOH and 15 mM ammonium aqueous solution clicked the peptide in less than 15 min (Fig. 4-5 F). Unwanted hydrolysis of the ester bond is reduced under these conditions and the purity of the converted peptide exceeds 95 % (Fig. 4-5 C), and should give a homogeneous monomeric state (Fezoui et al., 2000). But even the high solubility of the depsi-peptide and the low aggregation propensity (e.g. normally Aβ1-42 forms readily fibrils under acidic condition) did not exclude the formation of some ThT sensitive aggregates during work-up and storage of the peptide powder (Fig. 4-1 D). This could be due to intermolecular β-sheet formation especially between the C-termini of Aβ1-42 monomers (Tuchscherer et al., 2007). These aggregates were removed by cut-off filtration (10 kDa) of the depsi-peptide stock solution (un-converted peptide). The sequence-dependent loss of material was highest for more aggregation prone peptide Aβ1-42 (50 %) (Fig. 4-1 E). By comparison more than 90 % of the material was lost when the stock solution of the native peptide was filtered which could be due to oligomeric assemblies at basic pH (Bourhim et al., 2007). The presence of seeds in the untreated stock solution is further confirmed by the longer lag phase and the lower variability in the halftime of transition after the stock solution was filtered through a cut-off filter (Fig. 4-20 C) (Bieschke et al., 2008).

The reliable preparation of the stock solution using the depsi-peptide approach permitted the comparison of various peptide assemblies derived from Aβ fragments (initial state of Aβ1-40 compared to Aβ1-42 (Fig. 4-3 A) or Aβ1-40 compared to Aβ1-40 (A2V) mutation (Fig. 4-4 A)). The initial secondary structure state for all investigated Aβ fragments is mainly a statistical coil which conforms to literature data (Table 7-1). The two additional amino acids in Aβ1-42 increased slightly the β-sheet content. But no detectable changes in secondary structure were determined in a new mutation in the unordered N-terminus

(A2V) compared to the WT sequence (Di Fede et al., 2009) which was also supported by the identical shape of the secondary structure spectrum of the N-terminus hexapeptide (Fig. 4-4 B). Nevertheless the A2V mutation increased the propensity to aggregate (Di Fede et al., 2009; Kim and Hecht, 2008) as indicated by reduced lag phase in the in-situ ThT experiment (Fig. 4-20 A). This could be due to the higher hydrophobicity or β-sheet forming propensity of Valine over Alanine (Fig. 7-4). The binding of monomers to the structured nucleus is possibly governed by region other than the N-terminus (e.g. hydrophobic core), since binding of monomers of both variants to immobilised WT fibrils did not show any differences (Di Fede et al., 2009). Interestingly the elongation rates for both variants are similar in the in-situ ThT experiment. In NP the rate of fibril nucleation (lag phase) is the product of the monomer and nucleus concentration and the rate of fibril elongation is proportional to the monomer concentration (Powers and Powers, 2006). Since the lag phase is shorter in the MUT variant more oligomers should be present in the solution and hence should provide more sites for monomer addition and consequently should increase the rate compared to the WT peptide. Nevertheless, the models used to describe the aggregation kinetics of MUT and WT do not have to be the same. Due to the higher hydrophobicity favourable unordered aggregates could be formed which later reorganise to the more ordered amyloid structure (Auer et al., 2008; Cheon et al., 2007). Another influencing parameter is fibril fragmentation which was shown to dictate the rate of fibril elongation during agitation of β2-microglobulin on a plate reader (Xue et al., 2008) and could be the major process which deviates the rate from expected values.

The immediate formation of Aβ1-42 β-sheet structure at high peptide concentration (Fig. 4-12 D) could be an indication for lower energy barrier for monomer addition to the very first oligomers in solution (Auer et al., 2008). The monomer addition to fibrils of Aβ1-42 can be described by the NCC derived "Dock and Lock". Like Aβ1-40 (Cannon et al., 2004) and PrP82-146 (Gobbi et al., 2006), the model described the binding data of monomers to

fibrils immobilised on a SPR chip (Fig. 4-16). The initial binding step between Aβ1-42 monomers and Aβ1-42 fibrils has 2.9 times lower K_D than that previously reported using Aβ1-40 (123 μM) (Cannon et al., 2004) , mainly because of a 2-times slower dissociation rate constant (Table 4-2). The following conformational changes appeared not to be different between the two peptides.

5.2 Preformed assemblies and toxicity

We further characterised different assemblies of the Aβ1-42 peptide using protocols developed in this work (cut-off filtration of depsi-peptide and switching under slight basic condition, see section 7.3) or in the literature. This allowed preparation of different solution like initial state solution (immediately after dissolution of the basic stock solution in the buffer of interest), oligomers (Aβ derived diffusible ligands or ADDLs, (Lambert et al., 1998)), 22°C oligomers (Lauren et al., 2009) or fibrils (Stine et al., 2003). Results from physical-chemical experiments using the depsi-peptide approach (Fig. 4-6) strongly confirmed that the peptide is at its very initial state, possibly in the form of monomers (Hepler et al., 2006), although our data do not allow to exclude the presence of very small unstable oligomers in dynamic equilibrium with monomers (Bernstein et al., 2009; Bitan et al., 2003a; Rangachari et al., 2007). Interestingly the behaviour between fibrils and oligomers (ADDLs and 22°C oligomers) differed in SEC analysis. Most of the fibrils were blocked by the filter at the top of the SEC column, whereas ADDLs and 22°C oligomers show a second peak appearing in the SEC void volume which is greatly enhanced in the 22°C oligomers (Fig. 4-6 F) and which further correlated with the increase in ThT fluorescence (Fig. 4-28 D). This finding suggests that ADDLs and 22°C oligomers constitute a ThT sensitive β-sheet like state, as suggested by others (Finder and Glockshuber, 2007; Glabe, 2008). Recent data further support the toxic role of β-sheet assemblies which could be dimer up to tetramer in the case of Aβ1-40 (Ono et al., 2009). Since fibrils and oligomers are ThT sensitive, a similar structural motif could be present in

fibrils and toxic oligomers. The variance in toxicity could depend on the size of the otherwise similar structure. This is supported by the fact that only sonicated fibrils but not fibrils by themselves show a concentration dependent toxicity (Fig. 4-10 B). Nevertheless, we cannot exclude that the amount of other toxic oligomeric forms is enhanced after sonication due to the shift in the equilibrium since more monomers could be released from the fibrils to form toxic oligomeric species in solution (Pastor et al., 2008). In variance with the literature (Pastor et al., 2008) Aβ1-42 initial state solution is toxic similar to the ADDLs or 22°C oligomers solution (Fig. 4-10 A), but less toxic than sonicated fibrils (Fig. 4-10 B). This could be due to the rapid formation of toxic oligomers under experimental condition (Bitan et al., 2003a). In addition, toxic β-sheet species may be formed by interaction with the cellular membrane, since membrane mimicking reagents like SDS have been shown to induce stable toxic β-sheet oligomers (Barghorn et al., 2005a; Rangachari et al., 2007; Yu et al., 2009). The size of these oligomers is thought to be a dodecamer (Bernstein et al., 2009) possibly a basic unit of various detected toxic oligomers like the ADDLs (Roychaudhuri et al., 2009).

5.3 TC and its binding to Aβ assemblies

The methods used in this work - changes in CD values, SPR, fluorescence - investigating the binding of TC to the preformed fibrils were not able to detect differences compared to the control experiment (Fig. 4-23). Even given that SPR is sensitive enough to detect binding of CR or the Aβ1-6 hexapeptide (Di Fede et al., 2009) to fibrils, TC flown over preformed fibrils for long period of time did not alter the signal (Fig. 4-23 C). One reason could be that ligands with different modes of interaction to the fibril substructure could bind at different sites like fibril ends, between monomers of β-sheets or the fibril core at varying stoichiometry. For instance CR may interact with fibrillar β-sheets in 1:1 stoichiometric ratio of monomer (bound in the fibril) by binding to the fibril surface (Roterman et al., 2001) as also proposed for the Aβ peptide (Carter and Chou, 1998). The

surface binding is supported by the finding that the sensorgram in SPR of fibrils and sonicated fibrils are similar (Fig. 4-23 D). Nevertheless, ThT exhibiting a pronounced increase in fluorescence (Fig. 4-6 D) did not show binding to immobilised fibrils in SPR (Fig. 4-23 E). This could be explained by a low binding ratio 1:115 between the ligand and fibril bound monomer (LeVine, 2005) which would dramatically reduce the amount of compound bound to the fibril surface which is thought to be in a cavity of the fibril (Groenning et al., 2007). In addition, the two times lower molecular weight of ThT compared to CR could be responsible for the negative SPR, since under these circumstances the detection limit of the instrument could be reached. A low binding ratio could also explain the negative results in SPR experiments using TC. Inbar et al. also demonstrated the low amount of bound TC (Inbar et al., 2008). In this study the anti-body binding capability to preformed fibrils was reduced only by 20 % in the presence of TC with a notable low IC50 of 8.7 μM. Nevertheless, the unchanged fluorescence values reported in this work do not support this hypothesis, since TC can change its fluorescence spectrum upon binding to metal ions (Schneider et al., 2003). In the end, one question always stands out, since already the slightest variation in the fibril forming condition changes the morphology of the final aggregate (Petkova et al., 2005). "How relevant are these in-vitro formed structures?" Possibly the fibrils formed in this work vary in structure and stability compared to the aggregates formed by others (Ono and Yamada, 2006; Ono et al., 2003; Tagliavini et al., 2000). Nevertheless, TC has been reported to disaggregate fibrils derived from different peptide sequences which would suggest a more general mechanism. Additionally, the conditions used in other publication favour also the formation of off fibril pathway aggregates. The exclusive preparation of fibrils, like done in this work and shown by AFM and other techniques, allowed the investigation of the binding capability of the ligand to them.

A constantly claimed mechanism of action of TCs is the disaggregation of preformed fibrils (Forloni et al., 2001; Ono and Yamada, 2006). We followed the changes CD intensity at 215 nm and ThT fluorescence of fibrils and 22°C oligomers in the presence of TC over a time period of 10 h (Fig. 4-28). No changes were observed. This would not exclude the possibility that fibrils were fragmented, as was shown to happen in case of β2-microglobulin fibrils in the presence of ThT as result of laser irradiation (Ozawa et al., 2009). Nevertheless, the secondary structure is still in β-sheet and the ThT is as high as in the beginning of our experiment. In fact, fragmentation could induce toxicity due to the higher mobility of smaller species similar to the increase in toxicity of sonicated fibrils which could worsen the situation in-vivo (Fig. 4-10 B). Nevertheless, no reduction of the plaque load in an Aβ over expressing mouse model is seen after DC treatment which suggests that no disaggregation takes place in-vivo (Fig. 4-29).

5.4 TCs and the kinetics of fibril formation of Aβ

Binding to fibril surface shouldn't hinder the elongation of fibrils, especially when no secondary fibril growth on surface takes place. Aβ fibrils are thought to be long and unbranched (Fig. 4-23 E) (Andersen et al., 2009), which suggests no fibril surface induced fibril growth. The rate of elongation was tested by following the random-coil to β-sheet transition by in-situ ThT and CD experiment of Aβ1-40, Aβ1-42 and Aβ14-24 and binding of monomers to Aβ1-42 fibrils by SPR without and in presence of TC. Aβ14-24 has been demonstrated to be a convenient tool to test the potential of small compounds for altering the kinetics of aggregation (Camus et al., 2008). The model expresses the usual features of NP with lag phase and additional fibril growth (Fig. 4-18 C) which depend on the temperature and the peptide concentration (Fig. 4-18 D, E). Any change in the polymerization characteristic parameters (lag phase, rate of elongation, final plateau) could give information about the possible mechanism of action. Especially the change in the lag phase could indicate an interaction of the ligand with more toxic oligomers which are

thought to be formed in the early stages of the polymerization process. Nevertheless, despite of the differences of the final plateau values in the in-situ ThT experiment of Aβ1-40 depending on the TC concentration, no parameter of the kinetics was altered in any experiment carried out to investigate the effect of TC (Fig. 4-24). Several explanations for the difference in the final plateau of the in-situ ThT experiment are possible. First, the critical concentration of fibril formation is different and more unpolymerised monomers are in solution which then gives also different elongation rates. Second, the variation in fibrillar structure might alter the binding capability of ThT which in turn gives a different value but leaves the critical concentration unchanged. Under this assumption we normalised the traces with maximum ThT value. We found no change in the parameters of the kinetics. Third, the compound interferes with the ThT measurements. Several recent studies demonstrated the insufficiency of ThT fluorescence measurements to judge the potential of a compound and, more important showed that small compounds like Rasvertrol or Rifampicin bias the ThT results (Hudson et al., 2009; Meng et al., 2008). Fresh TC only slightly interfered with the ThT-test (Fig. 4-27 B), but decomposed TC, which is easily formed at 37°C and was even enhanced by increasing temperature (Fig. 4-25 C), reduced the ThT-value to nearly zero with a low IC50 (Fig. 4-27 B). This is possibly due to quenching since the absorbance of the decomposed TC increased at the ThT important emission wavelength at 482 nm (Fig. 4-27 A). This was confirmed in a fibril free high viscose aqueous glycerin solution (Fig. 4-27 C) which could be used as a general tool to investigate the interference of a compound with the ThT-test. The decomposition has an impact on the CD transition monitored at 215 nm as well, since it could diminish the total CD value at this wavelength (Fig. 4-27 D). Because of the instability of TC the incubation was restricted to 10 h. This excluded non agitated CD or ThT experiments together with the stirring experiments at low peptide concentration which gave a flow induced alignment of fibrils with a similar CD spectra seen by Linear

Dichroism (LD) spectroscopy (Fig. 4-13) (Dafforn et al., 2004) which is inverted in CD spectroscopy (Adachi et al., 2007). The invariance of the kinetic parameters further supports the finding that TC does not bind to the preformed assemblies discussed in the previous section.

The binding of monomers to immobilised fibrils in presence of TC probes also the association of TC to free monomers in solution. In aqueous solutions Aβ monomers appear to be largely unstructured with several regions adopting weak β-strand and α-helix conformations (Yang and Teplow, 2008). One can speculate that helix stabilization could hinder the aggregation to β-sheet containing assemblies (Nerelius et al., 2009), since the equilibrium could shift from helical to β-sheet secondary structure during aggregation (Takeda and Klimov, 2009). Interesting is the fact that TC was suggested to bind to α-helical prion fragments (Ronga et al., 2007). Nevertheless, the unchanged aggregation rate in the kinetic experiments and especially the unchanged SPR sensorgrams during the fibril elongation in the presence of TC did not support this mechanism of action.

Only a few kinetic data concerning the fibril formation of Aβ in the presence of TC are available in literature. A complete kinetic data set by means of a CD experiment showed no change of the lag phase of Aβ1-42 but a slower elongation rate (Bartolini et al., 2007). Nevertheless since the authors do not show the plateau after the transition, this change could also be due to a different β-sheet conformation, the decomposition of the TC during the experiment or the sedimentation of the aggregates. The only ThT-kinetic data available show a very high efficiency of reducing the fibril formation potential, fibril elongation and fibril destabilization by TC of the Aβ1-40 and Aβ1-42 (Ono and Yamada, 2006) and α-synuclein (Ono et al., 2006a). In these experiments a concentration dependent reduction of the ThT value at the plateau is observed (Fig. 5-1A). Nevertheless the normalised traces are nearly super-imposable (Fig. 5-1B), thus questioning the interpretation that the kinetics of fibril formation is affected by the compound. Furthermore, the time period of the

experiment was six days which could lead to false positive results due to TC decomposition.

A: B:

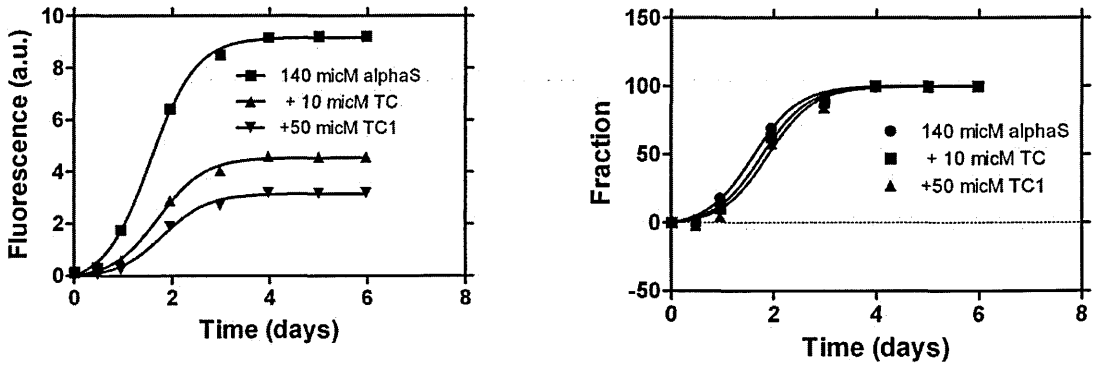

Fig. 5-1:Alpha synuclein in the presence of different concentration of Tetracycline (A) original data (B) normalization by the final value (Ono and Yamada, 2006)

In another study, Kirschner et al. used X-ray diffraction studies to determine the variation of the total amount of β-crystallite, the fibril length and the fibril width in the presence of anti-amyloidogenic compounds (Kirschner et al., 2008). TC was tried on Aβ11-25 and Aβ12-28. It was found that the length and the intersheet stacking of Aβ11-25 are not altered by the compound. Only the overall intensity (amount) is diminished (Fig. 5-2).

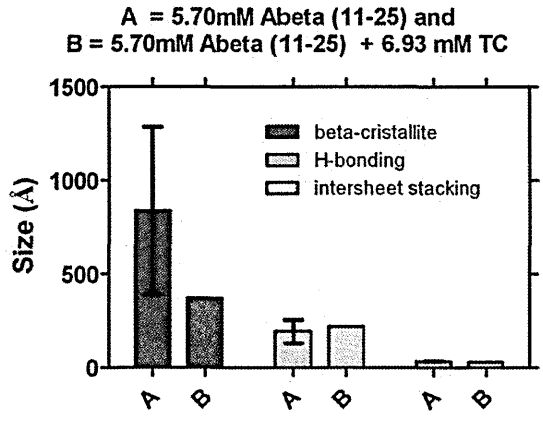

Fig. 5-2: Amount of β-structure, fibril length and intersheet stacking of Aβ11-25 with and without Tetracycline determined by X-ray diffraction patterns (adapted from Kirschner et al. (Kirschner et al., 2008))

In case of Aβ12-28 a concentration dependent decrease of the fibril length was observed. Nevertheless, this study uses extreme high peptide and compound concentrations which might produce aggregates which are not present in-vivo. Furthermore the high variability

of the results and the missing standard deviation for the experiment in the presence of the compound are not satisfactory. Another caveat in the experimental setup is the use of water for the preparation of the fibrils and stock solutions of the compounds. Since TC hydrochloride is used a change in the pH of the solution can be expected which could affect the aggregation process.

In comparing the in vitro studies reported in this thesis with the results of in-vivo or in-vitro experiments on the effect of TCs reported in literature, it cannot be ruled out that TCs may have alternative targets, not necessarily Aβ. In addition, toxic Aβ species other than the ones investigated may provide alternative sites of TCs action. Especially, the so called A11 positive pre-fibrillar oligomers (Kayed et al., 2003) which are different to the soluble fibrillar oligomers (e.g. ADDLs, amylospheroids) (Kayed et al., 2007; Noguchi et al., 2009) could not be detected under any of the experimental conditions used in this work (Fig. 4-8 B). For instance, it was shown that RTC inhibited the formation of A11 positive species but not the fibrillization of Aβ1-42 (Necula et al., 2007b). Nevertheless, RTC like TC is unstable and gave no reliable results from which we could draw a final conclusion (Fig. 4-26). It seems that the lag phase is not changed which would suggest the presence of only a small amount of RTC sensitive oligomers, if any, which do not change the overall monomer concentration significantly and hence do not alter the kinetics of fibril formation. Nevertheless, the relevance of A11 positive species can questioned since a recent study demonstrated that only the level of soluble fibrillar oligomers and not A11 positive pre-fibrillar oligomers correlated with the cognitive decline in transgenic mouse models (Tomic et al., 2009).

Finally, several studies focused on the therapeutic potential of TCs in AD suggesting that at least MC could act as neuroprotective agent affecting various pathways (Kim and Suh, 2009). MC reduces microgliosis, caspase-1 activity, formation of interleukin 1b, metalloprotease activity, and production of cyclooxygenase and prostaglandins. MC has

also been shown to reduce nitric oxide (NO) levels by inhibition of p38 activation (Lin et al., 2001). NOs are known to inhibit the mitochondrial respiration (Brown and Borutaite, 2006) which is thought to play an important role of mitochondrial dysfunction in the pathogenesis of AD. Interesting to this concern is the fact that oligomeric and fibrillar species of Aβ1-42 impair mitochondrial function in P301L tau transgenic mice (Eckert et al., 2008). TC has been found to decrease NO-levels as well (D'Agostino et al., 1998). Furthermore, the radical scavenging potential TCs could positively influence the symptoms of the disease (D'Agostino et al., 1998; Kim and Suh, 2009). Thus a range of mechanism other than direct action on Aβ species may be relevant to therapeutic application of TCs.

6 Conclusion

Thus, in conclusion, the possibility of TCs as therapeutics for AD as related to the specific target of suppression of amyloid formation appears not to be supported by the experiments reported here. However, the challenge of producing a reproducible system of amyloid fibril formation, monitored by AFM and other techniques, has created new opportunities for physical studies of an important polymerization process. Depsi-peptides permit a reliable and reproducible preparation of Aβ assemblies and greatly reduced the variability of a single kinetic experiment, which lowers the number of repetition and the amount of used material. The formation of the native sequence under slightly basic condition kept the hydrolysis of the ester bond at a minimum and allowed the preparation of the different Aβ species to investigate binding of Aβ ligands like monomers or small compounds by various physico-chemical techniques. In this way, it was shown that, similar to Aβ1-40, the fibril elongation of Aβ1-42 follows the "Dock and Lock" mechanism and that a mutation in the N-terminus (A2V) enhances the kinetics of fibril formation. In future work, kinetic studies of these systems can be extended by a) the additional knowledge of the formation of different oligomeric forms suitable for seeded growth of fibrils; and b) seeded polymerisation could now be used to allow better definition of the kinetic parameters for polymerization and depolymerisation. In addition, the structural studies on Aβ amyloids could be complemented by the preparative techniques developed here, to allow correlations between polymerization conditions and resultant structures to be sought under more controlled condition.

Care has to be taken if TCs are used in kinetic experiments, since their decomposition could interfere with the experimental outcome. We demonstrated for the first time that decomposed TC, but not fresh TC, dramatically reduced the ThT value. We propose the use of a fibril-free aqueous Glycerine solution to evaluate the disturbance of the ThT fluorescence by TCs and other compounds.

Taking into consideration the instability of TC, it was concluded that neither binding to preformed assemblies nor kinetic parameters are altered by the compound under condition applied in these studies. Since only monomers or fibrillar aggregates (oligomer or fibril) were possibly present in our studies, one possible target left for further investigation is A11 positive pre-fibrillar species. Nevertheless the multitude of targets of the compounds in various pathways of the brain could contribute even more to the positive effect of TCs in animal studies and might be also worth investigating.

7 Appendix

7.1 *Secondary structure of Aβ related fragments determined by various techniques*

Table 7-1: List of publication concerning the determination of the secondary structure of various Aβ fragments

Sequence	Structure/conformation	Experimental conditions	Methods	reference
Aß1-40	Cross-ß	water	FD	(Malinchik et al., 1998)
Aß1-28	Fibrillar, cross-ß	aqueous	EM, FD	(Kirschner et al., 1986)
Aß10-35	ß-sheet (parallel), in register	PH 3.7 or pH 7.4 STEM,	ssNMR	(Antzutkin et al., 2002)
Aß1-42	ß-sheet, in-register parallel	Aqueous, pH 7.4	EM, STEM, ssNMR	(Talafous et al., 1994)
Aß1-28	α-helix, bend at 12	Membrane mimic, SDS and TFE	NMR	(Talafous et al., 1994)
Aß1-40	1-10, disordered; 12-24 and 30-40, ß-strand; 25-29, a bend	Aqueous, pH 7.4	x-ray, EM, ssNMR	(Petkova et al., 2002)
Aß1-28	Random coil	Water (pH1-4)	CD	(Barrow and Zagorski, 1991)
Aß1-28	α-helix; increased temperature leads to decrease in helix, 13-20 remain most stable helix	TFE (4-7)	NMR	(Barrow and Zagorski, 1991)
Aß1-39	Random coil and ß-sheet	Aqueous (pH 7.3)	CD	(Barrow and Zagorski, 1991)
Aß1-39	α-helix	TFE (30%) (pH 1-4, 7-10)	CD	(Barrow and Zagorski, 1991)
Aß1-42	ß-sheet	water	CD	(Barrow and Zagorski, 1991)
Aß1-40	α-helix 10-24 and 28-42	SDS (pH 7.2)	NMR	(Shao et al., 1999)
Aß1-42	α-helix 10-24 and 28-42	SDS (pH 7.2)	NMR	(Shao et al., 1999)
Aß1-28	a-helix; increased temperature leads to decrease in helix, 13-20 remain most stable helix	TFE (4-7)	NMR	(Zagorski and Barrow, 1992)
Aß1-28	ß-sheet Water	(pH4-7)	CD	(Zagorski and Barrow, 1992)
Aß1-28	Not α-helical, extended strand	Water (pH5.6)	NMR	(Lee et al., 1995)
Aß1-28	C-terminal a-helix, N-terminal turn (flexible)	DMSO	NMR	(Sorimachi and Craik, 1994)
Aß1-39	ß-sheet (60%)	Aqueous (pH 7.4)	CD	(Shen and Murphy, 1995)
Aß12-28	a-helix 16-24	SDS (pH2.6)	NMR	(Fletcher and Keire, 1997)
Aß10-23	ß-sheet (antiparallel)	Solid state	FTIR	(Hilbich et al., 1991)

Aß10-43	80% ß-sheet	Water	CD	(Hilbich et al., 1991)
Aß10-43	28% α-helix	HFIP	CD	(Hilbich et al., 1991)
Aß25-35	ß-sheet PH5.5, pH 7.4 Aß29-42 ß-sheet (antiparallel)	Solid state	FTIR	(Hilbich et al., 1991)
Aß25-35	ß-sheet	Aqueous (pH 7.4)	CD	(Hilbich et al., 1991)
Aß10-35	ß-sheet (parallel), in register	Dried from water (pH 7.4)	ssNMR	(Benzinger et al., 1998)
Aß10-35	ß-sheet (parallel), in register	Dried from water (pH 7.4)	ssNMR	(Benzinger et al., 1998)
Aß10-35	ß-sheet (parallel), in register	Dried from water (pH 7.4)	ssNMR	(Burkoth et al., 2000)
Aß16-22	ß-sheets (antiparallel)	1.0 mM phosphate buffer, pH 7.0 EM,	ssNMR	(Balbach et al., 2000)
Aß25-35	ß-sheet > random coil (decreased concentration)	Aqueous (pH4, 5)	CD	(Terzi et al., 1994)
Aß34-42	ß-sheet (antiparallel)	aqueous	FTIR, ssNMR	(Lansbury et al., 1995)
Aß1-40	α-helix 15-36, kink 25-27	SDS (pH 5.1)	NMR	(Coles et al., 1998)
Aß1-40	α-helix 15-23, 31-35	TFE (40%) (pH 2.8)	NMR	(Sticht et al., 1995)
Aß1-40	ß-sheet (parallel, in-register)	Aqueous (pH 7.4)	ssNMR	(Antzutkin et al., 2000)
Aß1-40	ß-sheet (parallel, in-register), residue 1-9 without structure	PBS (140 mM NaCl, 3 mM KCl, 10 mM phosphate, pH 7.4)	ssNMR	(Balbach et al., 2002)
Aß1-42	ß-sheet 18-26, 31-42(parallel, in-register)	10 mM TRIS (150 mM NaCl, pD 7.7)	HDex-NMR	(Luhrs et al., 2005)
Aß11-25	β-sheet antiparallel (register pH dependent and differs to Aβ16-22); ssNMR and X-ray inconsistent	aqueous pH 7.4, 2.4	ssNMR, X-ray	(Petkova et al., 2004)
Aß1-40	Quaternary structure of fibrils		MD, theor. X-ray	(Buchete et al., 2005)
Aß1-40	Quaternary structure of fibrils		ssNMR	(Petkova et al., 2005)
Aß1-40	Random state of the initial solution	PB (pH 7.4)	CD	(Bieschke et al., 2008)
Aß1-42	Random state to β-sheet transition	PB (pH 7.4) + low amount of AcN	CD	(Bartolini et al., 2007)
Aß1-40/42	Random state of the initial solution	PB (pH 7.4)	CD	(Rangachari et al., 2007; Rangachari et al., 2006)
Aß1-40/42	α to β sheet transition	PB (pH 7.4) + SDS	CD	(Rangachari et al., 2007; Rangachari et al., 2006)
Aß1-40	Random state of the initial solution	PB (pH 7.4)	CD	(Gursky and Aleshkov,

				2000)
Aß1-40	Random state of the initial solution	Borate buffer (pH 9)	CD	(Klement et al., 2007)
Aß 1–9 Aß 1–16 Aß 1–28 Aß 12–28 Aß 16–21 Aß1-40	Random state of the initial solution	PB (pH 7.4)	CD	(Danielsson et al., 2005)
Aß 25–35	Anti-parallel β-sheet of the initial solution	PB (pH 7.4)	CD	(Danielsson et al., 2005)
Aß1-40/42	Random state of the initial solution	PB (pH 7.4)	CD	(Macao et al., 2008)

7.2 *Chemistry of solid state peptide synthesis (adapted from (Kirin et al., 2007)*

7.2.1 Fmoc deprotection

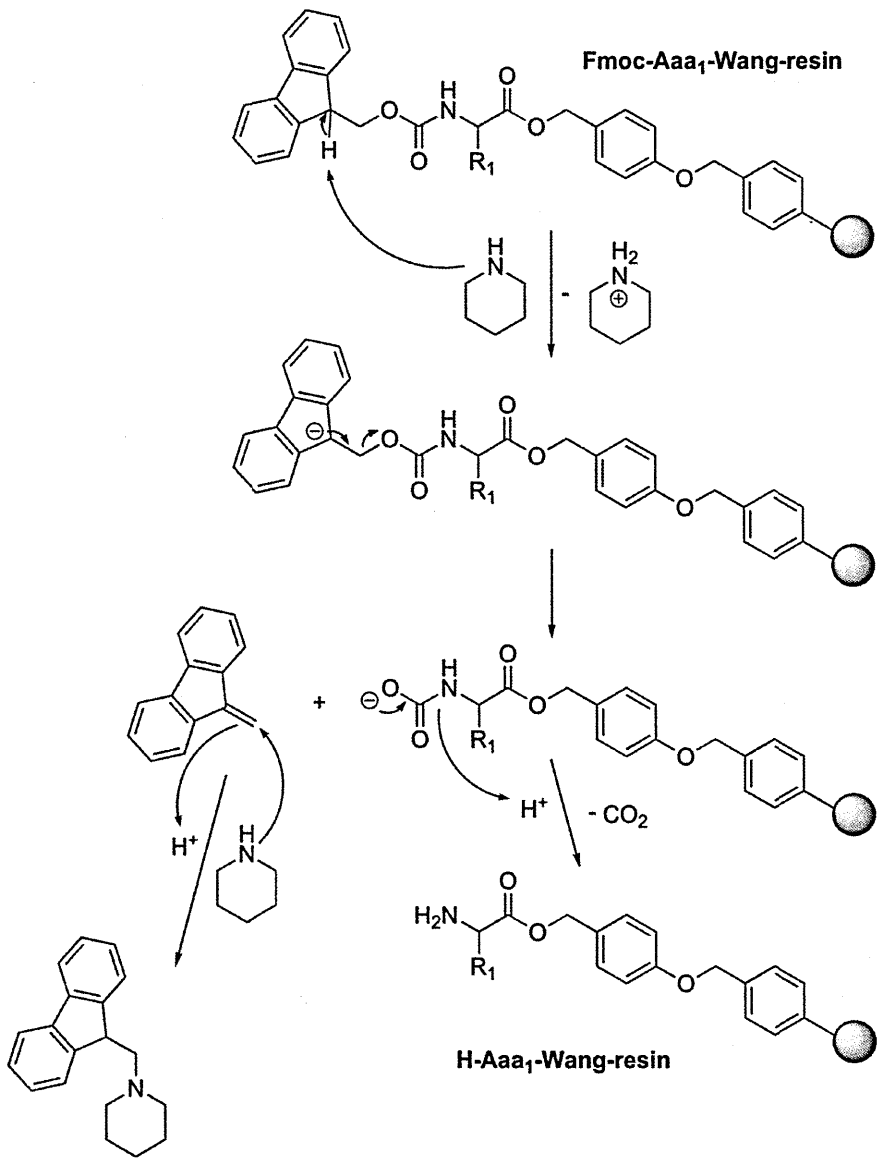

Fig. 7-1: Mechanism by arrow pushing of the removal of the Fmoc Nα-protecting group.

7.2.2 Amino acid coupling

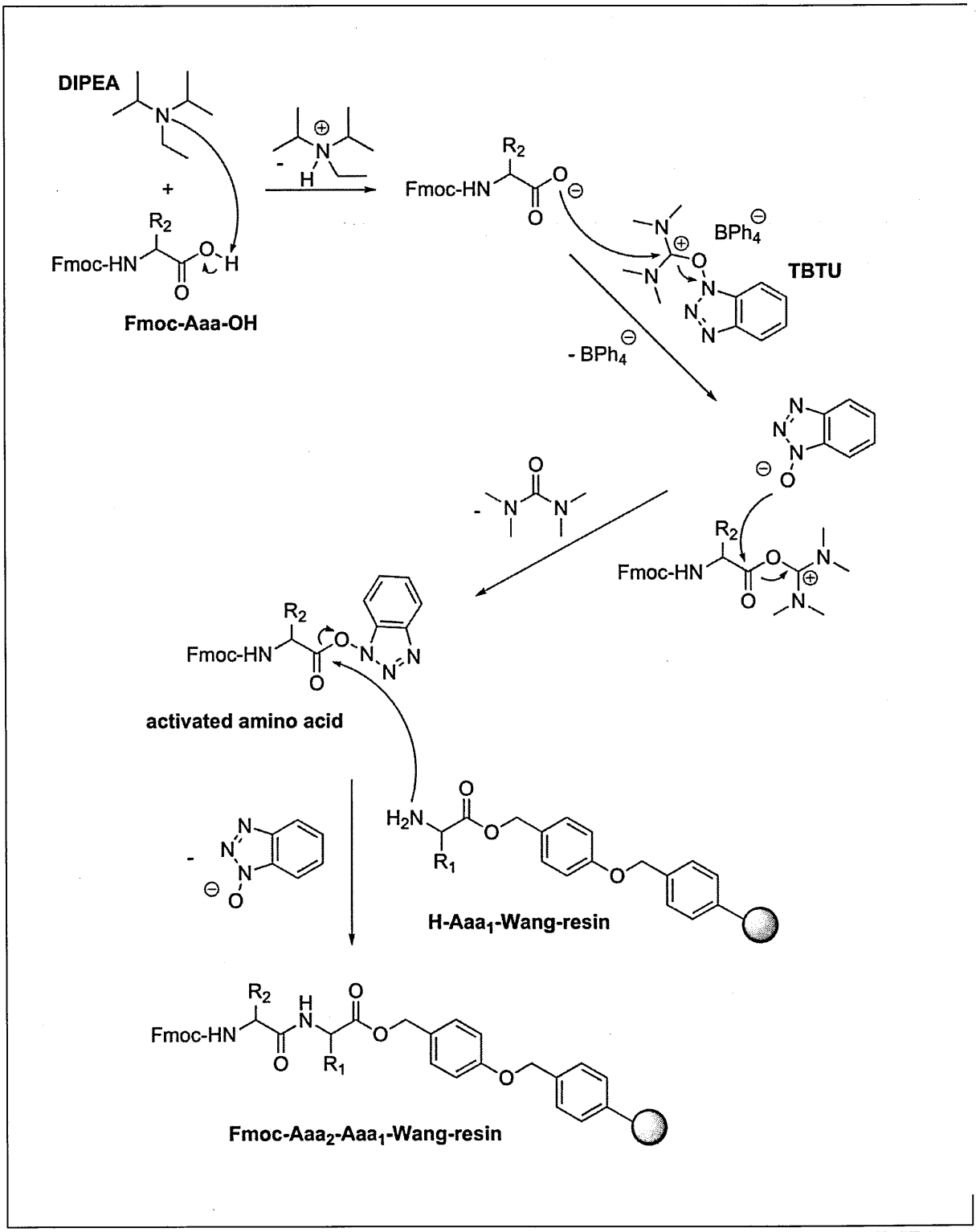

Fig. 7-2: Mechanism by arrow pushing of the coupling reaction using TBTU in the presence of DIEA.

7.2.3 Final deprotection from the resin and side chain deprotection

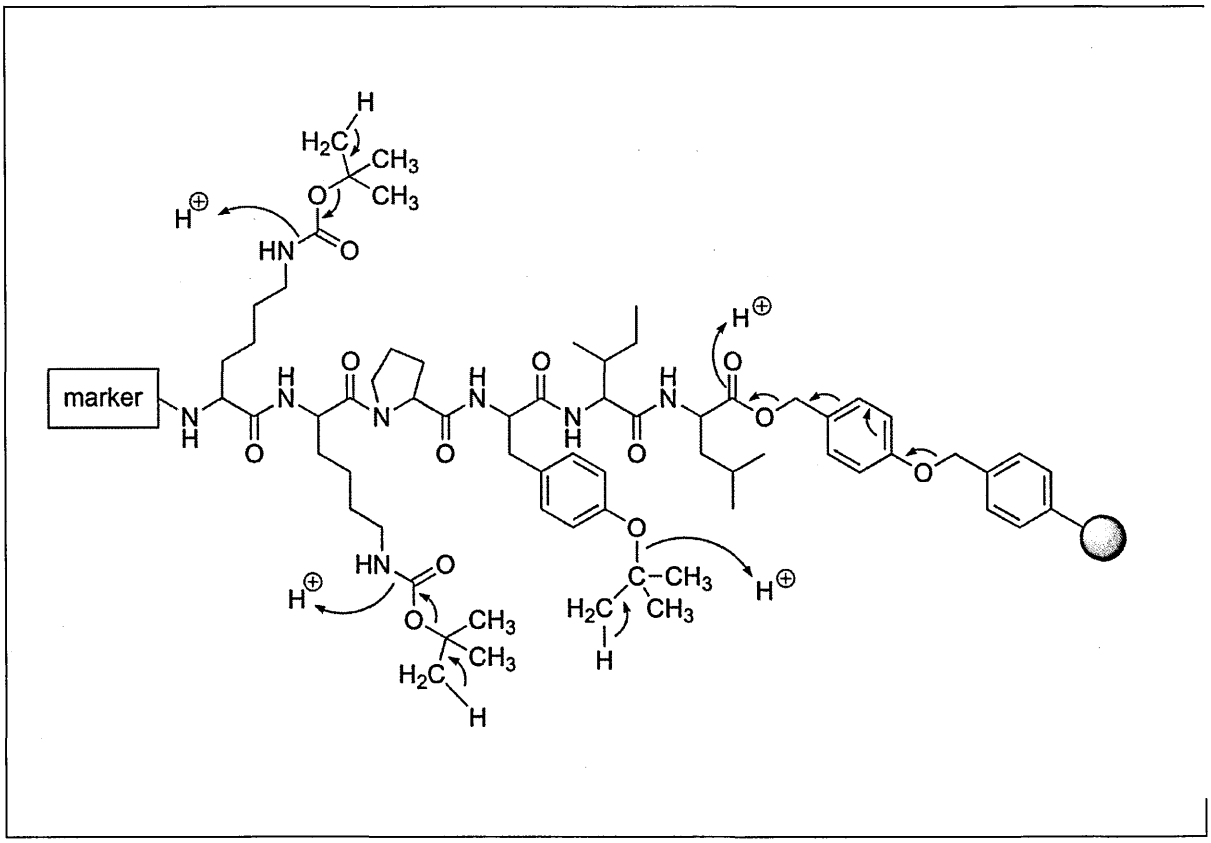

Fig. 7-3: Mechanism by arrow pushing of deprotection reaction of tBu and cleavage of a peptide from Wang resin.

7.3 Initial state and sample preparation

7.3.1 Preparation of stock solutions of Depsi-Aβ1-40/1-42

Depsi Aβ was dissolved in an acidic solution (TFA 0.02%, pH <3) at a concentration of about 1 mg/ml and centrifuged through a 10 kDa cut-off filter (YM-10, Millipore) at 14000g. The filter was washed two times by addition of same acidic solution and the centrifugation step was repeated. The loss of material using this procedure is around 40%. The final concentration of Aβ in the filtered solution was determined with UV-absorption, using the theoretical molar extinction coefficient at 280 nm (1490 M^{-1} cm^{-1}) (Pace et al., 1995) or at 214 nm like suggested by Kuipers et al. (Kuipers and Gruppen, 2007). Final concentration of Depsi Aβ1-42 was usually higher than 90 μM. This stock solution was flash frozen in dry ice/ethanol and stored at -80°C. These samples were used within 2 weeks.

7.3.2 Formation of native Aβ and sample preparations

The filtered acidic stock solution was concentrated with a 3 kDa cut off filter (YM-3, Millipore) to around 300 μM. Then, the native sequence was obtained by adding 0.5 M NaOH:ammonium (1:3) solution on ice to give a pH >10.5. This solution was diluted to 1 μM in PBS and used immediately ("initial state solution"). To prepare Aβ1-42 fibrils, the stock solution was diluted with water to 100 μM Aβ, acidified to pH 2.0 with 1 M HCl and left for 24 h at 37°C (Stine et al., 2003). To obtain Aβ1-42 oligomers, the stock solution was diluted to have 100 μM peptide in 50 mM phosphate buffer, 150 mM NaCl, pH 7.4, and incubated for 24 h at 4°C(Lambert et al., 1998).

7.4 *The sequence dependant properties which influence the aggregation of the Aβ mutation (A2V) compared to the WT sequence*

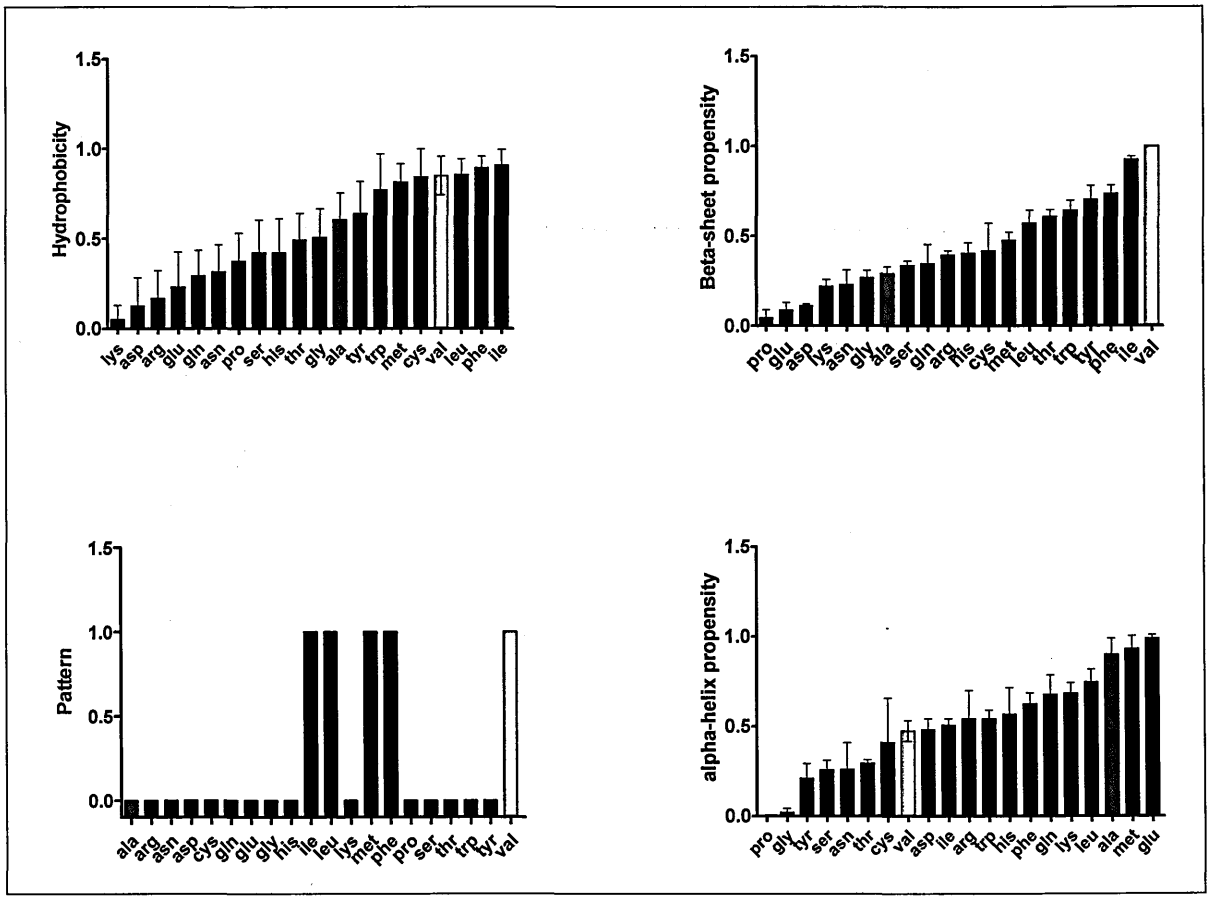

Fig. 7-4: The amino acid dependant hydrophobicity, β-sheet propensity, contribution to a hydrophilic, hydrophobic pattern and α-helix propensity; Alanine (WT) and Valine (MUT) are highlighted.

8 Bibliography

Adachi R, Yamaguchi K, Yagi H, Sakurai K, Naiki H and Goto Y (2007) Flow-induced alignment of amyloid protofilaments revealed by linear dichroism. *J Biol Chem* **282**(12):8978-8983.

Aitken JF, Loomes KM, Konarkowska B and Cooper GJ (2003) Suppression by polycyclic compounds of the conversion of human amylin into insoluble amyloid. *Biochem J* **374**(Pt 3):779-784.

Albert A (1953) Avidity of terramycin and aureomycin for metallic cations. *Nature* **172**(4370):201.

Albert A and Rees CW (1956) Avidity of the tetracyclines for the cations of metals. *Nature* **177**(4505):433-434.

Aleksandrov A and Simonson T (2009) Molecular mechanics models for tetracycline analogs. *J Comput Chem* **30**(2):243-255.

Ali FE, Separovic F, Barrow CJ, Cherny RA, Fraser F, Bush AI, Masters CL and Barnham KJ (2005) Methionine regulates copper/hydrogen peroxide oxidation products of Abeta. *J Pept Sci* **11**(6):353-360.

Allsop D, Mayes J, Moore S, Masad A and Tabner BJ (2008) Metal-dependent generation of reactive oxygen species from amyloid proteins implicated in neurodegenerative disease. *Biochem Soc Trans* **36**(Pt 6):1293-1298.

Alzheimer A (1907) Über eine eigenartige Erkrankung der Hirnrinde. *Zentralblatt für Nervenheilkunde und Psychiatrie* **30**:177-179.

Amblard M, Fehrentz JA, Martinez J and Subra G (2006) Methods and protocols of modern solid phase peptide synthesis. *Molecular Biotechnology* **33**(3):239-254.

Andersen CB, Yagi H, Manno M, Martorana V, Ban T, Christiansen G, Otzen DE, Goto Y and Rischel C (2009) Branching in amyloid fibril growth. *Biophys J* **96**(4):1529-1536.

Anderson HH (1955) Antibiotics Annual 1953-54: (Proceedings of the Symposium on Antibiotics), 632 pages, with index. HENRY WELCH, Ph.D., Chairman. Medical Encyclopedia, Inc., New York, 1953. *Am J Trop Med Hyg* **4**(1):157-a-.

Antzutkin ON, Balbach JJ, Leapman RD, Rizzo NW, Reed J and Tycko R (2000) Multiple quantum solid-state NMR indicates a parallel, not antiparallel, organization of beta-sheets in Alzheimer's beta-amyloid fibrils. *Proc Natl Acad Sci U S A* **97**(24):13045-13050.

Antzutkin ON, Leapman RD, Balbach JJ and Tycko R (2002) Supramolecular structural constraints on Alzheimer's beta-amyloid fibrils from electron microscopy and solid-state nuclear magnetic resonance. *Biochemistry* **41**(51):15436-15450.

Arendt T (2009) Synaptic degeneration in Alzheimer's disease. *Acta Neuropathol* **118**(1):167-179.

Auer S, Meersman F, Dobson CM and Vendruscolo M (2008) A generic mechanism of emergence of amyloid protofilaments from disordered oligomeric aggregates. *PLoS Comput Biol* **4**(11):e1000222.

Auer S, Trovato A and Vendruscolo M (2009) A condensation-ordering mechanism in nanoparticle-catalyzed peptide aggregation. *PLoS Comput Biol* **5**(8):e1000458.

Balbach JJ, Ishii Y, Antzutkin ON, Leapman RD, Rizzo NW, Dyda F, Reed J and Tycko R (2000) Amyloid fibril formation by A beta 16-22, a seven-residue fragment of the Alzheimer's beta-amyloid peptide, and structural characterization by solid state NMR. *Biochemistry* **39**(45):13748-13759.

Balbach JJ, Petkova AT, Oyler NA, Antzutkin ON, Gordon DJ, Meredith SC and Tycko R (2002) Supramolecular structure in full-length Alzheimer's beta-amyloid fibrils: evidence for a parallel beta-sheet organization from solid-state nuclear magnetic resonance. *Biophys J* **83**(2):1205-1216.

Barghorn S, Biernat J and Mandelkow E (2005a) Purification of recombinant tau protein and preparation of Alzheimer-paired helical filaments in vitro. *Methods Mol Biol* **299**:35-51.

Barghorn S, Nimmrich V, Striebinger A, Krantz C, Keller P, Janson B, Bahr M, Schmidt M, Bitner RS, Harlan J, Barlow E, Ebert U and Hillen H (2005b) Globular amyloid beta-peptide oligomer - a homogenous and stable neuropathological protein in Alzheimer's disease. *J Neurochem* **95**(3):834-847.

Barnham KJ and Bush AI (2008) Metals in Alzheimer's and Parkinson's diseases. *Curr Opin Chem Biol* **12**(2):222-228.

Barrow CJ and Zagorski MG (1991) Solution structures of beta peptide and its constituent fragments: relation to amyloid deposition. *Science* **253**(5016):179-182.

Barten DM and Albright CF (2008) Therapeutic strategies for Alzheimer's disease. *Mol Neurobiol* **37**(2-3):171-186.

Bartolini M, Bertucci C, Bolognesi ML, Cavalli A, Melchiorre C and Andrisano V (2007) Insight into the kinetic of amyloid beta (1-42) peptide self-aggregation: elucidation of inhibitors' mechanism of action. *Chembiochem* **8**(17):2152-2161.

Bates KA, Verdile G, Li QX, Ames D, Hudson P, Masters CL and Martins RN (2009) Clearance mechanisms of Alzheimer's amyloid-beta peptide: implications for therapeutic design and diagnostic tests. *Mol Psychiatry* **14**(5):469-486.

Benzinger TL, Gregory DM, Burkoth TS, Miller-Auer H, Lynn DG, Botto RE and Meredith SC (1998) Propagating structure of Alzheimer's beta-amyloid(10-35) is parallel beta-sheet with residues in exact register. *Proc Natl Acad Sci U S A* **95**(23):13407-13412.

Bernstein SL, Dupuis NF, Lazo ND, Wyttenbach T, Condron MM, Bitan G, Teplow DB, Shea J-E, Ruotolo BT, Robinson CV and Bowers MT (2009) Amyloid-beta protein oligomerization and the importance of tetramers and dodecamers in the aetiology of Alzheimer's disease. *Nat Chem* **1**(4):326-331.

Bieschke J, Siegel SJ, Fu Y and Kelly JW (2008) Alzheimer's Abeta peptides containing an isostructural backbone mutation afford distinct aggregate morphologies but analogous cytotoxicity. Evidence for a common low-abundance toxic structure(s)? *Biochemistry* **47**(1):50-59.

Bitan G, Kirkitadze MD, Lomakin A, Vollers SS, Benedek GB and Teplow DB (2003a) Amyloid beta -protein (Abeta) assembly: Abeta 40 and Abeta 42 oligomerize through distinct pathways. *Proc Natl Acad Sci U S A* **100**(1):330-335.

Bitan G, Tarus B, Vollers SS, Lashuel HA, Condron MM, Straub JE and Teplow DB (2003b) A molecular switch in amyloid assembly: Met35 and amyloid beta-protein oligomerization. *J Am Chem Soc* **125**(50):15359-15365.

Bitan G and Teplow DB (2004) Rapid photochemical cross-linking--a new tool for studies of metastable, amyloidogenic protein assemblies. *Acc Chem Res* **37**(6):357-364.

Blanchflower WJ, McCracken RJ and Rice DA (1989) Determination of chlortetracycline residues in tissues using high-performance liquid chromatography with fluorescence detection. *Analyst* **114**(4):421-423.

Bohrmann B, Adrian M, Dubochet J, Kuner P, Muller F, Huber W, Nordstedt C and Dobeli H (2000) Self-assembly of beta-amyloid 42 is retarded by small molecular ligands at the stage of structural intermediates. *J Struct Biol* **130**(2-3):232-246.

Boothe JH, Morton J, Petisi JP, Wilkinson RG and Williams JH (1953) TETRACYCLINE. *Journal of the American Chemical Society* **75**(18):4621-4621.

Bourhim M, Kruzel M, Srikrishnan T and Nicotera T (2007) Linear quantitation of Abeta aggregation using Thioflavin T: reduction in fibril formation by colostrinin. *J Neurosci Methods* **160**(2):264-268.

Bravman T, Bronner V, Lavie K, Notcovich A, Papalia GA and Myszka DG (2006) Exploring "one-shot" kinetics and small molecule analysis using the ProteOn XPR36 array biosensor. *Anal Biochem* **358**(2):281-288.

Brown GC and Borutaite V (2006) Interactions between nitric oxide, oxygen, reactive oxygen species and reactive nitrogen species. *Biochem Soc Trans* **34**(Pt 5):953-956.

Brunner R and Machek G (1962) *Die Antibiotica. Band I: Die großen Antibiotica. 1. Teil - Allgemeiner Teil, Penicillin + 2. Teil: Streptomycin, Chloramphenicol, Tetracycline*. Nürnberg, Hans Carl,.

Bryan PD, Hawkins KR, Stewart JT and Capomacchia AC (1992) Analysis of chlortetracycline by high performance liquid chromatography with postcolumn alkaline-induced fluorescence detection. *Biomed Chromatogr* **6**(6):305-310.

Buchete NV, Tycko R and Hummer G (2005) Molecular dynamics simulations of Alzheimer's beta-amyloid protofilaments. *J Mol Biol* **353**(4):804-821.

Burgos-Ramos E, Puebla-Jimenez L and Arilla-Ferreiro E (2008) Minocycline provides protection against beta-amyloid(25-35)-induced alterations of the somatostatin signaling pathway in the rat temporal cortex. *Neuroscience* **154**(4):1458-1466.

Burkoth TS, Benzinger TLS, Urban V, Morgan DM, Gregory DM, Thiyagarajan P, Botto RE, Meredith SC and Lynn DG (2000) Structure of the ?-amyloid(10-35) fibril. *Journal of the American Chemical Society* **122**(33):7883-7889.

Butterfield DA (2003) Amyloid beta-peptide [1-42]-associated free radical-induced oxidative stress and neurodegeneration in Alzheimer's disease brain: mechanisms and consequences. *Curr Med Chem* **10**(24):2651-2659.

Butterfield DA, Reed T, Newman SF and Sultana R (2007) Roles of amyloid beta-peptide-associated oxidative stress and brain protein modifications in the pathogenesis of Alzheimer's disease and mild cognitive impairment. *Free Radic Biol Med* **43**(5):658-677.

Camus MS, Dos Santos S, Chandravarkar A, Mandal B, Schmid AW, Tuchscherer G, Mutter M and Lashuel HA (2008) Switch-peptides: design and characterization of controllable super-amyloid-forming host-guest peptides as tools for identifying anti-amyloid agents. *Chembiochem* **9**(13):2104-2112.

Cannon MJ, Williams AD, Wetzel R and Myszka DG (2004) Kinetic analysis of beta-amyloid fibril elongation. *Anal Biochem* **328**(1):67-75.

Cardoso I, Merlini G and Saraiva MJ (2003) 4'-iodo-4'-deoxydoxorubicin and tetracyclines disrupt transthyretin amyloid fibrils in vitro producing noncytotoxic species: screening for TTR fibril disrupters. *FASEB J* **17**(8):803-809.

Cardoso I and Saraiva MJ (2006) Doxycycline disrupts transthyretin amyloid: evidence from studies in a FAP transgenic mice model. *FASEB J* **20**(2):234-239.

Carter DB and Chou KC (1998) A model for structure-dependent binding of Congo red to Alzheimer beta-amyloid fibrils. *Neurobiol Aging* **19**(1):37-40.

Caughey B and Lansbury PT (2003) Protofibrils, pores, fibrils, and neurodegeneration: separating the responsible protein aggregates from the innocent bystanders. *Annu Rev Neurosci* **26**:267-298.

Chan WC, White PD and NetLibrary I (2000) Fmoc solid phase peptide synthesis a practical approach, Oxford University Press, New York.

Charest MG, Siegel DR and Myers AG (2005) Synthesis of (-)-tetracycline. *J Am Chem Soc* **127**(23):8292-8293.

Chen YR and Glabe CG (2006) Distinct early folding and aggregation properties of Alzheimer amyloid-beta peptides Abeta40 and Abeta42: stable trimer or tetramer formation by Abeta42. *J Biol Chem* **281**(34):24414-24422.

Cheng IH, Palop JJ, Esposito LA, Bien-Ly N, Yan F and Mucke L (2004) Aggressive amyloidosis in mice expressing human amyloid peptides with the Arctic mutation. *Nat Med* **10**(11):1190-1192.

Cheon M, Chang I, Mohanty S, Luheshi LM, Dobson CM, Vendruscolo M and Favrin G (2007) Structural reorganisation and potential toxicity of oligomeric species formed during the assembly of amyloid fibrils. *PLoS Comput Biol* **3**(9):1727-1738.

Chimon S, Shaibat MA, Jones CR, Calero DC, Aizezi B and Ishii Y (2007) Evidence of fibril-like beta-sheet structures in a neurotoxic amyloid intermediate of Alzheimer's beta-amyloid. *Nat Struct Mol Biol.*

Chiti F and Dobson CM (2006) Protein misfolding, functional amyloid, and human disease. *Annu Rev Biochem* **75**:333-366.

Choi Y, Kim HS, Shin KY, Kim EM, Kim M, Park CH, Jeong YH, Yoo J, Lee JP, Chang KA, Kim S and Suh YH (2007) Minocycline attenuates neuronal cell death and improves cognitive impairment in Alzheimer's disease models. *Neuropsychopharmacology* **32**(11):2393-2404.

Chromy BA, Nowak RJ, Lambert MP, Viola KL, Chang L, Velasco PT, Jones BW, Fernandez SJ, Lacor PN, Horowitz P, Finch CE, Krafft GA and Klein WL (2003) Self-assembly of Abeta(1-42) into globular neurotoxins. *Biochemistry* **42**(44):12749-12760.

Chyung JH, Raper DM and Selkoe DJ (2005) Gamma-secretase exists on the plasma membrane as an intact complex that accepts substrates and effects intramembrane cleavage. *J Biol Chem* **280**(6):4383-4392.

Citron M, Vigo-Pelfrey C, Teplow DB, Miller C, Schenk D, Johnston J, Winblad B, Venizelos N, Lannfelt L and Selkoe DJ (1994) Excessive production of amyloid beta-protein by peripheral cells of symptomatic and presymptomatic patients carrying the Swedish familial Alzheimer disease mutation. *Proc Natl Acad Sci U S A* **91**(25):11993-11997.

Coan KE and Shoichet BK (2008) Stoichiometry and physical chemistry of promiscuous aggregate-based inhibitors. *J Am Chem Soc* **130**(29):9606-9612.

Coin I, Beerbaum M, Schmieder P, Bienert M and Beyermann M (2008) Solid-phase synthesis of a cyclodepsipeptide: cotransin. *Org Lett* **10**(17):3857-3860.

Coin I, Beyermann M and Bienert M (2007) Solid-phase peptide synthesis: from standard procedures to the synthesis of difficult sequences. *Nat Protoc* **2**(12):3247-3256.

Colaizzi JL and Klink PR (1969) pH-Partition behavior of tetracyclines. *J Pharm Sci* **58**(10):1184-1189.

Coles M, Bicknell W, Watson AA, Fairlie DP and Craik DJ (1998) Solution structure of amyloid beta-peptide(1-40) in a water-micelle environment. Is the membrane-spanning domain where we think it is? *Biochemistry* **37**(31):11064-11077.

Conover LH, Butler K, Johnston JD, Korst JJ and Woodward RB (1962) The Total Synthesis of 6-Demethyl-6-Deoxytetracycline. *Journal of the American Chemical Society* **84**(16):3222-3224.

Crews L, Tsigelny I, Hashimoto M and Masliah E (2009) Role of synucleins in Alzheimer's disease. *Neurotox Res* **16**(3):306-317.

D'Agostino P, Arcoleo F, Barbera C, Di Bella G, La Rosa M, Misiano G, Milano S, Brai M, Cammarata G, Feo S and Cillari E (1998) Tetracycline inhibits the nitric oxide synthase activity induced by endotoxin in cultured murine macrophages. *Eur J Pharmacol* **346**(2-3):283-290.

Dafforn TR, Rajendra J, Halsall DJ, Serpell LC and Rodger A (2004) Protein fiber linear dichroism for structure determination and kinetics in a low-volume, low-wavelength couette flow cell. *Biophys J* **86**(1 Pt 1):404-410.

Dahlgren KN, Manelli AM, Stine WB, Jr., Baker LK, Krafft GA and LaDu MJ (2002) Oligomeric and fibrillar species of amyloid-beta peptides differentially affect neuronal viability. *J Biol Chem* **277**(35):32046-32053.

Danielsson J, Jarvet J, Damberg P and Graslund A (2005) The Alzheimer beta-peptide shows temperature-dependent transitions between left-handed 3-helix, beta-strand and random coil secondary structures. *FEBS J* **272**(15):3938-3949.

Davis J, Xu F, Deane R, Romanov G, Previti ML, Zeigler K, Zlokovic BV and Van Nostrand WE (2004) Early-onset and robust cerebral microvascular accumulation of amyloid beta-protein in transgenic mice expressing low levels of a vasculotropic Dutch/Iowa mutant form of amyloid beta-protein precursor. *J Biol Chem* **279**(19):20296-20306.

De Almeida WB, Dos Santos HF and Zerner MC (1998) A theoretical study of the interaction of anhydrotetracycline with Al(III). *J Pharm Sci* **87**(9):1101-1108.

De Felice FG, Vieira MN, Saraiva LM, Figueroa-Villar JD, Garcia-Abreu J, Liu R, Chang L, Klein WL and Ferreira ST (2004) Targeting the neurotoxic species in Alzheimer's disease: inhibitors of Abeta oligomerization. *FASEB J* **18**(12):1366-1372.

De Felice FG, Wu D, Lambert MP, Fernandez SJ, Velasco PT, Lacor PN, Bigio EH, Jerecic J, Acton PJ, Shughrue PJ, Chen-Dodson E, Kinney GG and Klein WL (2008) Alzheimer's disease-type neuronal tau hyperphosphorylation induced by A beta oligomers. *Neurobiol Aging* **29**(9):1334-1347.

De Strooper B and Annaert W (2000) Proteolytic processing and cell biological functions of the amyloid precursor protein. *J Cell Sci* **113 (Pt 11)**:1857-1870.

Di Fede G, Catania M, Morbin M, Rossi G, Suardi S, Mazzoleni G, Merlin M, Giovagnoli AR, Prioni S, Erbetta A, Falcone C, Gobbi M, Colombo L, Bastone A, Beeg M, Manzoni C, Francescucci B, Spagnoli A, Cantu L, Del Favero E, Levy E, Salmona M and Tagliavini F (2009) A recessive mutation in the APP gene with dominant-negative effect on amyloidogenesis. *Science* **323**(5920):1473-1477.

Dolphin GT, Chierici S, Ouberai M, Dumy P and Garcia J (2008) A multimeric quinacrine conjugate as a potential inhibitor of Alzheimer's beta-amyloid fibril formation. *Chembiochem* **9**(6):952-963.

Dong J, Atwood CS, Anderson VE, Siedlak SL, Smith MA, Perry G and Carey PR (2003) Metal binding and oxidation of amyloid-beta within isolated senile plaque cores: Raman microscopic evidence. *Biochemistry* **42**(10):2768-2773.

Dos Santos S, Chandravarkar A, Mandal B, Mimna R, Murat K, Saucede L, Tella P, Tuchscherer G and Mutter M (2005) Switch-peptides: controlling self-assembly of amyloid beta-derived peptides in vitro by consecutive triggering of acyl migrations. *J Am Chem Soc* **127**(34):11888-11889.

Duarte HA, Carvalho S, Paniago EB and Simas AM (1999) Importance of tautomers in the chemical behavior of tetracyclinesdagger. *J Pharm Sci* **88**(1):111-120.

Duggar BM (1948) Aureomycin; a product of the continuing search for new antibiotics. *Ann N Y Acad Sci* **51**(Art. 2):177-181.

Durckheimer W (1975) Tetracyclines: chemistry, biochemistry, and structure-activity relations. *Angew Chem Int Ed Engl* **14**(11):721-734.

Dürckheimer W (1975) Tetracycline: Chemie, Biochemie und Struktur-Wirkungs-Beziehungen. *Angewandte Chemie* **87**(21):751-764.

Eckert A, Hauptmann S, Scherping I, Meinhardt J, Rhein V, Drose S, Brandt U, Fandrich M, Muller WE and Gotz J (2008) Oligomeric and fibrillar species of beta-amyloid (A beta 42) both impair mitochondrial function in P301L tau transgenic mice. *J Mol Med* **86**(11):1255-1267.

Eckman EA and Eckman CB (2005) Abeta-degrading enzymes: modulators of Alzheimer's disease pathogenesis and targets for therapeutic intervention. *Biochem Soc Trans* **33**(Pt 5):1101-1105.

Ehrnhoefer DE, Bieschke J, Boeddrich A, Herbst M, Masino L, Lurz R, Engemann S, Pastore A and Wanker EE (2008) EGCG redirects amyloidogenic polypeptides into unstructured, off-pathway oligomers. *Nat Struct Mol Biol* **15**(6):558-566.

Esler WP, Stimson ER, Jennings JM, Vinters HV, Ghilardi JR, Lee JP, Mantyh PW and Maggio JE (2000) Alzheimer's disease amyloid propagation by a template-dependent dock-lock mechanism. *Biochemistry* **39**(21):6288-6295.

Esteras-Chopo A, Pastor MT, Serrano L and Lopez de la Paz M (2008) New strategy for the generation of specific D-peptide amyloid inhibitors. *J Mol Biol* **377**(5):1372-1381.

Evans KC, Berger EP, Cho CG, Weisgraber KH and Lansbury PT, Jr. (1995) Apolipoprotein E is a kinetic but not a thermodynamic inhibitor of amyloid formation: implications for the pathogenesis and treatment of Alzheimer disease. *Proc Natl Acad Sci U S A* **92**(3):763-767.

Familian A, Boshuizen RS, Eikelenboom P and Veerhuis R (2006) Inhibitory effect of minocycline on amyloid beta fibril formation and human microglial activation. *Glia* **53**(3):233-240.

Familian A, Eikelenboom P and Veerhuis R (2007) Minocycline does not affect amyloid beta phagocytosis by human microglial cells. *Neurosci Lett* **416**(1):87-91.

Fandrich M, Meinhardt J and Grigorieff N (2009) Structural polymorphism of Alzheimer Abeta and other amyloid fibrils. *Prion* **3**(2):89-93.

Feng BY, Toyama BH, Wille H, Colby DW, Collins SR, May BC, Prusiner SB, Weissman J and Shoichet BK (2008) Small-molecule aggregates inhibit amyloid polymerization. *Nat Chem Biol* **4**(3):197-199.

Ferrao-Gonzales AD, Robbs BK, Moreau VH, Ferreira A, Juliano L, Valente AP, Almeida FC, Silva JL and Foguel D (2005) Controlling {beta}-amyloid oligomerization by the use of naphthalene sulfonates: trapping low molecular weight oligomeric species. *J Biol Chem* **280**(41):34747-34754.

Fezoui Y, Hartley DM, Harper JD, Khurana R, Walsh DM, Condron MM, Selkoe DJ, Lansbury PT, Jr., Fink AL and Teplow DB (2000) An improved method of preparing the amyloid beta-protein for fibrillogenesis and neurotoxicity experiments. *Amyloid* **7**(3):166-178.

Findeis MA (2000) Approaches to discovery and characterization of inhibitors of amyloid beta-peptide polymerization. *Biochim Biophys Acta* **1502**(1):76-84.

Finder VH and Glockshuber R (2007) Amyloid-beta aggregation. *Neurodegener Dis* **4**(1):13-27.

Fink AL (2006) The aggregation and fibrillation of alpha-synuclein. *Acc Chem Res* **39**(9):628-634.

Finlay AC, Hobby GL and et al. (1950) Terramycin, a new antibiotic. *Science* **111**(2874):85.

Fletcher TG and Keire DA (1997) The interaction of beta-amyloid protein fragment (12-28) with lipid environments. *Protein Sci* **6**(3):666-675.

Forloni G, Colombo L, Girola L, Tagliavini F and Salmona M (2001) Anti-amyloidogenic activity of tetracyclines: studies in vitro. *FEBS Lett* **487**(3):404-407.

Forloni G, Salmona M, Marcon G and Tagliavini F (2009) Tetracyclines and prion infectivity. *Infect Disord Drug Targets* **9**(1):23-30.

Fraser PE, Nguyen JT, Chin DT and Kirschner DA (1992) Effects of sulfate ions on Alzheimer beta/A4 peptide assemblies: implications for amyloid fibril-proteoglycan interactions. *J Neurochem* **59**(4):1531-1540.

Fuentealba RA, Farias G, Scheu J, Bronfman M, Marzolo MP and Inestrosa NC (2004) Signal transduction during amyloid-beta-peptide neurotoxicity: role in Alzheimer disease. *Brain Res Brain Res Rev* **47**(1-3):275-289.

Gallardo G, Schluter OM and Sudhof TC (2008) A molecular pathway of neurodegeneration linking alpha-synuclein to ApoE and Abeta peptides. *Nat Neurosci* **11**(3):301-308.

Ganguli M, Dodge HH, Chen P, Belle S and DeKosky ST (2000) Ten-year incidence of dementia in a rural elderly US community population: the MoVIES Project. *Neurology* **54**(5):1109-1116.

Gellermann GP, Byrnes H, Striebinger A, Ullrich K, Mueller R, Hillen H and Barghorn S (2008) Abeta-globulomers are formed independently of the fibril pathway. *Neurobiol Dis* **30**(2):212-220.

Gellermann GP, Ullrich K, Tannert A, Unger C, Habicht G, Sauter SR, Hortschansky P, Horn U, Mollmann U, Decker M, Lehmann J and Fandrich M (2006) Alzheimer-like plaque formation by human macrophages is reduced by fibrillation inhibitors and lovastatin. *J Mol Biol* **360**(2):251-257.

Gendron TF and Petrucelli L (2009) The role of tau in neurodegeneration. *Mol Neurodegener* **4**:13.

Gervais F, Paquette J, Morissette C, Krzywkowski P, Yu M, Azzi M, Lacombe D, Kong X, Aman A, Laurin J, Szarek WA and Tremblay P (2007) Targeting soluble Abeta peptide with Tramiprosate for the treatment of brain amyloidosis. *Neurobiol Aging* **28**(4):537-547.

Glabe CG (2008) Structural classification of toxic amyloid oligomers. *J Biol Chem* **283**(44):29639-29643.

Glenner GG and Wong CW (1984) Alzheimer's disease: initial report of the purification and characterization of a novel cerebrovascular amyloid protein. *Biochem Biophys Res Commun* **120**(3):885-890.

Goate A, Chartier-Harlin MC, Mullan M, Brown J, Crawford F, Fidani L, Giuffra L, Haynes A, Irving N, James L and et al. (1991) Segregation of a missense mutation in the amyloid precursor protein gene with familial Alzheimer's disease. *Nature* **349**(6311):704-706.

Gobbi M, Colombo L, Morbin M, Mazzoleni G, Accardo E, Vanoni M, Del Favero E, Cantu L, Kirschner DA, Manzoni C, Beeg M, Ceci P, Ubezio P, Forloni G, Tagliavini F and Salmona M (2006) Gerstmann-Straussler-Scheinker disease amyloid protein polymerizes according to the "dock-and-lock" model. *J Biol Chem* **281**(2):843-849.

Goldgaber D, Lerman MI, McBride OW, Saffiotti U and Gajdusek DC (1987) Characterization and chromosomal localization of a cDNA encoding brain amyloid of Alzheimer's disease. *Science* **235**(4791):877-880.

Goldsbury CS, Wirtz S, Muller SA, Sunderji S, Wicki P, Aebi U and Frey P (2000) Studies on the in vitro assembly of a beta 1-40: implications for the search for a beta fibril formation inhibitors. *J Struct Biol* **130**(2-3):217-231.

Gonzalez-Scarano F and Baltuch G (1999) Microglia as mediators of inflammatory and degenerative diseases. *Annu Rev Neurosci* **22**:219-240.

Gordon DJ, Tappe R and Meredith SC (2002) Design and characterization of a membrane permeable N-methyl amino acid-containing peptide that inhibits Abeta1-40 fibrillogenesis. *J Pept Res* **60**(1):37-55.

Groenning M, Olsen L, van de Weert M, Flink JM, Frokjaer S and Jorgensen FS (2007) Study on the binding of Thioflavin T to beta-sheet-rich and non-beta-sheet cavities. *J Struct Biol* **158**(3):358-369.

Grutzendler J, Helmin K, Tsai J and Gan WB (2007) Various dendritic abnormalities are associated with fibrillar amyloid deposits in Alzheimer's disease. *Ann N Y Acad Sci* **1097**:30-39.

Gude M, Ryf J and White PD (2002) An accurate method for the quantitation of Fmoc-derivatized solid phase supports. *Letters in Peptide Science* **9**(4):203-206.

Gursky O and Aleshkov S (2000) Temperature-dependent beta-sheet formation in beta-amyloid Abeta(1-40) peptide in water: uncoupling beta-structure folding from aggregation. *Biochim Biophys Acta* **1476**(1):93-102.

Ha C, Ryu J and Park CB (2007) Metal ions differentially influence the aggregation and deposition of Alzheimer's beta-amyloid on a solid template. *Biochemistry* **46**(20):6118-6125.

Halling-Sorensen B, Sengelov G and Tjornelund J (2002) Toxicity of tetracyclines and tetracycline degradation products to environmentally relevant bacteria, including selected tetracycline-resistant bacteria. *Arch Environ Contam Toxicol* **42**(3):263-271.

Hamaguchi T, Ono K and Yamada M (2006) Anti-amyloidogenic therapies: strategies for prevention and treatment of Alzheimer's disease. *Cell Mol Life Sci* **63**(13):1538-1552.

Hardy J and Selkoe DJ (2002) The amyloid hypothesis of Alzheimer's disease: progress and problems on the road to therapeutics. *Science* **297**(5580):353-356.

Harper JD and Lansbury PT, Jr. (1997) Models of amyloid seeding in Alzheimer's disease and scrapie: mechanistic truths and physiological consequences of the time-dependent solubility of amyloid proteins. *Annu Rev Biochem* **66**:385-407.

Hepler RW, Grimm KM, Nahas DD, Breese R, Dodson EC, Acton P, Keller PM, Yeager M, Wang H, Shughrue P, Kinney G and Joyce JG (2006) Solution state characterization of amyloid beta-derived diffusible ligands. *Biochemistry* **45**(51):15157-15167.

Herzig MC, Winkler DT, Burgermeister P, Pfeifer M, Kohler E, Schmidt SD, Danner S, Abramowski D, Sturchler-Pierrat C, Burki K, van Duinen SG, Maat-Schieman ML, Staufenbiel M, Mathews PM and Jucker M (2004) Abeta is targeted to the vasculature in a mouse model of hereditary cerebral hemorrhage with amyloidosis. *Nat Neurosci* **7**(9):954-960.

Hilbich C, Kisters-Woike B, Reed J, Masters CL and Beyreuther K (1991) Aggregation and secondary structure of synthetic amyloid beta A4 peptides of Alzheimer's disease. *J Mol Biol* **218**(1):149-163.

Honson NS and Kuret J (2008) Tau aggregation and toxicity in tauopathic neurodegenerative diseases. *J Alzheimers Dis* **14**(4):417-422.

Hortschansky P, Schroeckh V, Christopeit T, Zandomeneghi G and Fandrich M (2005) The aggregation kinetics of Alzheimer's beta-amyloid peptide is controlled by stochastic nucleation. *Protein Sci* **14**(7):1753-1759.

Hou L, Shao H, Zhang Y, Li H, Menon NK, Neuhaus EB, Brewer JM, Byeon IJ, Ray DG, Vitek MP, Iwashita T, Makula RA, Przybyla AB and Zagorski MG (2004) Solution NMR studies of the A beta(1-40) and A beta(1-42) peptides establish that the Met35 oxidation state affects the mechanism of amyloid formation. *J Am Chem Soc* **126**(7):1992-2005.

Howlett DR, George AR, Owen DE, Ward RV and Markwell RE (1999a) Common structural features determine the effectiveness of carvedilol, daunomycin and rolitetracycline as inhibitors of Alzheimer beta-amyloid fibril formation. *Biochem J* **343 Pt 2**:419-423.

Howlett DR, Jennings KH, Lee DC, Clark MS, Brown F, Wetzel R, Wood SJ, Camilleri P and Roberts GW (1995) Aggregation state and neurotoxic properties of Alzheimer beta-amyloid peptide. *Neurodegeneration* **4**(1):23-32.

Howlett DR, Perry AE, Godfrey F, Swatton JE, Jennings KH, Spitzfaden C, Wadsworth H, Wood SJ and Markwell RE (1999b) Inhibition of fibril formation in beta-amyloid peptide by a novel series of benzofurans. *Biochem J* **340 (Pt 1)**:283-289.

Huang H and Rabenstein DL (1999) A cleavage cocktail for methionine-containing peptides. *J Pept Res* **53**(5):548-553.

Hudson SA, Ecroyd H, Kee TW and Carver JA (2009) The thioflavin T fluorescence assay for amyloid fibril detection can be biased by the presence of exogenous compounds. *FEBS J* **276**(20):5960-5972.

Hunter CL, Quintero EM, Gilstrap L, Bhat NR and Granholm AC (2004) Minocycline protects basal forebrain cholinergic neurons from mu p75-saporin immunotoxic lesioning. *Eur J Neurosci* **19**(12):3305-3316.

Hureau C and Faller P (2009) Abeta-mediated ROS production by Cu ions: Structural insights, mechanisms and relevance to Alzheimer's disease. *Biochimie*.

Hussar DA, Niebergall PJ, Sugita ET and Doluisio JT (1968) Aspects of the epimerization of certain tetracycline derivatives. *J Pharm Pharmacol* **20**(7):539-546.

Ikonomovic MD, Abrahamson EE, Isanski BA, Debnath ML, Mathis CA, Dekosky ST and Klunk WE (2006) X-34 labeling of abnormal protein aggregates during the progression of Alzheimer's disease. *Methods Enzymol* **412**:123-144.

Inbar P, Bautista MR, Takayama SA and Yang J (2008) Assay to screen for molecules that associate with Alzheimer's related beta-amyloid fibrils. *Anal Chem* **80**(9):3502-3506.

Inouye H and Kirschner DA (2000) A beta fibrillogenesis: kinetic parameters for fibril formation from congo red binding. *J Struct Biol* **130**(2-3):123-129.

Jahn TR, Makin OS, Morris KL, Marshall KE, Tian P, Sikorski P and Serpell LC (2009) The Common Architecture of Cross-beta Amyloid. *J Mol Biol*.

Kaiser E, Colescott RL, Bossinger CD and Cook PI (1970) Color test for detection of free terminal amino groups in the solid-phase synthesis of peptides. *Anal Biochem* **34**(2):595-598.

Kawahara M, Arispe N, Kuroda Y and Rojas E (1997) Alzheimer's disease amyloid beta-protein forms Zn(2+)-sensitive, cation-selective channels across excised membrane patches from hypothalamic neurons. *Biophys J* **73**(1):67-75.

Kayed R, Head E, Sarsoza F, Saing T, Cotman CW, Necula M, Margol L, Wu J, Breydo L, Thompson JL, Rasool S, Gurlo T, Butler P and Glabe CG (2007) Fibril specific, conformation dependent antibodies recognize a generic epitope common to amyloid fibrils and fibrillar oligomers that is absent in prefibrillar oligomers. *Mol Neurodegener* **2**:18.

Kayed R, Head E, Thompson JL, McIntire TM, Milton SC, Cotman CW and Glabe CG (2003) Common structure of soluble amyloid oligomers implies common mechanism of pathogenesis. *Science* **300**(5618):486-489.

Keil U, Bonert A, Marques CA, Scherping I, Weyermann J, Strosznajder JB, Muller-Spahn F, Haass C, Czech C, Pradier L, Muller WE and Eckert A (2004) Amyloid beta-induced changes in nitric oxide production and mitochondrial activity lead to apoptosis. *J Biol Chem* **279**(48):50310-50320.

Kelly SM, Jess TJ and Price NC (2005) How to study proteins by circular dichroism. *Biochim Biophys Acta* **1751**(2):119-139.

Kennedy DG, McCracken RJ, Carey MP, Blanchflower WJ and Hewitt SA (1998) Iso- and epi-iso-chlortetracycline and the principal metabolites of chlortetracycline in the hen's egg. *J Chromatogr A* **812**(1-2):327-337.

Kheterpal I, Chen M, Cook KD and Wetzel R (2006) Structural differences in Abeta amyloid protofibrils and fibrils mapped by hydrogen exchange--mass spectrometry with on-line proteolytic fragmentation. *J Mol Biol* **361**(4):785-795.

Kim HS and Suh YH (2009) Minocycline and neurodegenerative diseases. *Behav Brain Res* **196**(2):168-179.

Kim J, Basak JM and Holtzman DM (2009) The role of apolipoprotein E in Alzheimer's disease. *Neuron* **63**(3):287-303.

Kim W and Hecht MH (2008) Mutations enhance the aggregation propensity of the Alzheimer's A beta peptide. *J Mol Biol* **377**(2):565-574.

Kirin SI, Noor F, Metzler-Nolte N and Mier W (2007) Manual solid-phase peptide synthesis of metallocene-peptide bioconjugates. *Journal of Chemical Education* **84**(1):108-111.

Kirschner DA, Abraham C and Selkoe DJ (1986) X-ray diffraction from intraneuronal paired helical filaments and extraneuronal amyloid fibers in Alzheimer disease indicates cross-beta conformation. *Proc Natl Acad Sci U S A* **83**(2):503-507.

Kirschner DA, Gross AA, Hidalgo MM, Inouye H, Gleason KA, Abdelsayed GA, Castillo GM, Snow AD, Pozo-Ramajo A, Petty SA and Decatur SM (2008) Fiber diffraction as a screen for amyloid inhibitors. *Curr Alzheimer Res* **5**(3):288-307.

Klement K, Wieligmann K, Meinhardt J, Hortschansky P, Richter W and Fandrich M (2007) Effect of different salt ions on the propensity of aggregation and on the structure of Alzheimer's abeta(1-40) amyloid fibrils. *J Mol Biol* **373**(5):1321-1333.

Kodali R and Wetzel R (2007) Polymorphism in the intermediates and products of amyloid assembly. *Curr Opin Struct Biol* **17**(1):48-57.

Koffie RM, Meyer-Luehmann M, Hashimoto T, Adams KW, Mielke ML, Garcia-Alloza M, Micheva KD, Smith SJ, Kim ML, Lee VM, Hyman BT and Spires-Jones TL (2009) Oligomeric amyloid beta associates with postsynaptic densities and correlates with excitatory synapse loss near senile plaques. *Proc Natl Acad Sci U S A* **106**(10):4012-4017.

Koo EH and Squazzo SL (1994) Evidence that production and release of amyloid beta-protein involves the endocytic pathway. *J Biol Chem* **269**(26):17386-17389.

Kowalewski T and Holtzman DM (1999) In situ atomic force microscopy study of Alzheimer's beta-amyloid peptide on different substrates: new insights into mechanism of beta-sheet formation. *Proc Natl Acad Sci U S A* **96**(7):3688-3693.

Kraus RL, Pasieczny R, Lariosa-Willingham K, Turner MS, Jiang A and Trauger JW (2005) Antioxidant properties of minocycline: neuroprotection in an oxidative stress assay and direct radical-scavenging activity. *J Neurochem* **94**(3):819-827.

Krone MG, Baumketner A, Bernstein SL, Wyttenbach T, Lazo ND, Teplow DB, Bowers MT and Shea JE (2008) Effects of familial Alzheimer's disease mutations on the folding nucleation of the amyloid beta-protein. *J Mol Biol* **381**(1):221-228.

Kuipers BJ and Gruppen H (2007) Prediction of molar extinction coefficients of proteins and peptides using UV absorption of the constituent amino acids at 214 nm to enable quantitative reverse phase high-performance liquid chromatography-mass spectrometry analysis. *J Agric Food Chem* **55**(14):5445-5451.

Kuschinsky G and Lüllmann H (1981) *Kurzes Lehrbuch der Pharmakologie und Toxikologie*. Stuttgart / Thieme.

Lambert MP, Barlow AK, Chromy BA, Edwards C, Freed R, Liosatos M, Morgan TE, Rozovsky I, Trommer B, Viola KL, Wals P, Zhang C, Finch CE, Krafft GA and Klein WL (1998) Diffusible, nonfibrillar ligands derived from Abeta1-42 are potent central nervous system neurotoxins. *Proc Natl Acad Sci U S A* **95**(11):6448-6453.

Lanig H, Gottschalk M, Schneider S and Clark T (1999) Conformational Analysis of Tetracycline using Molecular Mechanical and Semiempirical MO-Calculations. *Journal of Molecular Modeling* **5**(3):46-62.

Lansbury PT, Jr., Costa PR, Griffiths JM, Simon EJ, Auger M, Halverson KJ, Kocisko DA, Hendsch ZS, Ashburn TT, Spencer RG and et al. (1995) Structural model for the beta-amyloid fibril based on interstrand alignment of an antiparallel-sheet comprising a C-terminal peptide. *Nat Struct Biol* **2**(11):990-998.

Lashuel HA, Hartley DM, Balakhaneh D, Aggarwal A, Teichberg S and Callaway DJ (2002) New class of inhibitors of amyloid-beta fibril formation. Implications for the mechanism of pathogenesis in Alzheimer's disease. *J Biol Chem* **277**(45):42881-42890.

Lauren J, Gimbel DA, Nygaard HB, Gilbert JW and Strittmatter SM (2009) Cellular prion protein mediates impairment of synaptic plasticity by amyloid-beta oligomers. *Nature* **457**(7233):1128-1132.

Lee JP, Stimson ER, Ghilardi JR, Mantyh PW, Lu YA, Felix AM, Llanos W, Behbin A, Cummings M, Van Criekinge M and et al. (1995) 1H NMR of A beta amyloid peptide congeners in water solution. Conformational changes correlate with plaque competence. *Biochemistry* **34**(15):5191-5200.

Lendel C, Bertoncini CW, Cremades N, Waudby CA, Vendruscolo M, Dobson CM, Schenk D, Christodoulou J and Toth G (2009) On the mechanism of non-specific inhibitors of protein aggregation: dissecting the interactions of -synuclein with Congo red and Lacmoid. *Biochemistry*.

Lesne S, Koh MT, Kotilinek L, Kayed R, Glabe CG, Yang A, Gallagher M and Ashe KH (2006) A specific amyloid-beta protein assembly in the brain impairs memory. *Nature* **440**(7082):352-357.

LeVine H, 3rd (2005) Multiple ligand binding sites on A beta(1-40) fibrils. *Amyloid* **12**(1):5-14.

LeVine H, 3rd (2007) Small molecule inhibitors of Abeta assembly. *Amyloid* **14**(3):185-197.

Levy-Lahad E, Wasco W, Poorkaj P, Romano DM, Oshima J, Pettingell WH, Yu CE, Jondro PD, Schmidt SD, Wang K and et al. (1995) Candidate gene for the chromosome 1 familial Alzheimer's disease locus. *Science* **269**(5226):973-977.

Liang Y, Denton MB and Bates RB (1998) Stability studies of tetracycline in methanol solution. *Journal of Chromatography A* **827**(1):45-55.

Lim KH (2006) A weakly clustered N terminus inhibits Abeta(1-40) amyloidogenesis. *Chembiochem* **7**(11):1662-1666.

Lin S, Wei X, Xu Y, Yan C, Dodel R, Zhang Y, Liu J, Klaunig JE, Farlow M and Du Y (2003) Minocycline blocks 6-hydroxydopamine-induced neurotoxicity and free radical production in rat cerebellar granule neurons. *Life Sciences* **72**(14):1635-1641.

Lin S, Zhang Y, Dodel R, Farlow MR, Paul SM and Du Y (2001) Minocycline blocks nitric oxide-induced neurotoxicity by inhibition p38 MAP kinase in rat cerebellar granule neurons. *Neurosci Lett* **315**(1-2):61-64.

Lomakin A, Chung DS, Benedek GB, Kirschner DA and Teplow DB (1996) On the nucleation and growth of amyloid beta-protein fibrils: detection of nuclei and quantitation of rate constants. *Proc Natl Acad Sci U S A* **93**(3):1125-1129.

Lord A, Kalimo H, Eckman C, Zhang XQ, Lannfelt L and Nilsson LN (2006) The Arctic Alzheimer mutation facilitates early intraneuronal Abeta aggregation and senile plaque formation in transgenic mice. *Neurobiol Aging* **27**(1):67-77.

Lorenzo A and Yankner BA (1994) Beta-amyloid neurotoxicity requires fibril formation and is inhibited by congo red. *Proc Natl Acad Sci U S A* **91**(25):12243-12247.

Luhrs T, Ritter C, Adrian M, Riek-Loher D, Bohrmann B, Dobeli H, Schubert D and Riek R (2005) 3D structure of Alzheimer's amyloid-beta(1-42) fibrils. *Proc Natl Acad Sci U S A* **102**(48):17342-17347.

Macao B, Hoyer W, Sandberg A, Brorsson AC, Dobson CM and Hard T (2008) Recombinant amyloid beta-peptide production by coexpression with an affibody ligand. *BMC Biotechnol* **8**:82.

Mahley RW and Huang Y (2006) Apolipoprotein (apo) E4 and Alzheimer's disease: unique conformational and biophysical properties of apoE4 can modulate neuropathology. *Acta Neurol Scand Suppl* **185**:8-14.

Malinchik SB, Inouye H, Szumowski KE and Kirschner DA (1998) Structural analysis of Alzheimer's beta(1-40) amyloid: protofilament assembly of tubular fibrils. *Biophys J* **74**(1):537-545.

Malmo C, Vilasi S, Iannuzzi C, Tacchi S, Cametti C, Irace G and Sirangelo I (2006) Tetracycline inhibits W7FW14F apomyoglobin fibril extension and keeps the amyloid protein in a pre-fibrillar, highly cytotoxic state. *FASEB J* **20**(2):346-347.

Marder O and Albericio F (2004) Industrial Application of Coupling Reagents in Peptides. *ChemInform* **35**(24).

Martell MJ, Jr. and Boothe JH (1967) The 6-deoxytetracyclines. VII. Alkylated aminotetracyclines possessing unique antibacterial activity. *J Med Chem* **10**(1):44-46.

Martinez EE and Shimoda W (1989) Liquid chromatographic determination of epimerization of chlortetracycline residue to 4-epi-chlortetracycline residue in animal feed, using McIlvain's buffer as extractant. *J Assoc Off Anal Chem* **72**(5):848-850.

McCormick JRD, Fox SM, Smith LL, Bitler BA, Reichenthal J, Origoni VE, Muller WH, Winterbottom R and Doerschuk AP (1957) Studies of the Reversible Epimerization Occurring in the Tetracycline Family. The Preparation, Properties and Proof of Structure of Some 4-epi-Tetracyclines. *Journal of the American Chemical Society* **79**(11):2849-2858.

McLaurin J, Cecal R, Kierstead ME, Tian X, Phinney AL, Manea M, French JE, Lambermon MH, Darabie AA, Brown ME, Janus C, Chishti MA, Horne P, Westaway D, Fraser PE, Mount HT, Przybylski M and St George-Hyslop P (2002) Therapeutically effective antibodies against amyloid-beta peptide target amyloid-beta residues 4-10 and inhibit cytotoxicity and fibrillogenesis. *Nat Med* **8**(11):1263-1269.

McLaurin J and Chakrabartty A (1997) Characterization of the interactions of Alzheimer beta-amyloid peptides with phospholipid membranes. *Eur J Biochem* **245**(2):355-363.

McLaurin J, Franklin T, Fraser PE and Chakrabartty A (1998) Structural transitions associated with the interaction of Alzheimer beta-amyloid peptides with gangliosides. *J Biol Chem* **273**(8):4506-4515.

McLaurin J, Golomb R, Jurewicz A, Antel JP and Fraser PE (2000) Inositol stereoisomers stabilize an oligomeric aggregate of Alzheimer amyloid beta peptide and inhibit abeta -induced toxicity. *J Biol Chem* **275**(24):18495-18502.

Meinhardt J, Tartaglia GG, Pawar A, Christopeit T, Hortschansky P, Schroeckh V, Dobson CM, Vendruscolo M and Fandrich M (2007) Similarities in the thermodynamics and kinetics of aggregation of disease-related Abeta(1-40) peptides. *Protein Sci* **16**(6):1214-1222.

Meng F, Marek P, Potter KJ, Verchere CB and Raleigh DP (2008) Rifampicin does not prevent amyloid fibril formation by human islet amyloid polypeptide but does inhibit fibril thioflavin-T interactions: implications for mechanistic studies of beta-cell death. *Biochemistry* **47**(22):6016-6024.

Merrifield RB (1963) Solid Phase Peptide Synthesis. I. The Synthesis of a Tetrapeptide. *Journal of the American Chemical Society* **85**(14):2149-2154.

Merrifield RB (1965) Automated synthesis of peptides. *Science* **150**(693):178-185.

Minati L, Edginton T, Bruzzone MG and Giaccone G (2009) Current concepts in Alzheimer's disease: a multidisciplinary review. *Am J Alzheimers Dis Other Demen* **24**(2):95-121.

Miravalle L, Tokuda T, Chiarle R, Giaccone G, Bugiani O, Tagliavini F, Frangione B and Ghiso J (2000) Substitutions at codon 22 of Alzheimer's abeta peptide induce diverse conformational changes and apoptotic effects in human cerebral endothelial cells. *J Biol Chem* **275**(35):27110-27116.

Mitscher LA, Bonacci AC and Sokoloski TD (1968) Circular dichroism and solution conformation of the tetracycline antibiotics. *Tetrahedron Lett* **51**:5361-5364.

Mitscher LA, Slater-Eng B and Sokoloski TD (1972) Circular dichroism measurements of the tetracyclines. IV. 5-Hydroxylated derivatives. *Antimicrob Agents Chemother* **2**(2):66-72.

Miyoshi K (2009) What is 'early onset dementia'? *Psychogeriatrics* **9**(2):67-72.

Morimoto A, Irie K, Murakami K, Masuda Y, Ohigashi H, Nagao M, Fukuda H, Shimizu T and Shirasawa T (2004) Analysis of the secondary structure of beta-amyloid (Abeta42) fibrils by systematic proline replacement. *J Biol Chem* **279**(50):52781-52788.

Moss MA, Varvel NH, Nichols MR, Reed DK and Rosenberry TL (2004) Nordihydroguaiaretic acid does not disaggregate beta-amyloid(1-40) protofibrils but does inhibit growth arising from direct protofibril association. *Mol Pharmacol* **66**(3):592-600.

Mucke L (2009) Neuroscience: Alzheimer's disease. *Nature* **461**(7266):895-897.

Murakami K, Irie K, Morimoto A, Ohigashi H, Shindo M, Nagao M, Shimizu T and Shirasawa T (2002) Synthesis, aggregation, neurotoxicity, and secondary structure of various A beta 1-42 mutants of familial Alzheimer's disease at positions 21-23. *Biochem Biophys Res Commun* **294**(1):5-10.

Muxfeldt H, Haas G, Hardtmann G, Kathawala F, Mooberry JB and Vedejs E (1979) Tetracyclines. 9. Total synthesis of dl-terramycin. *Journal of the American Chemical Society* **101**(3):689-701.

Myszka DG and Morton TA (1998) CLAMP: a biosensor kinetic data analysis program. *Trends Biochem Sci* **23**(4):149-150.

Naggar V, Daabis NA and Motawi MM (1974a) Effect of solubilizers on the stability of tetracycline. *Pharmazie* **29**(2):126-129.

Naggar V, Daabis NA and Motawi MM (1974b) Solubilization of tetracycline and oxytetracycline. *Pharmazie* **29**(2):122-125.

Nakamura T, Watanabe A, Fujino T, Hosono T and Michikawa M (2009) Apolipoprotein E4 (1-272) fragment is associated with mitochondrial proteins and affects mitochondrial function in neuronal cells. *Mol Neurodegener* **4**:35.

Necula M, Breydo L, Milton S, Kayed R, van der Veer WE, Tone P and Glabe CG (2007a) Methylene blue inhibits amyloid Abeta oligomerization by promoting fibrillization. *Biochemistry* **46**(30):8850-8860.

Necula M, Kayed R, Milton S and Glabe CG (2007b) Small molecule inhibitors of aggregation indicate that amyloid beta oligomerization and fibrillization pathways are independent and distinct. *J Biol Chem* **282**(14):10311-10324.

Nelson ML, Ismail MY, McIntyre L, Bhatia B, Viski P, Hawkins P, Rennie G, Andorsky D, Messersmith D, Stapleton K, Dumornay J, Sheahan P, Verma AK, Warchol T and Levy SB (2003) Versatile and facile synthesis of diverse semisynthetic tetracycline derivatives via Pd-catalyzed reactions. *J Org Chem* **68**(15):5838-5851.

Nelson R and Eisenberg D (2006) Recent atomic models of amyloid fibril structure. *Curr Opin Struct Biol* **16**(2):260-265.

Nerelius C, Sandegren A, Sargsyan H, Raunak R, Leijonmarck H, Chatterjee U, Fisahn A, Imarisio S, Lomas DA, Crowther DC, Stromberg R and Johansson J (2009) Alpha-helix targeting reduces amyloid-beta peptide toxicity. *Proc Natl Acad Sci U S A* **106**(23):9191-9196.

Neugroschl J and Sano M (2009) An update on treatment and prevention strategies for Alzheimer's disease. *Curr Neurol Neurosci Rep* **9**(5):368-376.

Nguyen PH, Li MS, Stock G, Straub JE and Thirumalai D (2007) Monomer adds to preformed structured oligomers of Abeta-peptides by a two-stage dock-lock mechanism. *Proc Natl Acad Sci U S A* **104**(1):111-116.

NIH (2008) Alzheimer's Disease: Unraveling the Mystery. *Publication Number: 08-3782* **http://www.nia.nih.gov/Alzheimers/Publications/Unraveling/**.

Nilsberth C, Westlind-Danielsson A, Eckman CB, Condron MM, Axelman K, Forsell C, Stenh C, Luthman J, Teplow DB, Younkin SG, Naslund J and Lannfelt L (2001) The 'Arctic' APP mutation (E693G) causes Alzheimer's disease by enhanced Abeta protofibril formation. *Nat Neurosci* **4**(9):887-893.

Nishitsuji K, Tomiyama T, Ishibashi K, Ito K, Teraoka R, Lambert MP, Klein WL and Mori H (2009) The E693Delta mutation in amyloid precursor protein increases intracellular accumulation of amyloid beta oligomers and causes endoplasmic reticulum stress-induced apoptosis in cultured cells. *Am J Pathol* **174**(3):957-969.

Noguchi A, Matsumura S, Dezawa M, Tada M, Yanazawa M, Ito A, Akioka M, Kikuchi S, Sato M, Ideno S, Noda M, Fukunari A, Muramatsu SI, Itokazu Y, Sato K, Takahashi H, Teplow DB, Nabeshima YI, Kakita A, Imahori K and Hoshi M (2009) Isolation and characterization of patient-derived, toxic, high-mass amyloid {beta}-protein (A{beta}) assembly from Alzheimer's disease brains. *J Biol Chem.*

Novak-Pekli M, el-Hadi Mesbah M and Petho G (1996) Equilibrium studies on tetracycline-metal ion systems. *J Pharm Biomed Anal* **14**(8-10):1025-1029.

O'Nuallain B, Thakur AK, Williams AD, Bhattacharyya AM, Chen S, Thiagarajan G and Wetzel R (2006) Kinetics and thermodynamics of amyloid assembly using a high-performance liquid chromatography-based sedimentation assay. *Methods Enzymol* **413**:34-74.

Ono K, Condron MM and Teplow DB (2009) Structure-neurotoxicity relationships of amyloid {beta}-protein oligomers. *Proc Natl Acad Sci U S A.*

Ono K, Hasegawa K, Naiki H and Yamada M (2004a) Anti-amyloidogenic activity of tannic acid and its activity to destabilize Alzheimer's beta-amyloid fibrils in vitro. *Biochim Biophys Acta* **1690**(3):193-202.

Ono K, Hasegawa K, Naiki H and Yamada M (2004b) Curcumin has potent anti-amyloidogenic effects for Alzheimer's beta-amyloid fibrils in vitro. *J Neurosci Res* **75**(6):742-750.

Ono K, Hirohata M and Yamada M (2006a) Alpha-lipoic acid exhibits anti-amyloidogenicity for beta-amyloid fibrils in vitro. *Biochem Biophys Res Commun* **341**(4):1046-1052.

Ono K, Naiki H and Yamada M (2006b) The development of preventives and therapeutics for Alzheimer's disease that inhibit the formation of beta-amyloid fibrils (fAbeta), as well as destabilize preformed fAbeta. *Curr Pharm Des* **12**(33):4357-4375.

Ono K and Yamada M (2006) Antioxidant compounds have potent anti-fibrillogenic and fibril-destabilizing effects for alpha-synuclein fibrils in vitro. *J Neurochem* **97**(1):105-115.

Ono K, Yoshiike Y, Takashima A, Hasegawa K, Naiki H and Yamada M (2003) Potent anti-amyloidogenic and fibril-destabilizing effects of polyphenols in vitro: implications for the prevention and therapeutics of Alzheimer's disease. *J Neurochem* **87**(1):172-181.

Opazo C, Huang X, Cherny RA, Moir RD, Roher AE, White AR, Cappai R, Masters CL, Tanzi RE, Inestrosa NC and Bush AI (2002) Metalloenzyme-like activity of Alzheimer's disease beta-amyloid. Cu-dependent catalytic conversion of dopamine, cholesterol, and biological reducing agents to neurotoxic H(2)O(2). *J Biol Chem* **277**(43):40302-40308.

Ozawa D, Yagi H, Ban T, Kameda A, Kawakami T, Naiki H and Goto Y (2009) Destruction of amyloid fibrils of a beta2-microglobulin fragment by laser beam irradiation. *J Biol Chem* **284**(2):1009-1017.

Pace CN, Vajdos F, Fee L, Grimsley G and Gray T (1995) How to measure and predict the molar absorption coefficient of a protein. *Protein Sci* **4**(11):2411-2423.

Pallitto MM, Ghanta J, Heinzelman P, Kiessling LL and Murphy RM (1999) Recognition sequence design for peptidyl modulators of beta-amyloid aggregation and toxicity. *Biochemistry* **38**(12):3570-3578.

Paravastu AK, Qahwash I, Leapman RD, Meredith SC and Tycko R (2009) Seeded growth of beta-amyloid fibrils from Alzheimer's brain-derived fibrils produces a distinct fibril structure. *Proc Natl Acad Sci U S A* **106**(18):7443-7448.

Pastor MT, Kummerer N, Schubert V, Esteras-Chopo A, Dotti CG, Lopez de la Paz M and Serrano L (2008) Amyloid toxicity is independent of polypeptide sequence, length and chirality. *J Mol Biol* **375**(3):695-707.

Petkova AT, Buntkowsky G, Dyda F, Leapman RD, Yau WM and Tycko R (2004) Solid state NMR reveals a pH-dependent antiparallel beta-sheet registry in fibrils formed by a beta-amyloid peptide. *J Mol Biol* **335**(1):247-260.

Petkova AT, Ishii Y, Balbach JJ, Antzutkin ON, Leapman RD, Delaglio F and Tycko R (2002) A structural model for Alzheimer's beta -amyloid fibrils based on experimental constraints from solid state NMR. *Proc Natl Acad Sci U S A* **99**(26):16742-16747.

Petkova AT, Leapman RD, Guo Z, Yau WM, Mattson MP and Tycko R (2005) Self-propagating, molecular-level polymorphism in Alzheimer's beta-amyloid fibrils. *Science* **307**(5707):262-265.

Podlisny MB, Ostaszewski BL, Squazzo SL, Koo EH, Rydell RE, Teplow DB and Selkoe DJ (1995) Aggregation of secreted amyloid beta-protein into sodium dodecyl sulfate-stable oligomers in cell culture. *J Biol Chem* **270**(16):9564-9570.

Powers ET and Powers DL (2006) The kinetics of nucleated polymerizations at high concentrations: amyloid fibril formation near and above the "supercritical concentration". *Biophys J* **91**(1):122-132.

Priller C, Bauer T, Mitteregger G, Krebs B, Kretzschmar HA and Herms J (2006) Synapse formation and function is modulated by the amyloid precursor protein. *J Neurosci* **26**(27):7212-7221.

Puglielli L, Friedlich AL, Setchell KD, Nagano S, Opazo C, Cherny RA, Barnham KJ, Wade JD, Melov S, Kovacs DM and Bush AI (2005) Alzheimer disease beta-amyloid activity mimics cholesterol oxidase. *J Clin Invest* **115**(9):2556-2563.

Qin Z, Hu D, Han S, Hong DP and Fink AL (2007) Role of different regions of alpha-synuclein in the assembly of fibrils. *Biochemistry* **46**(46):13322-13330.

Quintana C, Bellefqih S, Laval JY, Guerquin-Kern JL, Wu TD, Avila J, Ferrer I, Arranz R and Patino C (2006) Study of the localization of iron, ferritin, and hemosiderin in Alzheimer's disease hippocampus by analytical microscopy at the subcellular level. *J Struct Biol* **153**(1):42-54.

Rangachari V, Moore BD, Reed DK, Sonoda LK, Bridges AW, Conboy E, Hartigan D and Rosenberry TL (2007) Amyloid-beta(1-42) rapidly forms protofibrils and oligomers by distinct pathways in low concentrations of sodium dodecylsulfate. *Biochemistry* **46**(43):12451-12462.

Rangachari V, Reed DK, Moore BD and Rosenberry TL (2006) Secondary structure and interfacial aggregation of amyloid-beta(1-40) on sodium dodecyl sulfate micelles. *Biochemistry* **45**(28):8639-8648.

Reddy PH (2009) Amyloid beta, mitochondrial structural and functional dynamics in Alzheimer's disease. *Exp Neurol* **218**(2):286-292.

Reinke AA and Gestwicki JE (2007) Structure-activity relationships of amyloid beta-aggregation inhibitors based on curcumin: influence of linker length and flexibility. *Chem Biol Drug Des* **70**(3):206-215.

Remmers EG, Sieger GM and Doerschuk AP (1963) Some Observations on the Kinetics of the C.4 Epimerization of Tetracycline. *J Pharm Sci* **52**:752-756.

Rogers J, Strohmeyer R, Kovelowski CJ and Li R (2002) Microglia and inflammatory mechanisms in the clearance of amyloid beta peptide. *Glia* **40**(2):260-269.

Ronga L, Langella E, Palladino P, Marasco D, Tizzano B, Saviano M, Pedone C, Improta R and Ruvo M (2007) Does tetracycline bind helix 2 of prion? An integrated spectroscopical and computational study of the interaction between the antibiotic and alpha helix 2 human prion protein fragments. *Proteins* **66**(3):707-715.

Roterman I, KrUl M, Nowak M, Konieczny L, Rybarska J, Stopa B, Piekarska B and Zemanek G (2001) Why Congo red binding is specific for amyloid proteins - model studies and a computer analysis approach. *Med Sci Monit* 7(4):771-784.

Rovelet-Lecrux A, Hannequin D, Raux G, Le Meur N, Laquerriere A, Vital A, Dumanchin C, Feuillette S, Brice A, Vercelletto M, Dubas F, Frebourg T and Campion D (2006) APP locus duplication causes autosomal dominant early-onset Alzheimer disease with cerebral amyloid angiopathy. *Nat Genet* **38**(1):24-26.

Roychaudhuri R, Yang M, Hoshi MM and Teplow DB (2009) Amyloid beta-protein assembly and Alzheimer disease. *J Biol Chem* **284**(8):4749-4753.

Ryu JK and McLarnon JG (2006) Minocycline or iNOS inhibition block 3-nitrotyrosine increases and blood-brain barrier leakiness in amyloid beta-peptide-injected rat hippocampus. *Exp Neurol* **198**(2):552-557.

Salehi A and Swaab DF (1999) Diminished neuronal metabolic activity in Alzheimer's disease. Review article. *J Neural Transm* **106**(9-10):955-986.

Sawaya MR, Sambashivan S, Nelson R, Ivanova MI, Sievers SA, Apostol MI, Thompson MJ, Balbirnie M, Wiltzius JJ, McFarlane HT, Madsen AO, Riekel C and Eisenberg D (2007) Atomic structures of amyloid cross-beta spines reveal varied steric zippers. *Nature* **447**(7143):453-457.

Schmidt M, Sachse C, Richter W, Xu C, Fandrich M and Grigorieff N (2009) Comparison of Alzheimer A{beta}(1-40) and A{beta}(1-42) amyloid fibrils reveals similar protofilament structures. *Proc Natl Acad Sci U S A.*

Schmitt MO and Schneider S (2006) Novel insight into the protonation-deprotonation equilibria of tetracycline, sancycline and 10-propoxy-sancycline in aqueous solution. I. Analysis of the pH-dependent UV/vis absorption spectra by the SVD technique. *Zeitschrift fur Physikalische Chemie* **220**(4):441-475.

Schmitt MO, Schneider S and Nelson ML (2007) Novel insight into the protonation-deprotonation equilibria of tetracycline and several derivatives in aqueous solution. II. Analysis of the pH-dependent fluorescence spectra by the SVD technique. *Zeitschrift fur Physikalische Chemie* **221**(2):235-271.

Schnappinger D and Hillen W (1996) Tetracyclines: antibiotic action, uptake, and resistance mechanisms. *Arch Microbiol* **165**(6):359-369.

Schneider S, Schmitt MO, Brehm G, Reiher M, Matousek P and Towrie M (2003) Fluorescence kinetics of aqueous solutions of tetracycline and its complexes with Mg2+ and Ca2+. *Photochem Photobiol Sci* **2**(11):1107-1117.

Sciarretta KL, Gordon DJ and Meredith SC (2006) Peptide-based inhibitors of amyloid assembly. *Methods Enzymol* **413**:273-312.

Seabrook TJ, Jiang L, Maier M and Lemere CA (2006) Minocycline affects microglia activation, Abeta deposition, and behavior in APP-tg mice. *Glia* **53**(7):776-782.

Serio TR, Cashikar AG, Kowal AS, Sawicki GJ, Moslehi JJ, Serpell L, Arnsdorf MF and Lindquist SL (2000) Nucleated conformational conversion and the replication of conformational information by a prion determinant. *Science* **289**(5483):1317-1321.

Shankar GM, Li S, Mehta TH, Garcia-Munoz A, Shepardson NE, Smith I, Brett FM, Farrell MA, Rowan MJ, Lemere CA, Regan CM, Walsh DM, Sabatini BL and Selkoe DJ (2008) Amyloid-beta protein dimers isolated directly from Alzheimer's brains impair synaptic plasticity and memory. *Nat Med* **14**(8):837-842.

Shao H, Jao S, Ma K and Zagorski MG (1999) Solution structures of micelle-bound amyloid beta-(1-40) and beta-(1-42) peptides of Alzheimer's disease. *J Mol Biol* **285**(2):755-773.

Shen CL and Murphy RM (1995) Solvent effects on self-assembly of beta-amyloid peptide. *Biophys J* **69**(2):640-651.

Sherrington R, Rogaev EI, Liang Y, Rogaeva EA, Levesque G, Ikeda M, Chi H, Lin C, Li G, Holman K and et al. (1995) Cloning of a gene bearing missense mutations in early-onset familial Alzheimer's disease. *Nature* **375**(6534):754-760.

Shi J, Perry G, Smith MA and Friedland RP (2000) Vascular abnormalities: the insidious pathogenesis of Alzheimer's disease. *Neurobiol Aging* **21**(2):357-361.

Simons LJ, Caprathe BW, Callahan M, Graham JM, Kimura T, Lai Y, LeVine H, 3rd, Lipinski W, Sakkab AT, Tasaki Y, Walker LC, Yasunaga T, Ye Y, Zhuang N and Augelli-Szafran CE (2009) The synthesis and structure-activity relationship of substituted N-phenyl anthranilic acid analogs as amyloid aggregation inhibitors. *Bioorg Med Chem Lett* **19**(3):654-657.

Smith DL, Woodman B, Mahal A, Sathasivam K, Ghazi-Noori S, Lowden PA, Bates GP and Hockly E (2003) Minocycline and doxycycline are not beneficial in a model of Huntington's disease. *Ann Neurol* **54**(2):186-196.

Soeborg T, Ingerslev F and Halling-Sorensen B (2004) Chemical stability of chlortetracycline and chlortetracycline degradation products and epimers in soil interstitial water. *Chemosphere* **57**(10):1515-1524.

Sohma Y, Hayashi Y, Kimura M, Chiyomori Y, Taniguchi A, Sasaki M, Kimura T and Kiso Y (2005) The 'O-acyl isopeptide method' for the synthesis of difficult sequence-containing peptides: application to the synthesis of Alzheimer's disease-related amyloid beta peptide (Abeta) 1-42. *J Pept Sci* **11**(8):441-451.

Sohma Y and Kiso Y (2006) "Click peptides"--chemical biology-oriented synthesis of Alzheimer's disease-related amyloid beta peptide (abeta) analogues based on the "O-acyl isopeptide method". *Chembiochem* **7**(10):1549-1557.

Sohma Y, Sasaki M, Hayashi Y, Kimura T and Kiso Y (2004a) Design and synthesis of a novel water-soluble A?1-42 isopeptide: An efficient strategy for the preparation of Alzheimer's disease-related peptide, A?1-42, via O-N intramolecular acyl migration reaction. *Tetrahedron Letters* **45**(31):5965-5968.

Sohma Y, Sasaki M, Hayashi Y, Kimura T and Kiso Y (2004b) Design and synthesis of a novel water-soluble A[beta]1-42 isopeptide: an efficient strategy for the preparation of Alzheimer's disease-related peptide, A[beta]1-42, via O-N intramolecular acyl migration reaction. *Tetrahedron Letters* **45**(31):5965-5968.

Sohma Y, Yoshiya T, Taniguchi A, Kimura T, Hayashi Y and Kiso Y (2007) Development of O-acyl isopeptide method. *Biopolymers* **88**(2):253-262.

Sorimachi K and Craik DJ (1994) Structure determination of extracellular fragments of amyloid proteins involved in Alzheimer's disease and Dutch-type hereditary cerebral haemorrhage with amyloidosis. *Eur J Biochem* **219**(1-2):237-251.

Soto C (1999) Plaque busters: strategies to inhibit amyloid formation in Alzheimer's disease. *Mol Med Today* **5**(8):343-350.

Soto C, Kindy MS, Baumann M and Frangione B (1996) Inhibition of Alzheimer's amyloidosis by peptides that prevent beta-sheet conformation. *Biochem Biophys Res Commun* **226**(3):672-680.

Stephens CR, Murai K, Rennhard HH, Conover LH and Brunings KJ (1958) HYDROGENOLYSIS STUDIES IN THE TETRACYCLINE SERIES: -6-DEOXYTETRACYCLINES. *Journal of the American Chemical Society* **80**(19):5324-5325.

Sticht H, Bayer P, Willbold D, Dames S, Hilbich C, Beyreuther K, Frank RW and Rosch P (1995) Structure of amyloid A4-(1-40)-peptide of Alzheimer's disease. *Eur J Biochem* **233**(1):293-298.

Stine WB, Jr., Dahlgren KN, Krafft GA and LaDu MJ (2003) In vitro characterization of conditions for amyloid-beta peptide oligomerization and fibrillogenesis. *J Biol Chem* **278**(13):11612-11622.

Stoltenberg M, Bruhn M, Sondergaard C, Doering P, West MJ, Larsen A, Troncoso JC and Danscher G (2005) Immersion autometallographic tracing of zinc ions in Alzheimer beta-amyloid plaques. *Histochem Cell Biol* **123**(6):605-611.

Stsiapura VI, Maskevich AA, Kuzmitsky VA, Uversky VN, Kuznetsova IM and Turoverov KK (2008) Thioflavin T as a Molecular Rotor: Fluorescent Properties of Thioflavin T in Solvents with Different Viscosity. *J Phys Chem B.*

Sun C, Wang Q, Brubaker JD, Wright PM, Lerner CD, Noson K, Charest M, Siegel DR, Wang YM and Myers AG (2008a) A robust platform for the synthesis of new tetracycline antibiotics. *J Am Chem Soc* **130**(52):17913-17927.

Sun Y, Zhang G, Hawkes CA, Shaw JE, McLaurin J and Nitz M (2008b) Synthesis of scyllo-inositol derivatives and their effects on amyloid beta peptide aggregation. *Bioorg Med Chem* **16**(15):7177-7184.

Tagliavini F, Forloni G, Colombo L, Rossi G, Girola L, Canciani B, Angeretti N, Giampaolo L, Peressini E, Awan T, De Gioia L, Ragg E, Bugiani O and Salmona M (2000) Tetracycline affects abnormal properties of synthetic PrP peptides and PrP(Sc) in vitro. *J Mol Biol* **300**(5):1309-1322.

Takeda T and Klimov DK (2009) Interpeptide interactions induce helix to strand structural transition in Abeta peptides. *Proteins* **77**(1):1-13.

Talafous J, Marcinowski KJ, Klopman G and Zagorski MG (1994) Solution structure of residues 1-28 of the amyloid beta-peptide. *Biochemistry* **33**(25):7788-7796.

Tanaka M, Chien P, Naber N, Cooke R and Weissman JS (2004) Conformational variations in an infectious protein determine prion strain differences. *Nature* **428**(6980):323-328.

Taniguchi A, Sohma Y, Hirayama Y, Mukai H, Kimura T, Hayashi Y, Matsuzaki K and Kiso Y (2009) "Click peptide": pH-triggered in situ production and aggregation of monomer Abeta1-42. *Chembiochem* **10**(4):710-715.

Teplow DB (2006) Preparation of amyloid beta-protein for structural and functional studies. *Methods Enzymol* **413**:20-33.

Teplow DB, Lazo ND, Bitan G, Bernstein S, Wyttenbach T, Bowers MT, Baumketner A, Shea JE, Urbanc B, Cruz L, Borreguero J and Stanley HE (2006) Elucidating amyloid beta-protein folding and assembly: A multidisciplinary approach. *Acc Chem Res* **39**(9):635-645.

Terzi E, Holzemann G and Seelig J (1994) Reversible random coil-beta-sheet transition of the Alzheimer beta-amyloid fragment (25-35). *Biochemistry* **33**(6):1345-1350.

Tew DJ, Bottomley SP, Smith DP, Ciccotosto GD, Babon J, Hinds MG, Masters CL, Cappai R and Barnham KJ (2008) Stabilization of neurotoxic soluble beta-sheet-rich conformations of the Alzheimer's disease amyloid-beta peptide. *Biophys J* **94**(7):2752-2766.

Thinakaran G and Koo EH (2008) Amyloid precursor protein trafficking, processing, and function. *J Biol Chem* **283**(44):29615-29619.

Tickler AK, Clippingdale AB and Wade JD (2004) Amyloid-beta as a "difficult sequence" in solid phase peptide synthesis. *Protein Pept Lett* **11**(4):377-384.

Tjernberg LO, Lilliehook C, Callaway DJ, Naslund J, Hahne S, Thyberg J, Terenius L and Nordstedt C (1997) Controlling amyloid beta-peptide fibril formation with protease-stable ligands. *J Biol Chem* **272**(19):12601-12605.

Tjernberg LO, Naslund J, Lindqvist F, Johansson J, Karlstrom AR, Thyberg J, Terenius L and Nordstedt C (1996) Arrest of beta-amyloid fibril formation by a pentapeptide ligand. *J Biol Chem* **271**(15):8545-8548.

Tomic JL, Pensalfini A, Head E and Glabe CG (2009) Soluble fibrillar oligomer levels are elevated in Alzheimer's disease brain and correlate with cognitive dysfunction. *Neurobiol Dis.*

Tuchscherer G, Chandravarkar A, Camus MS, Berard J, Murat K, Schmid A, Mimna R, Lashuel HA and Mutter M (2007) Switch-peptides as folding precursors in self-assembling peptides and amyloid fibrillogenesis. *Biopolymers* **88**(2):239-252.

Turner PR, O'Connor K, Tate WP and Abraham WC (2003) Roles of amyloid precursor protein and its fragments in regulating neural activity, plasticity and memory. *Prog Neurobiol* **70**(1):1-32.

Tycko R (2006) Solid-state NMR as a probe of amyloid structure. *Protein Pept Lett* **13**(3):229-234.

Uversky VN and Fink AL (2004) Conformational constraints for amyloid fibrillation: the importance of being unfolded. *Biochim Biophys Acta* **1698**(2):131-153.

Valincius G, Heinrich F, Budvytyte R, Vanderah DJ, McGillivray DJ, Sokolov Y, Hall JE and Losche M (2008) Soluble amyloid beta-oligomers affect dielectric membrane properties by bilayer insertion and domain formation: implications for cell toxicity. *Biophys J* **95**(10):4845-4861.

Van Nostrand WE, Melchor JP, Cho HS, Greenberg SM and Rebeck GW (2001) Pathogenic effects of D23N Iowa mutant amyloid beta -protein. *J Biol Chem* **276**(35):32860-32866.

Verdier Y, Zarandi M and Penke B (2004) Amyloid beta-peptide interactions with neuronal and glial cell plasma membrane: binding sites and implications for Alzheimer's disease. *J Pept Sci* **10**(5):229-248.

Walsh DM, Lomakin A, Benedek GB, Condron MM and Teplow DB (1997) Amyloid beta-protein fibrillogenesis. Detection of a protofibrillar intermediate. *J Biol Chem* **272**(35):22364-22372.

Wang H, Kakizawa T, Taniguchi A, Mizuguchi T, Kimura T and Kiso Y (2009) Synthesis of amyloid beta peptide 1-42 (E22Delta) click peptide: pH-triggered in situ production of its native form. *Bioorg Med Chem* **17**(14):4881-4887.

Weng N, Roets E, Busson R and Hoogmartens J (1990) Separation of keto-enol tautomers of chlortetracycline and 4-epichlortetracycline by liquid chromatography on poly(styrene-divinylbenzene)copolymer. *J Pharm Biomed Anal* **8**(8-12):881-889.

Wessels JM, Ford WE, Szymczak W and Schneider S (1998) The Complexation of Tetracycline and Anhydrotetracycline with Mg2+ and Ca2+: A Spectroscopic Study. *The Journal of Physical Chemistry B* **102**(46):9323-9331.

Wetzel R, Shivaprasad S and Williams AD (2007) Plasticity of amyloid fibrils. *Biochemistry* **46**(1):1-10.

Williams AD, Portelius E, Kheterpal I, Guo JT, Cook KD, Xu Y and Wetzel R (2004) Mapping abeta amyloid fibril secondary structure using scanning proline mutagenesis. *J Mol Biol* **335**(3):833-842.

Williams AD, Sega M, Chen M, Kheterpal I, Geva M, Berthelier V, Kaleta DT, Cook KD and Wetzel R (2005) Structural properties of Abeta protofibrils stabilized by a small molecule. *Proc Natl Acad Sci U S A* **102**(20):7115-7120.

Wöhr T (1995) Pseudo-prolines in peptide synthesis: Direct insertion of serine and threonine derived oxazolidines in dipeptides. *Tetrahedron Letters* **36**(22):3847-3848.

Wood SJ, Maleeff B, Hart T and Wetzel R (1996) Physical, morphological and functional differences between ph 5.8 and 7.4 aggregates of the Alzheimer's amyloid peptide Abeta. *J Mol Biol* **256**(5):870-877.

Xue WF, Homans SW and Radford SE (2008) Systematic analysis of nucleation-dependent polymerization reveals new insights into the mechanism of amyloid self-assembly. *Proc Natl Acad Sci U S A* **105**(26):8926-8931.

Yang F, Lim GP, Begum AN, Ubeda OJ, Simmons MR, Ambegaokar SS, Chen PP, Kayed R, Glabe CG, Frautschy SA and Cole GM (2005) Curcumin inhibits formation of amyloid beta oligomers and fibrils, binds plaques, and reduces amyloid in vivo. *J Biol Chem* **280**(7):5892-5901.

Yang M and Teplow DB (2008) Amyloid beta-protein monomer folding: free-energy surfaces reveal alloform-specific differences. *J Mol Biol* **384**(2):450-464.

Yip CM, Elton EA, Darabie AA, Morrison MR and McLaurin J (2001) Cholesterol, a modulator of membrane-associated Abeta-fibrillogenesis and neurotoxicity. *J Mol Biol* **311**(4):723-734.

Yu L, Edalji R, Harlan JE, Holzman TF, Lopez AP, Labkovsky B, Hillen H, Barghorn S, Ebert U, Richardson PL, Miesbauer L, Solomon L, Bartley D, Walter K, Johnson RW, Hajduk PJ and Olejniczak ET (2009) Structural Characterization of a Soluble Amyloid beta-Peptide Oligomer. *Biochemistry.*

Yun S, Urbanc B, Cruz L, Bitan G, Teplow DB and Stanley HE (2007) Role of electrostatic interactions in amyloid beta-protein (A beta) oligomer formation: a discrete molecular dynamics study. *Biophys J* **92**(11):4064-4077.

Zagorski MG and Barrow CJ (1992) NMR studies of amyloid beta-peptides: proton assignments, secondary structure, and mechanism of an alpha-helix----beta-sheet conversion for a homologous, 28-residue, N-terminal fragment. *Biochemistry* **31**(24):5621-5631.

Zagorski MG, Yang J, Shao H, Ma K, Zeng H and Hong A (1999) Methodological and chemical factors affecting amyloid beta peptide amyloidogenicity. *Methods Enzymol* **309**:189-204.

Zhanel GG, Homenuik K, Nichol K, Noreddin A, Vercaigne L, Embil J, Gin A, Karlowsky JA and Hoban DJ (2004) The glycylcyclines: a comparative review with the tetracyclines. *Drugs* **64**(1):63-88.

Zhang R, Hu X, Khant H, Ludtke SJ, Chiu W, Schmid MF, Frieden C and Lee JM (2009) Interprotofilament interactions between Alzheimer's Abeta1-42 peptides in amyloid fibrils revealed by cryoEM. *Proc Natl Acad Sci U S A* **106**(12):4653-4658.

Zhang S, Iwata K, Lachenmann MJ, Peng JW, Li S, Stimson ER, Lu Y, Felix AM, Maggio JE and Lee JP (2000) The Alzheimer's peptide a beta adopts a collapsed coil structure in water. *J Struct Biol* **130**(2-3):130-141.

Zhao Y, Ci Y and Chang W (1997) Fluorescence enhancing by alkaline degradation of tetracycline antibiotics and its application. *Science in China Series B: Chemistry* **40**(4):434-441.

Zhu X, Smith MA, Honda K, Aliev G, Moreira PI, Nunomura A, Casadesus G, Harris PL, Siedlak SL and Perry G (2007) Vascular oxidative stress in Alzheimer disease. *J Neurol Sci* **257**(1-2):240-246.